INTERNATIONAL ATOMIC ENERGY AGENCY
UNITED NATIONS EDUCATIONAL, SCIENTIFIC AND CULTURAL ORGANIZATION
INTERNATIONAL CENTRE FOR THEORETICAL PHYSICS
I.C.T.P., P.O. BOX 586, 34100 TRIESTE, ITALY, CABLE: CENTRATOM TRIESTE

H4.SMR/842-12

Conference on
Ultrafast Transmission Systems in Optical Fibres

13 - 17 February 1995

Optoelectronic Switches, Modulators and Semiconductor Amplifier Gates for High Speed Fibre-Transmission Systems

H. Melchior

Swiss Federal Institute of Technology
Zurich, Switzerland

Conference on Ultrafast Transmission Systems in Optical Fibers

International Centre for Theoretical Physics
Trieste, February 13 to 17 1995

Optoelectronic Switches Modulators and Semiconductor Amplifier Gates for High Speed Fibre-Transmission Systems

Hans Melchior
Swiss Federal Institute of Technology
CH-8093 Zurich
Switzerland
Tel.: ++41 1 633 2101
Fax: ++41 1 633 1109
E-mail: h.melchior@iqe.phys.ethz.ch

01

ETH Eidgenössische Technische Hochschule Zürich

HIGH-SPEED PHOTONIC WAVEGUIDE SWITCH ARRAYS and OPTICAL AMPLIFIER GATES IN InGaAsP/InP for COMMUNICATIONS APPLICATIONS

- Introductory Overview
- Planar Compound Semiconductor Waveguide Space Switches
  - Operational Principles
    Linear and Quadratic Electro-optic Effects
    in Bulk and Quantum Well Semiconductors
  - Implementations
    Directional Coupler Switches
    Digital Optical Switches
    Mach Zehnder Interferometer Switches
- Semiconductor Optical Amplifier Gate-Switches
- Conclusions

02

ETH Eidgenössische Technische Hochschule Zürich

Overview

Optical switches, modulators and amplifier gates rely on controlled optical and electro-optical interactions of light passing through suitably chosen electro-optic materials and devices.

In electro-optic materials like $LiNbO_3$ the phase of an optical wave can be controlled through the linear electro-optic effect by an electric field.

In the form of integrated waveguide arrays, such electro-optic modulators and switches are useful for high speed modulation and for the routing and switching of single and multi-wavelength fiber-optic signal transmission channels.

In liquid-crystal light valves a number of electro-optic and light scattering effects are being exploited for the parallel processing of optical signals.

Semiconductor-optoelectronic materials offer, besides the linear electro-optic effect and optical amplification, a rich variety of pronounced carrier density and electric field related optoelectronic interactions, that make possible both, integrated optic waveguide switch arrays for telecommunications and planar modulator and switch arrays that work in transmission or reflection for optical interconnects and parallel optical signal processing.

This presentation combines an introductory overview over the various electro-optic effects used in optical modulators, switches and amplifier gates with details of state of the art implementations. The physical effects include the linear and quadratic electro-optic effect of the dielectric electro-optic materials.

For semiconductors the number of useful electro-optic effects is extended to include in addition optical amplification and the carrier density related band-filling, bandgap shrinkage and free-carrier plasma effects and the band-to-band tunneling induced electrorefraction and absorption at high electric fields. In multiple-quantum wells there are pronounced electric-field induced shifts in absorption edges and large changes in refractive indices.

Major types of integrated optic waveguide switches, modulators and semiconductor amplifier gates will be discussed, Beginning with the principle of phase modulation by changes in refractive index and its exploitation in waveguide coupler switches Mach-Zehnder Interferometers. Other switch principles rely on adiabatic beam transformations on total internal reflection. Examples of waveguide switch and array designs and application possibilities are mentioned together with their use in the modulation, switching and routing of optical communication signals.

The optical modulators include electroabsorption and refractive index modulators. Optical space switches both in single switch and switch array from include directional coupler switches, Mach-Zehnder interferometer switches, digital optical switches and total internal reflection switches. High-speed optical switches with gain are feasible in direct bandgap semiconductor materials.

Quantum-well electroabsorption modulators and optically controlled bistable switching devices are presented as examples of optical switching devices arranged in a plane and optimally combined with electronics for optical signal processing utilizing highly multiparallel optical beam arrangements.

An outlook towards more futuristic optical signal processing device concepts for optical wavelength conversion and all-optical switching will be included. Key requirements for optical switches, modulators and amplifier gates will be mentioned. They include low optical losses, high-speed operation, low polarization sensitivity, high on-off ratios and low cross-talk.

Optoelectronic Switches Modulators and Semiconductor Amplifier Gates for High Speed Fiber-Transmission Systems

➡ Motivation for Optical Switching in High Speed Fiber Optical Communication Networks

⇨ Basic Concepts of Optical Switches, Modulators and Semiconductor Optical Amplifier Gates

⇨ Physical Effects exploited in Waveguide Type Optical Switches, Modulators and Semiconductor Optical Amplifier Gates

⇨ Implementations of High Speed Optical Modulators

⇨ Implementations of High Speed Waveguide Type Space Switches

⇨ Semiconductor Optical Amplifier Gates and Wavelength Converters

⇨ Summary and Conclusions

ETH Eidgenössische Technische Hochschule Zürich

trieste1995/4

05

Fiber Optical Communication Systems and Networks

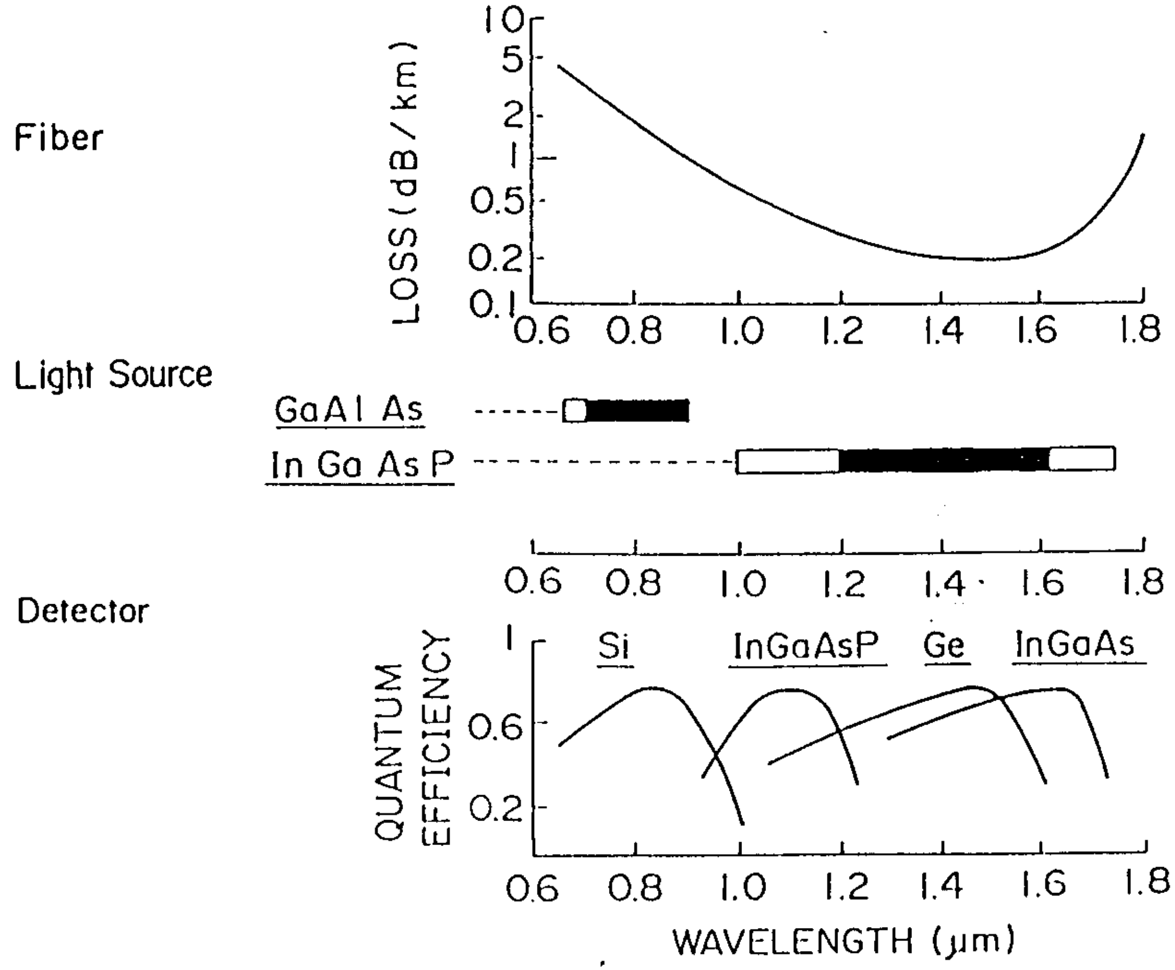

TRAFFIC CHARACTERISTICS OF BROADBAND SERVICES

(S. Weinstein, *IEEE Spectrum*, November, 1987)

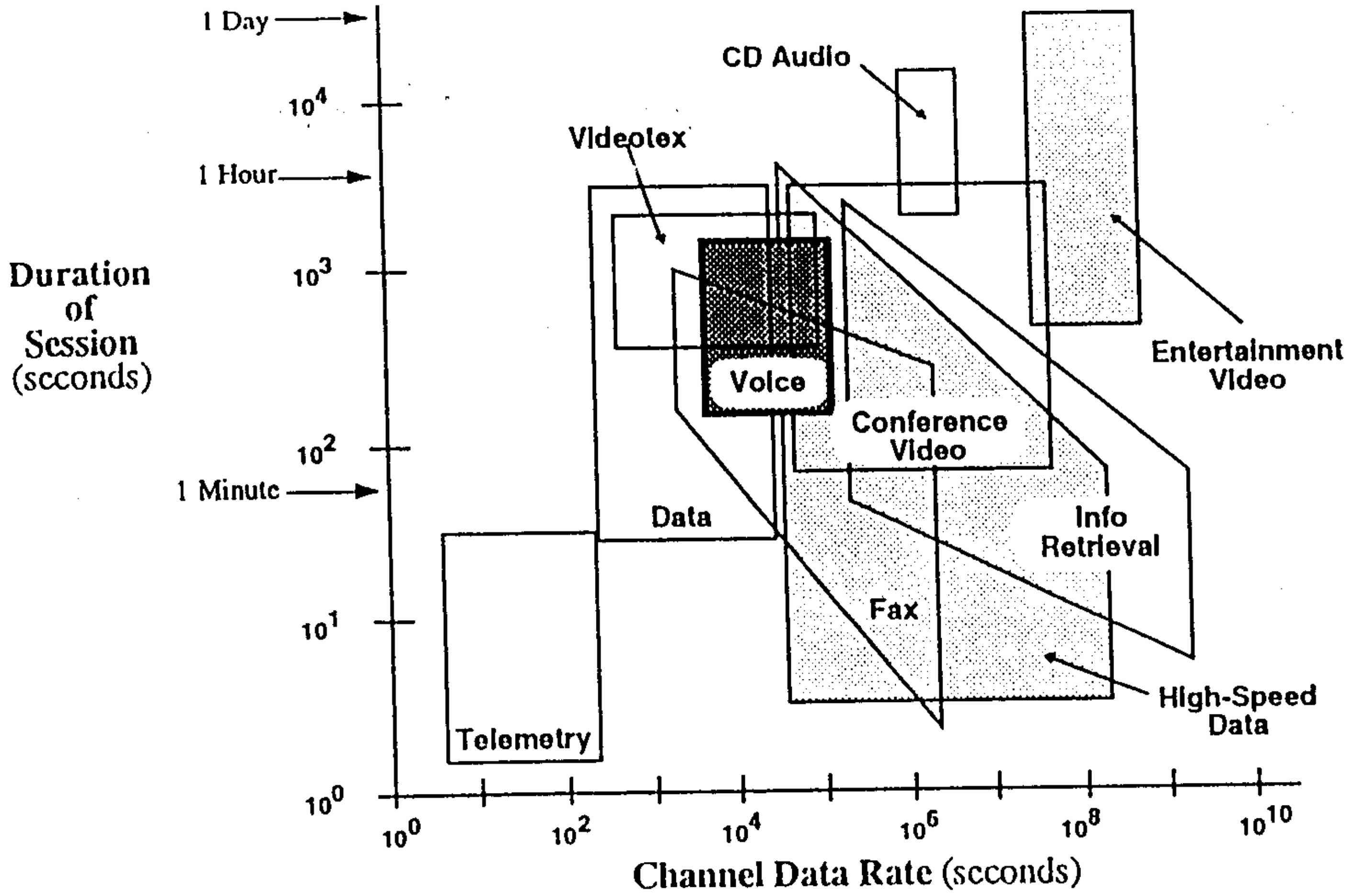

Information Transmission Capacity of Silica-Glass Fibers

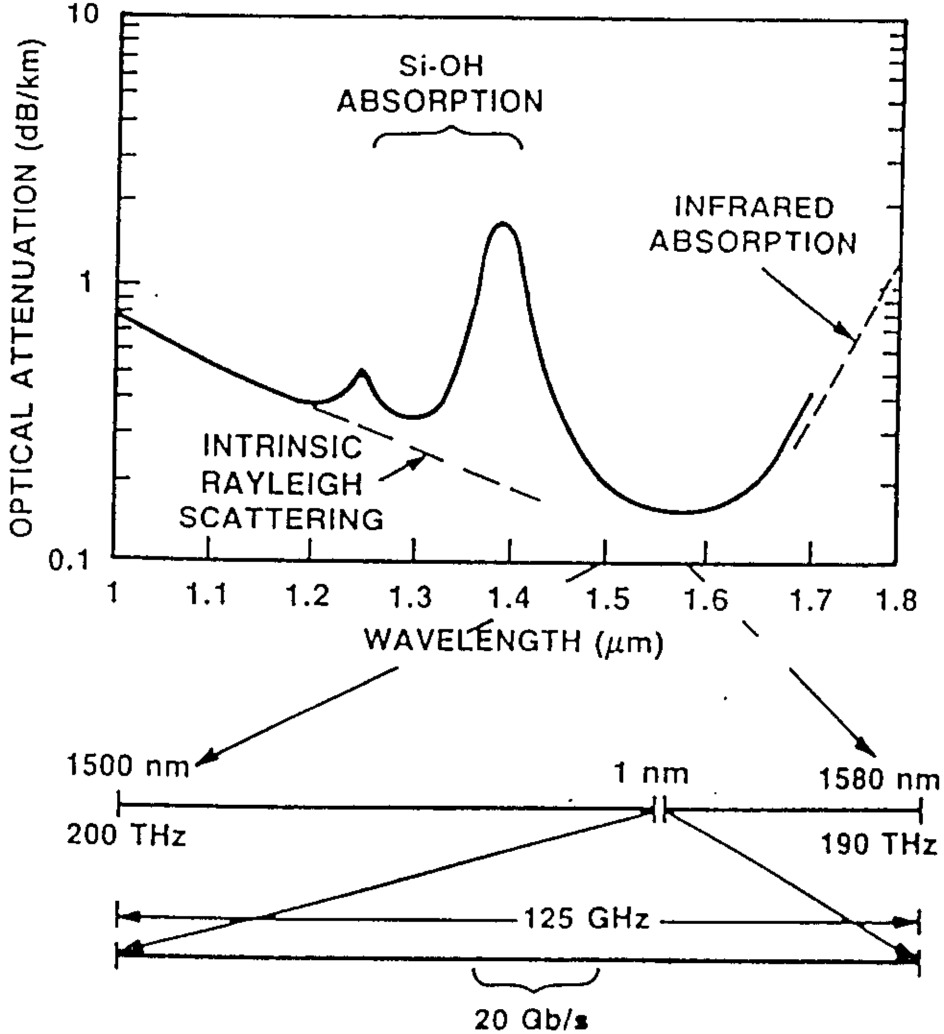

80

HIGH-SPEED OPTICAL TRANSMITTER WITH PULSED LASER AND OPTICAL MODULATOR

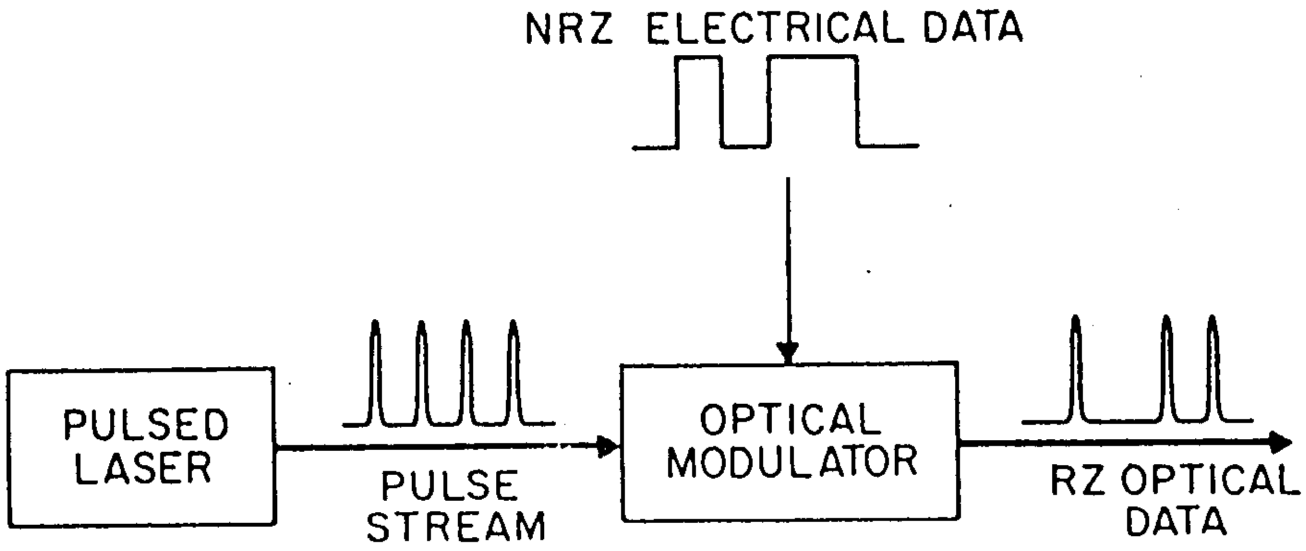

60

ETH Eidgenössische Technische Hochschule Zürich

OPTICAL SPACE SWITCH

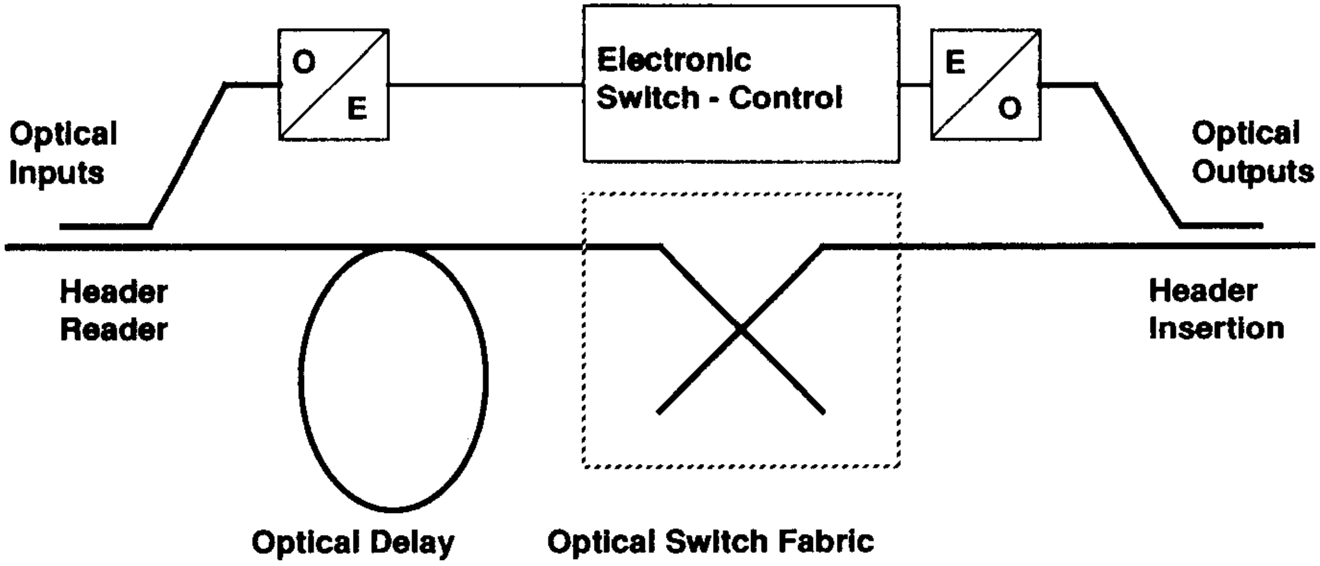

Combins optically transparent switch fabric with delay lines, electronic header reader and switch control

Fully Implemented Strictly Non-blocking 16x16 Photonic Switching System Composed of 23 Lithium Niobate Modules

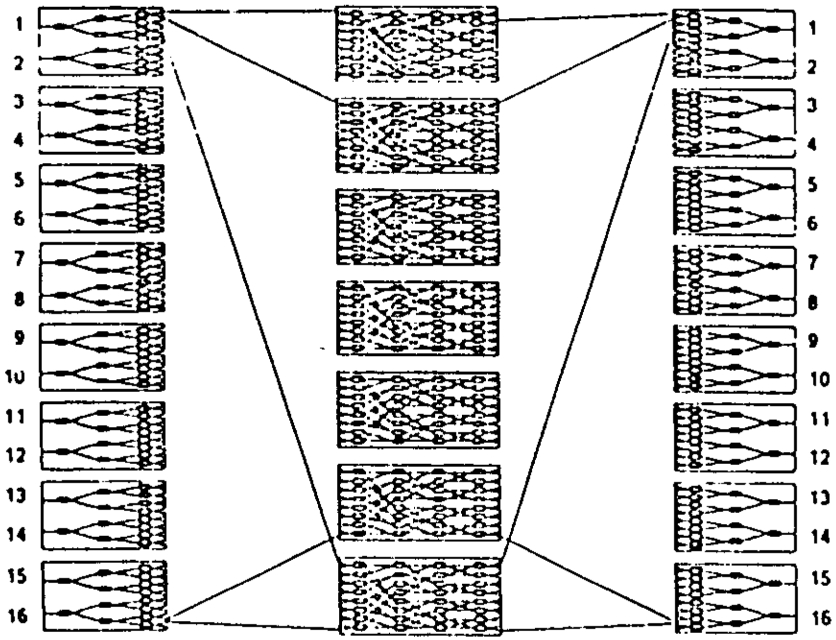

Extended 16x16 Generalized Shuffle Network

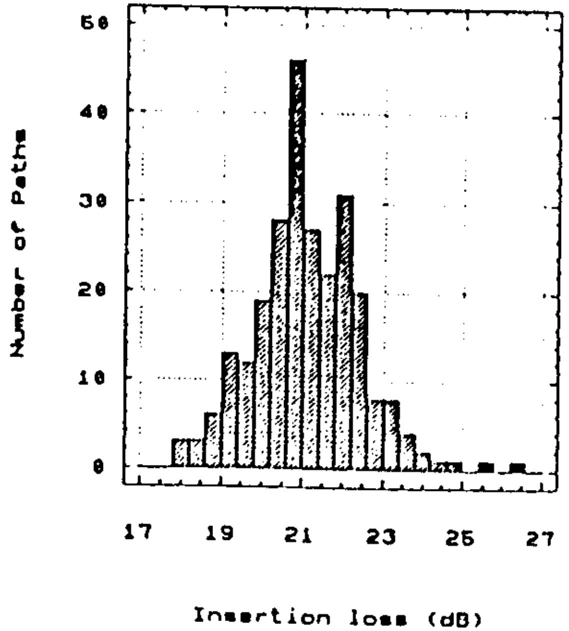

Overall Input to Output Losses

ATT Bell Labs, OFC/IOOC'93

Eidgenössische Technische Hochschule Zürich

Optoelectronic Switches Modulators and Semiconductor Amplifier Gates for High Speed Fiber-Transmission Systems

⇒ Motivation for Optical Switching in High Speed Fiber Optical Communication Networks

➡ Basic Concepts of Optical Switches, Modulators and Semiconductor Optical Amplifier Gates

⇒ Physical Effects exploited in Waveguide Type Optical Switches, Modulators and Semiconductor Optical Amplifier Gates

⇒ Implementations of High Speed Optical Modulators

⇒ Implementations of High Speed Waveguide Type Space Switches

⇒ Semiconductor Optical Amplifier Gates and Wavelength Converters

⇒ Summary and Conclusions

ETH Eidgenössische Technische Hochschule Zürich

OPTICAL SWITCHES AND MODULATOR

Bulk Optics

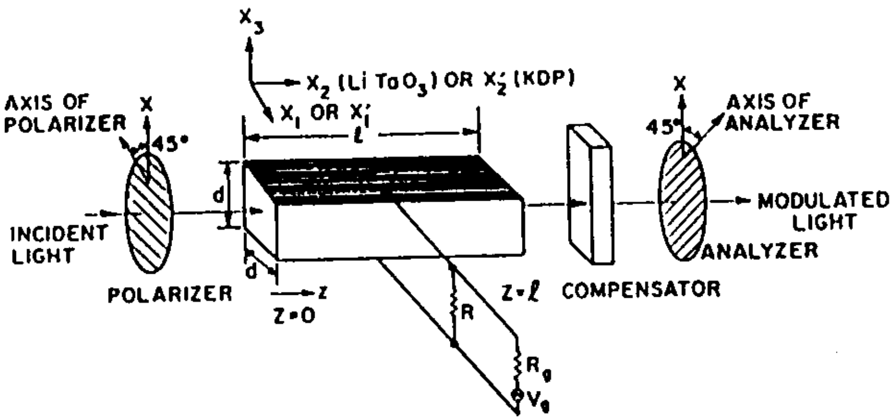

Free Space Switches

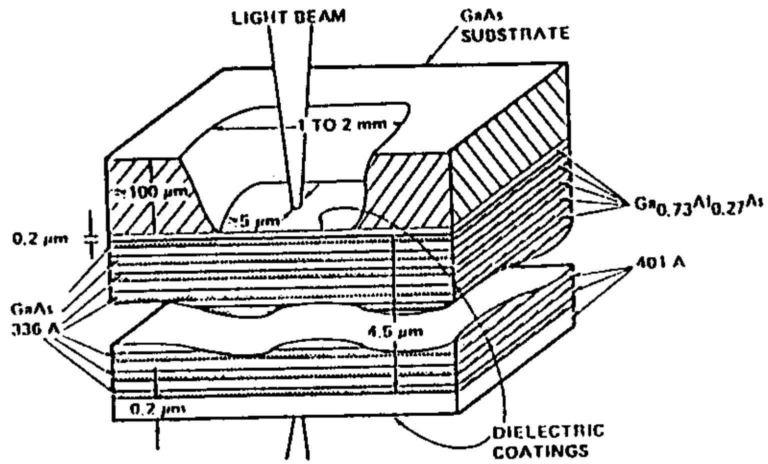

Guided Wave Switches (Directional Coupler Switch using Electro-Optic Effect in n^--n^+GaAs Rib-Waveguides)

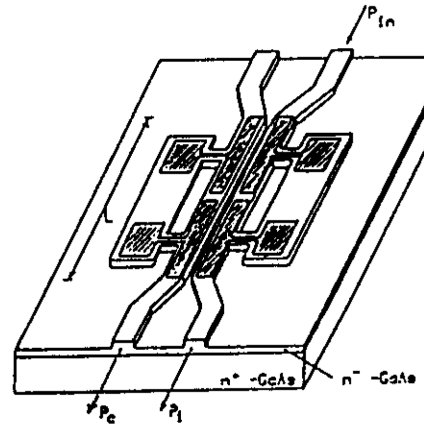

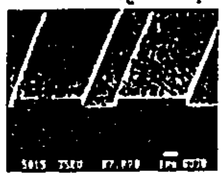

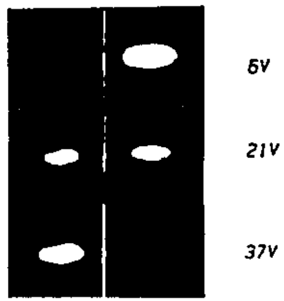

(ETH-Z 1989)

Eidgenössische Technische Hochschule Zürich

OPTICAL WAVEGUIDES

Optical waveguides are structures in dielectric or magnetic materials that are used to confine and guide electromagnetic waves at optical frequencies.

Basic principle: Optical waveguiding, i.e. guidance and propagation of electromagnetic waves takes place along regions with enhanced optical refractive index, respectively along regions with enhanced dielectric constant ε or magnetic permittivity μ.

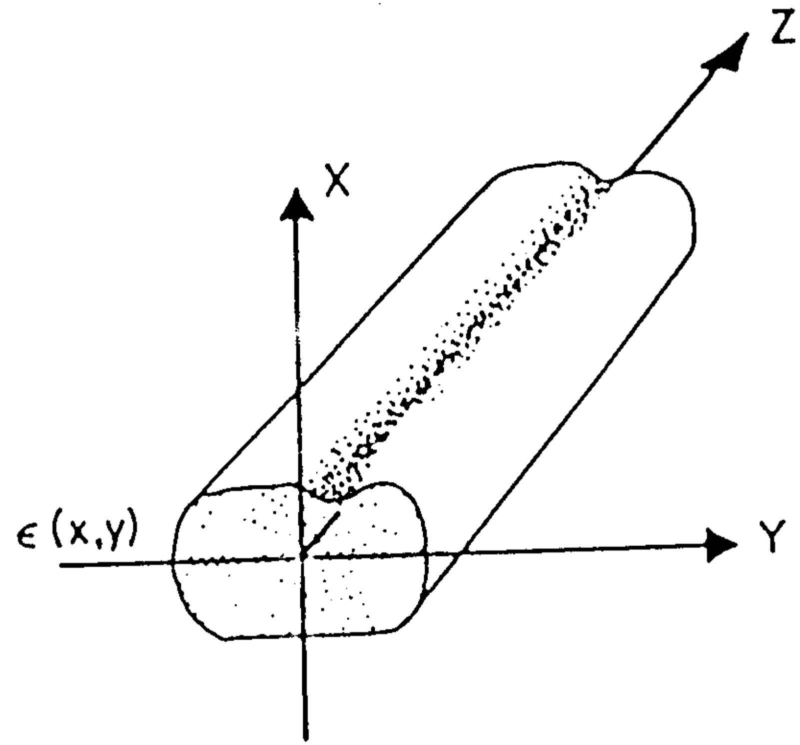

Dielectric Waveguide allowing Wave Propagation in ±z-Direction.

OPTICAL WAVEGUIDES

Optical Fiber

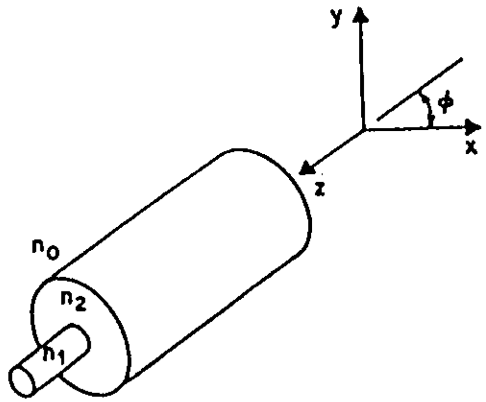

Planar Thin Film Waveguide
"Slab Waveguide"

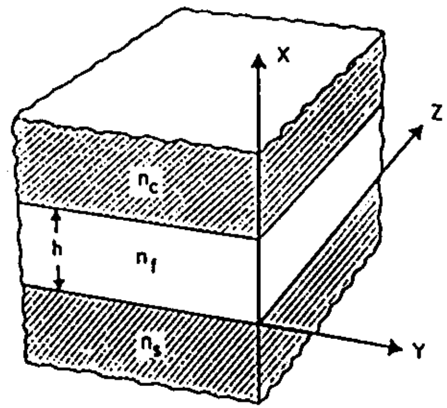

Two Dimensional
Thin Film
Waveguide

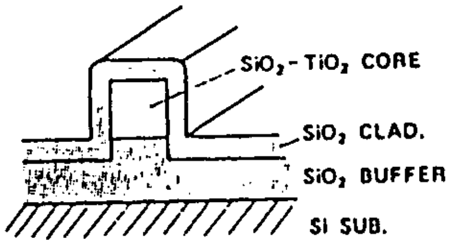

ETH Eidgenössische Technische Hochschule Zürich

IMPLEMENTATIONS OF OPTICAL SINGLE AND MULTI-MODE WAVEGUIDE COMPONENTS

Circularly Symmetric Structures

↓

Optical Fibers
SiO_2

Organics

Integrated Waveguides in Planar Technologies

Waveguides in Three-Dimensional Structures

Organics

Glass

Silica on Silicon

Electro-Optic Materials

$LiNbO_3$

III-V Compound Semiconductors

AlGaAs/GaAs
InGaAsP/InP

Other Semiconductors

GeSi/Si

ETH Eidgenössische Technische Hochschule Zürich

SILICA ON SILICON INTEGRATED OPTIC WAVEGUIDE CIRCUITS

Single mode optical waveguide circuits made either from SiO_2:P/SiO_2 on Silicon with core sizes of a few micrometers, or from Si_3N_4/SiO_2 on Silicon with smaller waveguide cores, both with low losses and well advanced technologies, offer advantages for the integration of passive optical waveguide components.

Silica on Silicon integrated waveguides are suitable as a mounting board technique for the interconnection of active optical device chips, passive waveguide circuits and interconnections with fibers. This technology is thus of practical importance for optical fiber networks.

4x4 SILICA ON SILICON WAVEGUIDE SWITCHES

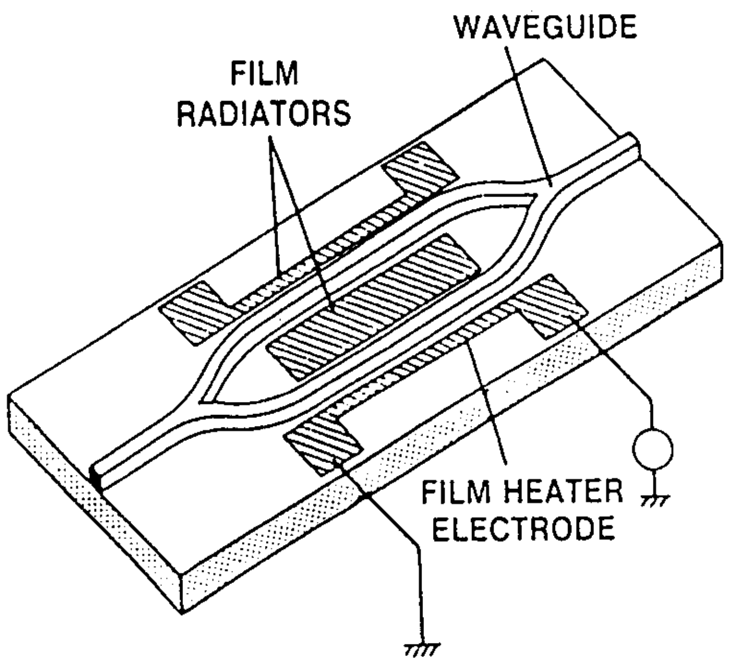

MACH-ZEHNDER
INTERFEROMETER GATE

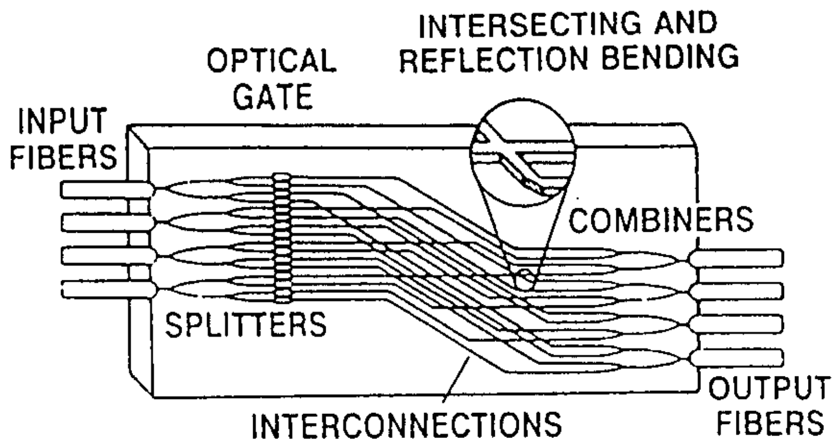

4 x 4 OPTICAL GATE MATRIX
SWITCH CONFIGURATION

A. Himeno and M. Kobayshi, Elect. Letter. 23, 887 (1987)

INTEGRATED OPTIC COMPONENTS

Active devices (switches, modulators, etc.) can be interconnected on a single substrate

Materials - Ti : $LiNbO_3$
GaAs
InGaAsP/InP
Glass
Si

Problem areas - Connecting in and out
Polarization sensitivity
Matching fiber profile
Overall performance, cross talk, loss, environmental stability

Fabrication Of Ti-Indiffused Waveguides In Lithium Niobate

1. EXPOSE WAVEGUIDE PATTERN

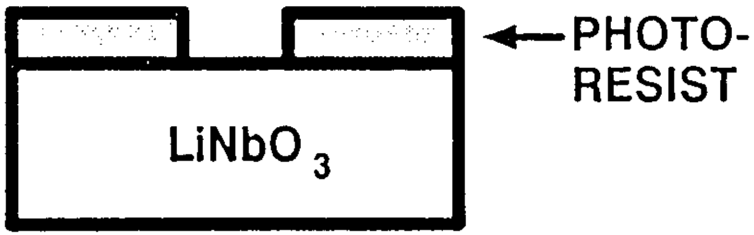

2. DEPOSIT TITANIUM DOPANT

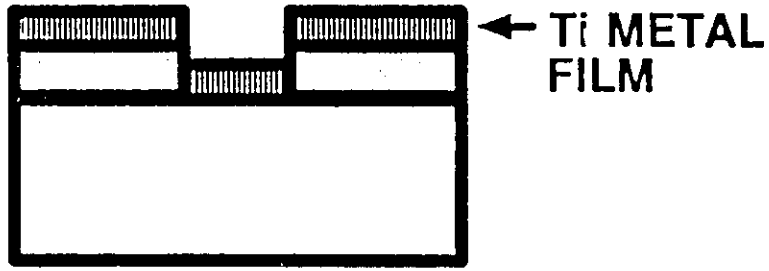

3. LIFTOFF

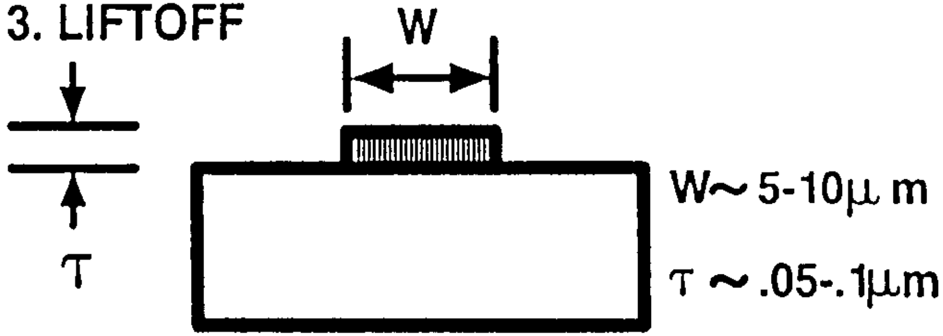

4. DIFFUSE

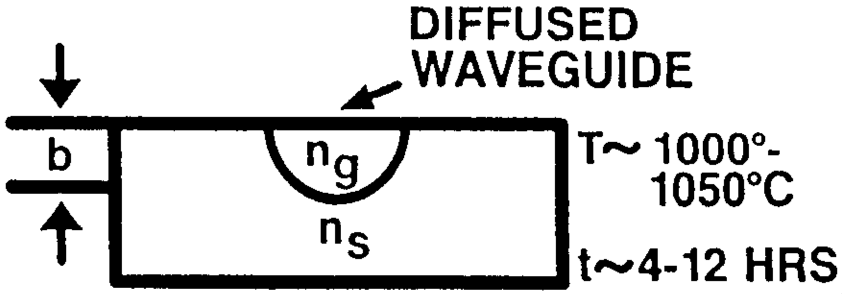

$n_g - n_s = f(\tau, T, t) \sim .005\text{-}.01$

Semiconductor Waveguide Fabrication

RIB

INVERTED RIB

DEPOSIT/
PATTERN
MASK

ETCH, STRIP
MASK

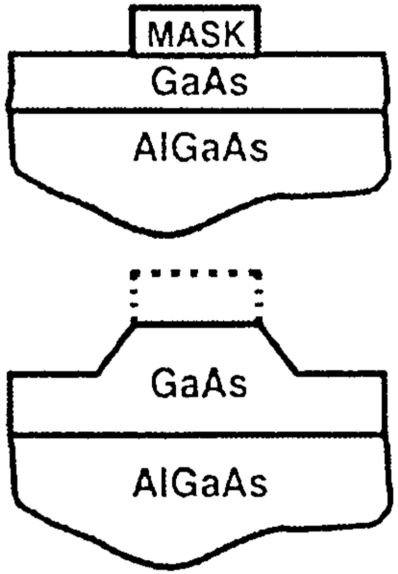

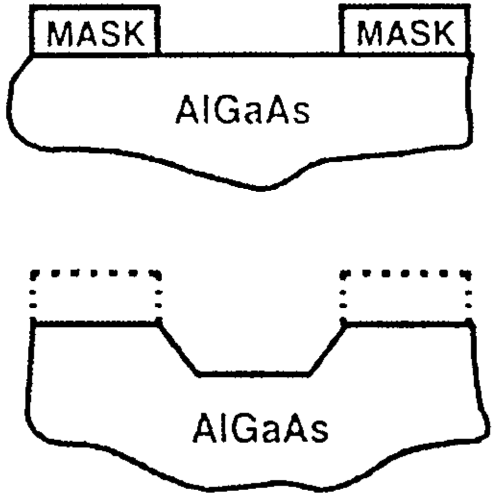

TYPICAL
RIB
GUIDE

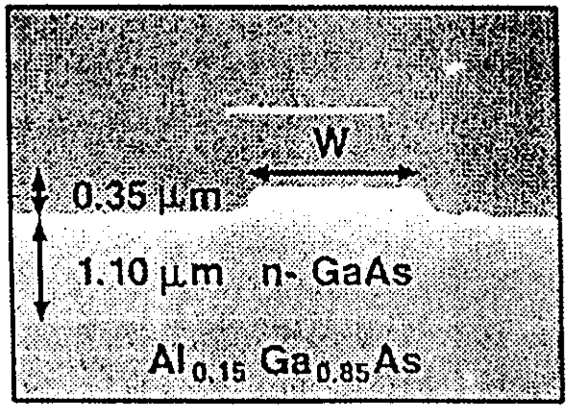

EPITAXIAL
REGROWTH

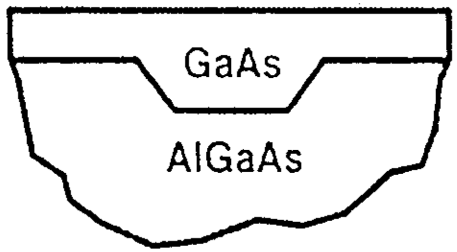

WAVEGUIDE–STRUCTURES

RIB–WAVEGUIDES

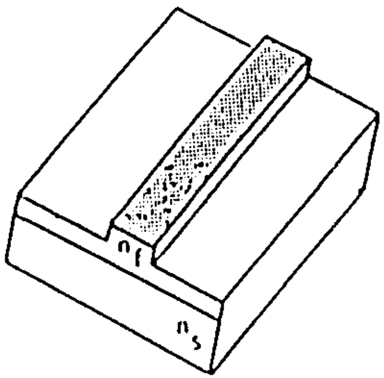

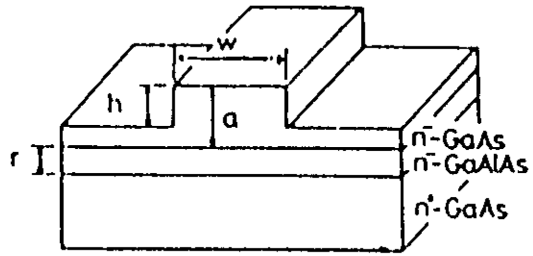

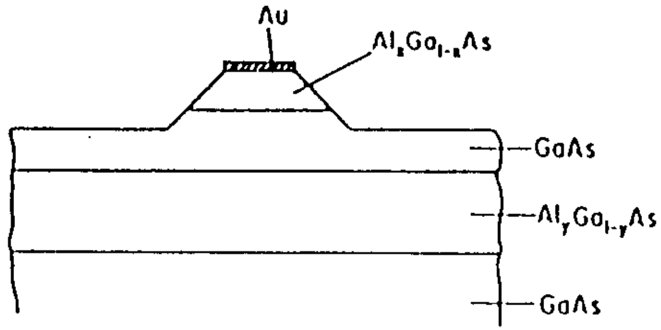

$n^- - n^+$ GaAs
$n^- - n^+$ InP

Single
Heterostructure
GaAs/AlGaAs
InGaAsP/InP

Double
Heterostructure
GaAs/AlGaAs
InGaAsP/InP

PHOTONIC SPACE DIVISION SWITCH

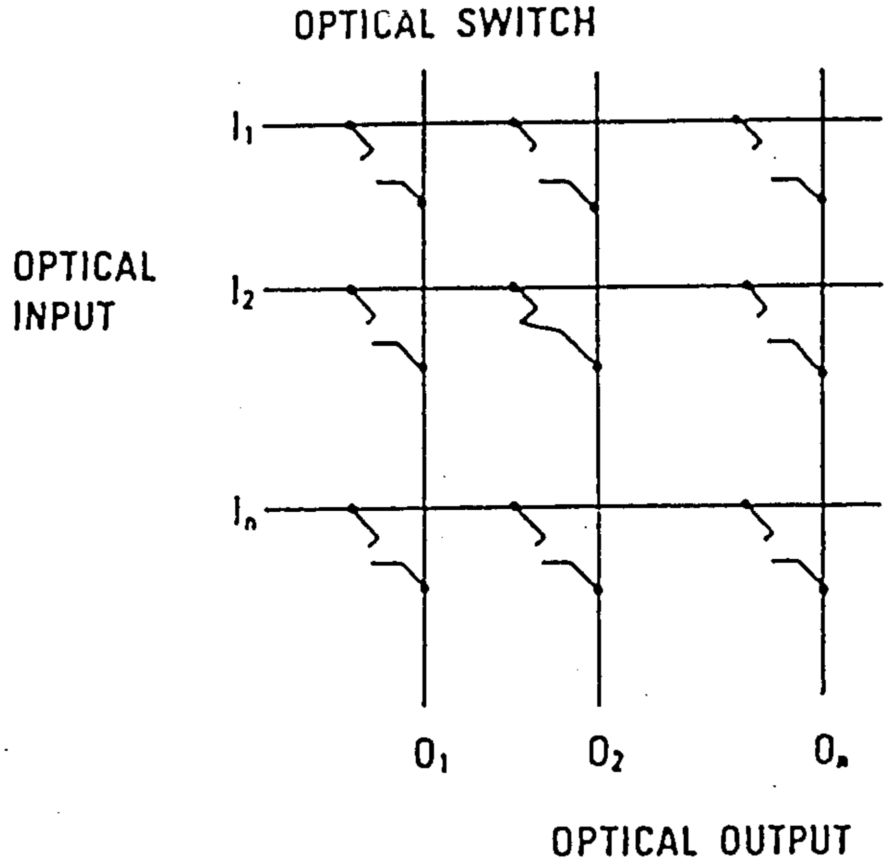

WAVEGUIDE SPACE SWITCHES AND MODULATORS

- **LiNbO3 - Electro-optic Effect Devices**
- **InP- and GaAs III-V Compound Semiconductors**

Interferometric Devices | Mode Converters | Reflection Type | Optical Gates

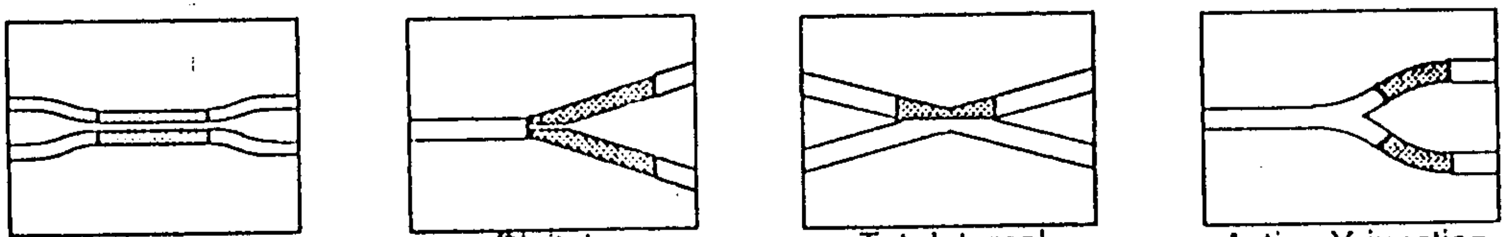

Directional Coupler | Digital Optical Switch | TotalInternal Reflection Switch | Active Y-junction Switch

Refractive index modulation | Absorption modulation

ETH Eidgenössische Technische Hochschule Zürich

OPTICAL WAVEGUIDE MODULATORS AND SWITCHES

- Phase Modulators
- Mach Zehnder Waveguide Interferometers
- Directional Couplers
- Total Internal Reflection Switches
- Digital Optical Switches

Optoelectronic Switches Modulators and Semiconductor Amplifier Gates for High Speed Fiber-Transmission Systems

- ⇒ Motivation for Optical Switching in High Speed Fiber Optical Communication Networks
- ⇒ Basic Concepts of Optical Switches, Modulators and Semiconductor Optical Amplifier Gates
- ➡ Physical Effects exploited in Waveguide Type Optical Switches, Modulators and Semiconductor Optical Amplifier Gates
- ⇒ Implementations of High Speed Optical Modulators
- ⇒ Implementations of High Speed Waveguide Type Space Switches
- ⇒ Semiconductor Optical Amplifier Gates and Wavelength Converters
- ⇒ Summary and Conclusions

ETH Eidgenössische Technische Hochschule Zürich

ENERGY BANDGAPS AND LATTICE CONSTANTS OF $In_{1-x}Ga_x As_yP_{1-y}/InP$ QUATERARIES

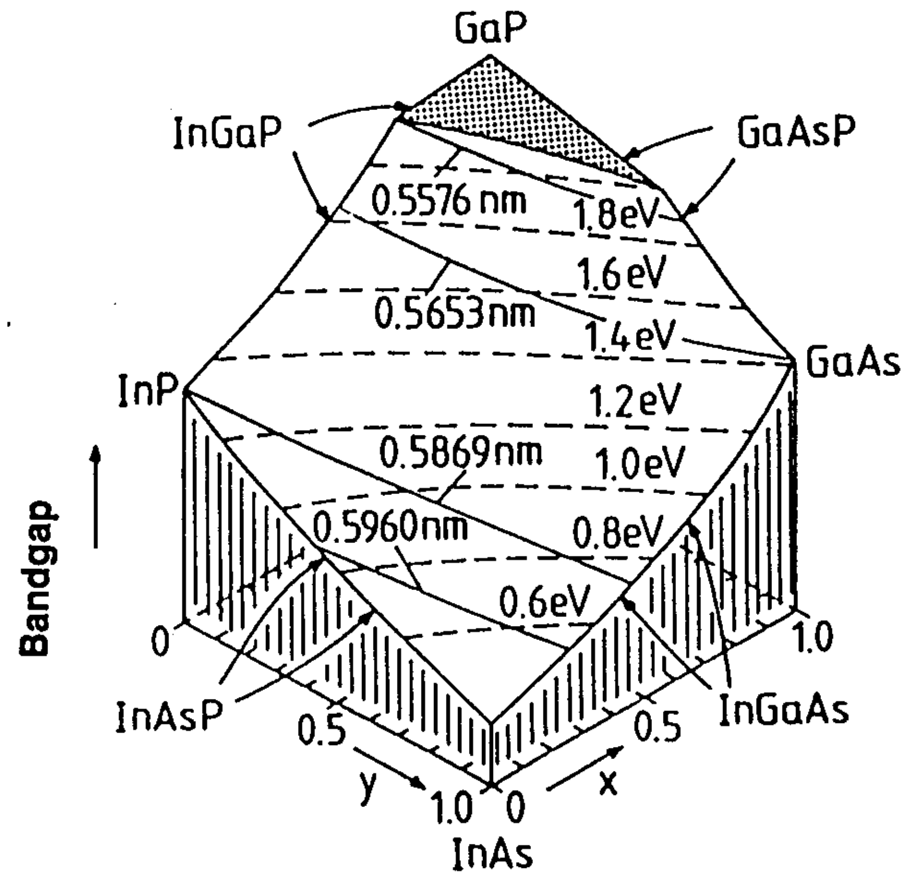

ETH Eidgenössische Technische Hochschule Zürich

MINIMUM BANDGAP VERSUS LATTICE CONSTANT OF COLOMN IV, III-V AND II-VI SEMICONDUCTORS

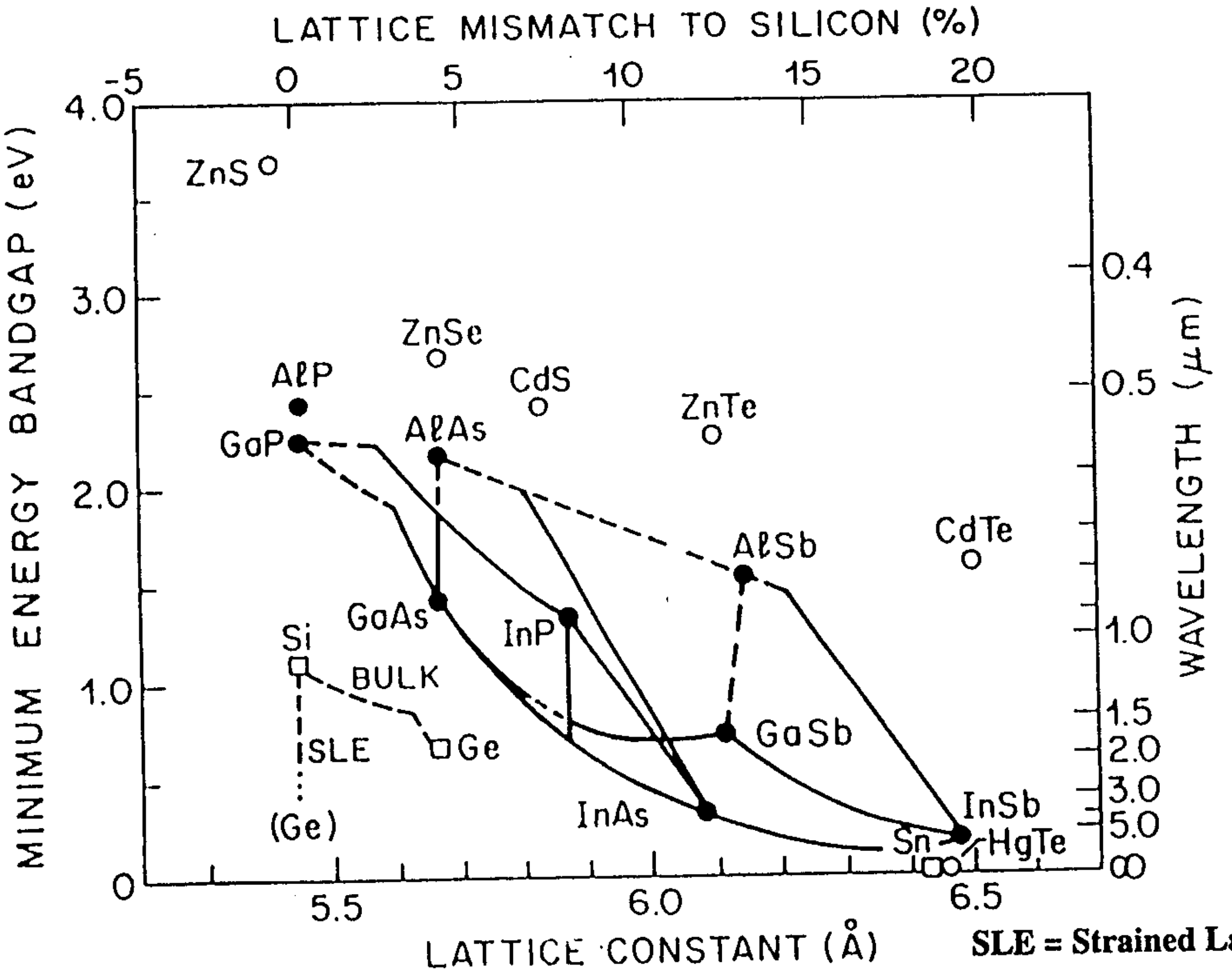

SLE = Strained Layer Epitaxy

Optical Refractive Index of
$Al_xGa_{1-x}As$ and $In_{1-x}Ga_xAs_yP_{1-y}$/InP (y= 2.197x)

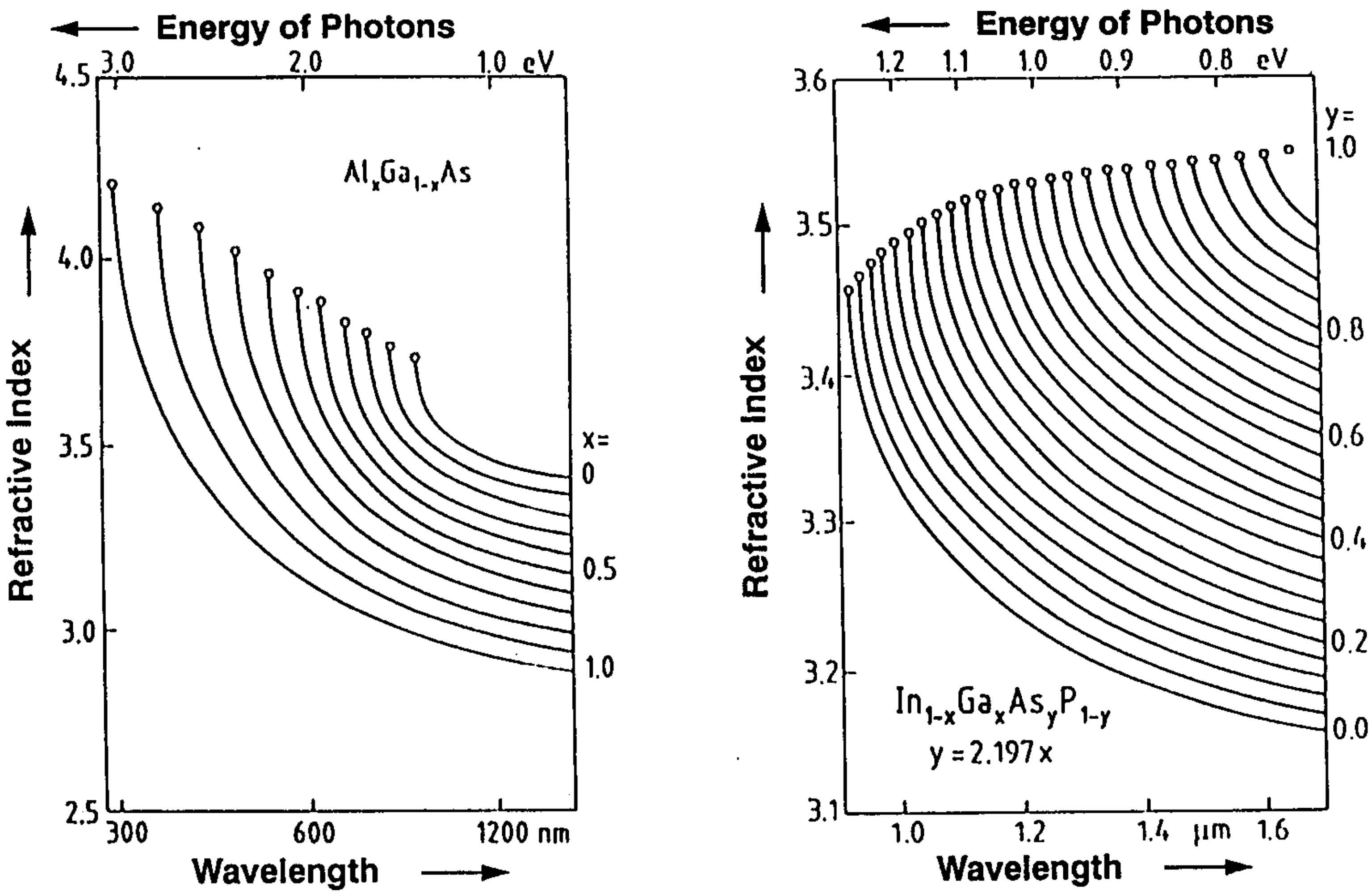

CEI

OPTICAL ABSORPTION OF AlGaAs AND InGaAs

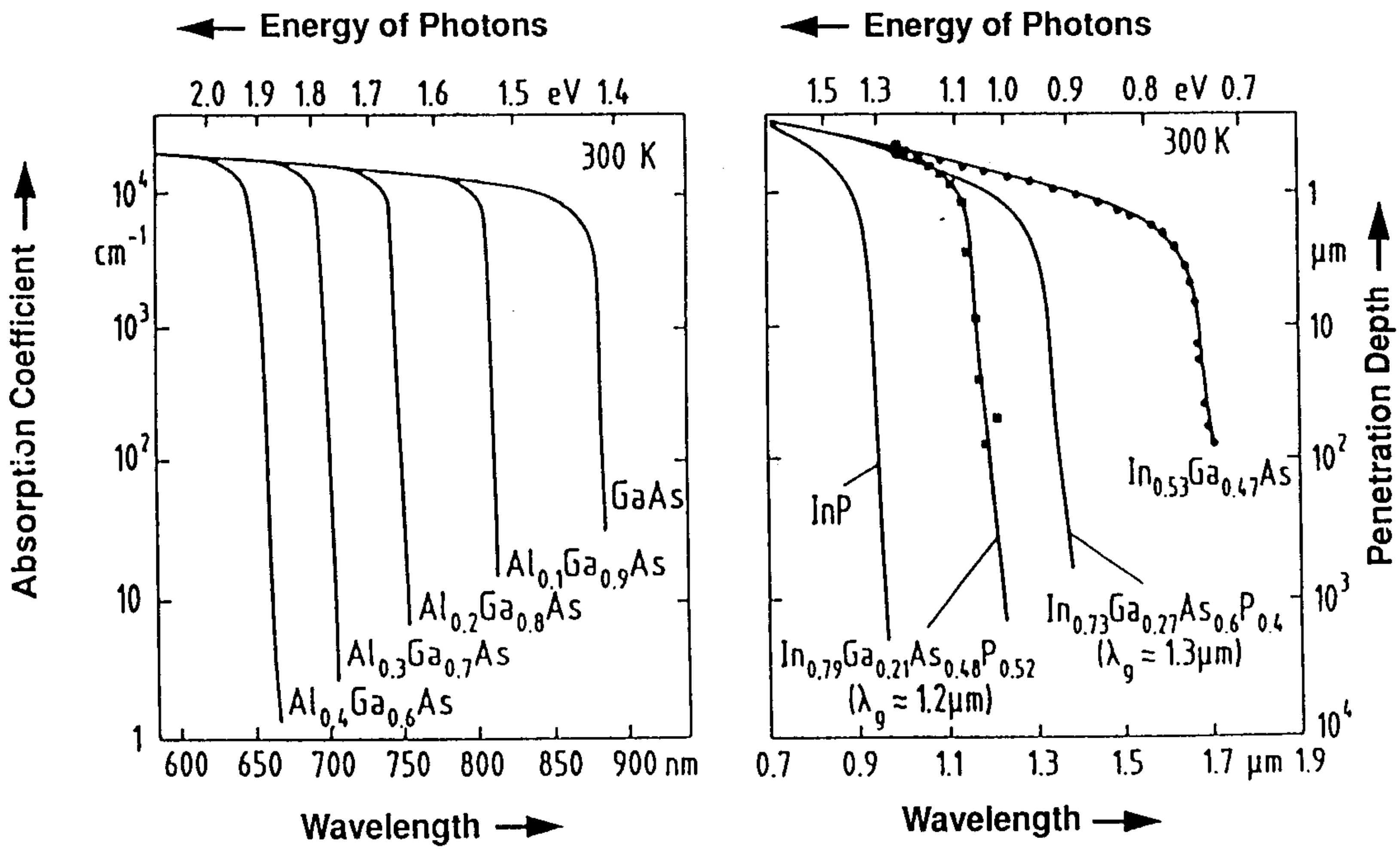

30

Eidgenössische Technische Hochschule Zürich

OPTICAL LOSSES DUE TO FREE CARRIER ABSORPTION AT INFRARED WAVELENGTHS IN SEMICONDUCTORS

At infrared wavelengths, beyond the absorption edge of band-to-band carrier excitation, semiconductors can still show appreciable absorption due to free-carrier excitation within the valence and conduction bands. Free carrier absorption coefficients

$$\alpha \sim N\lambda^{p}$$

increase propertional with carrier densities N and overproportional p ~ 2 to 3 with wavelength λ.

Free-Carrier Absorption of n-GaAs and n-InP at Infrared Wavelengths

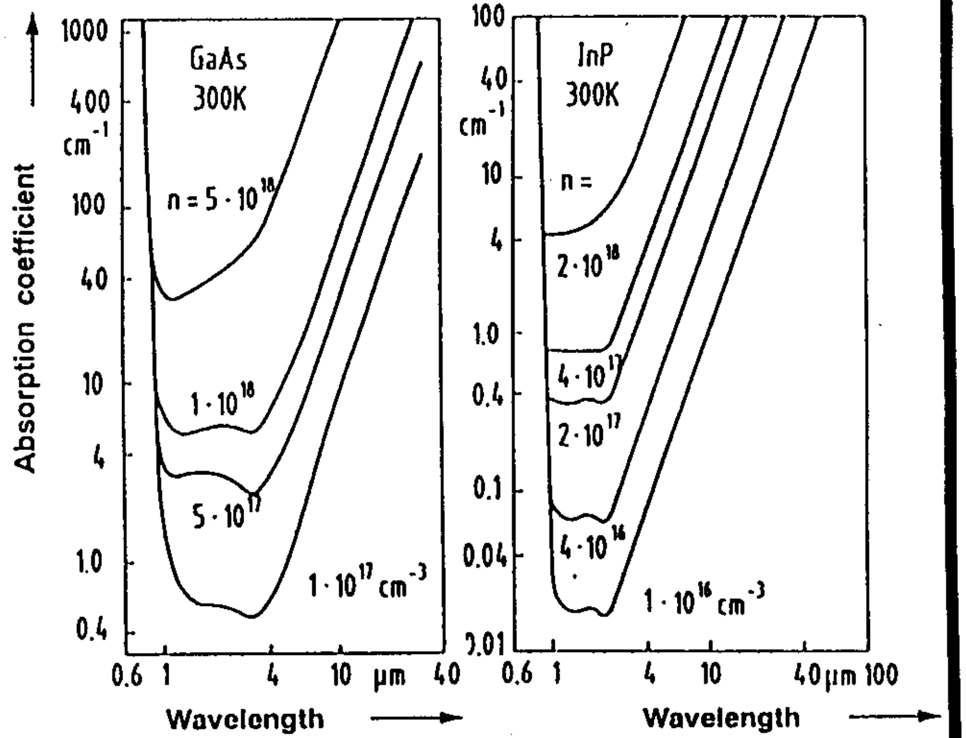

ELECTRO-OPTIC EFFECTS IN CUBIC CRYSTALS

- Linear electrooptic effect leads to crystal orientation and polarization sensitive modulators and switches.
- Quadratic electrooptic effect is isotropic and leads to crystal orientation and polarization insensitive switches and modulators.
- Carrier density related refractive index changes are isotropic leading to polarisation independent modulators and switches.
- Electric field induced refractive effects are usually isotropic, leading to polarization insensitive modulators and switches.

LINEAR AND QUADRATIC ELECTRO-OPTIC EFFECTS

Origin: Nonlinear polarizability of lattice electrons

- **Linear Electro-Optic Effect**
  Pockels Effect

  Observed in non-centrosymmetric crystals and materials

$$\Delta n_{TE} = \frac{n^3}{2} r_{41} E_{el}$$

(100) InP or GaAs, E_{el}//[100]
anisotropic

- **Quadratic Electro-Optic Effect**

  Kerr Effect

  Small effect, present in all materials

$$\Delta n = \frac{n^3}{2} R_{Kerr} E_{el}$$

Primarly exploited in LiNbO3 space switches.
Also used in GaAs and InP switches and modulators.

LINEAR AND QUADRATIC ELECTRO-OPTIC EFFECTS IN III-V COMPOUND SEMICONDUCTORS

Electro-optic effects due to bound valence band electrons

$$\Delta n = \frac{n_0^3}{2}\left(\pm r E_{el} + R \cdot E_{el}^2\right)$$

Δn = Refractive index change induced by electric fields

E_{el} = Electric field

n_0 = Refractive index of material at wavelength of operation

r = Linear electrooptic coefficient (Pockels-effect), depends on crystal class, direction of electrical and optical fields and polarization

R = Quadratic electrooptic coefficient (Kerr-effect), isotropic for $\bar{4}3m$ crystals and polarization insensitive

GaAs: $r_{41} = -1.5 \cdot 10^{-10} \frac{cm}{V}$ at 1.3 µm

InP: $r_{41} = -1.4 \cdot 10^{-12} \frac{cm}{V}$ at 1.5 µm

Eidgenössische Technische Hochschule Zürich

LINEAR ELECTROOPTIC PROPERTIES OF CRYSTAL CLASS $\bar{4}3m$ III-V COMPOUND SEMICONDUCTORS

(001)-Crystal and Wafer Orientation

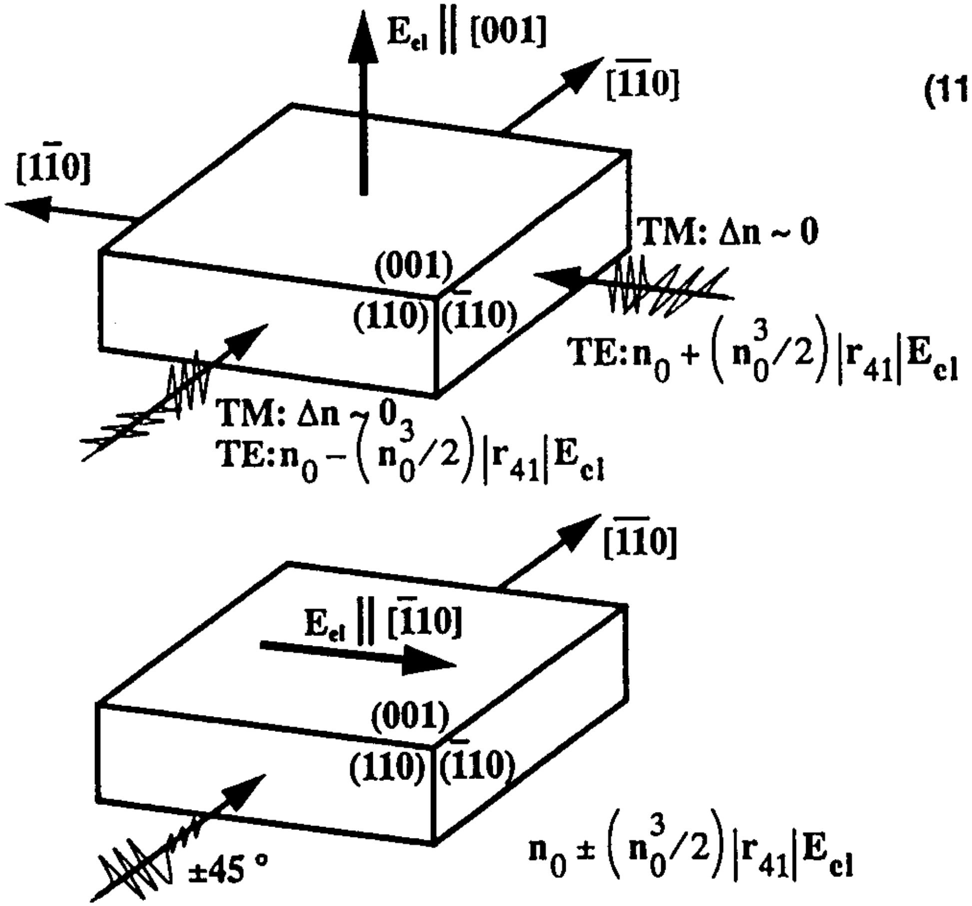

(111)-Crystal and Wafer Orientation

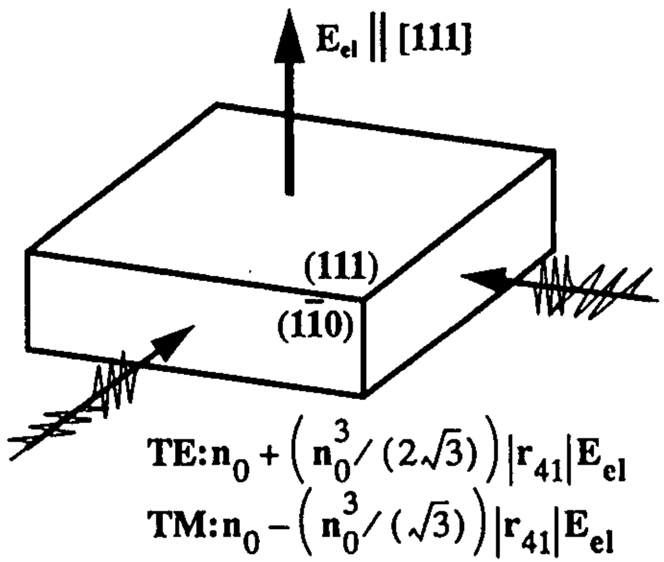

35

Electro-optic Devices

the electro-optic effects in crystals—the effect of an applied electric field on the propagation of electromagnetic radiation can be used to build light modulators, spectral tunable filters, electro-optic filters, beam deflectors, and so on. The use of electro-optic modulation offers the possibility of manipulating a laser beam or controlling the signal radiation at high speeds (up to the multigigahertz region), since no mechanical moving parts are involved.

ELECTRO-OPTIC LIGHT MODULATORS

The basic principle involved is that the application of the electric field changes the index ellipsoid. Consequently, the index of refraction of the crystal for the linearly polarized normal modes depends on the field strength. It is clear that the phase shift of these normal modes passing through the crystal depends on the index of refraction. After traversing a distance L in the crystal, the change in phase shift due to the applied electric field is typically

$$\Delta\phi = \frac{\pi}{\lambda} n^3 r E L,$$

where λ is the wavelength of the light, n is the index of refraction, r is the relevant electro-optic coefficient, and E is the applied electric field.

Electro-Optic Modulators Using Cubic Crystals. Cubic crystals are optically isotropic (no birefringence) and therefore offer a wide field of view in many optical systems. Here we consider the case of crystals of the $\bar{4}3m$ symmetry (zinc blende) group. Examples of this group are InAs, CuCl, GaAs, and CdTe.

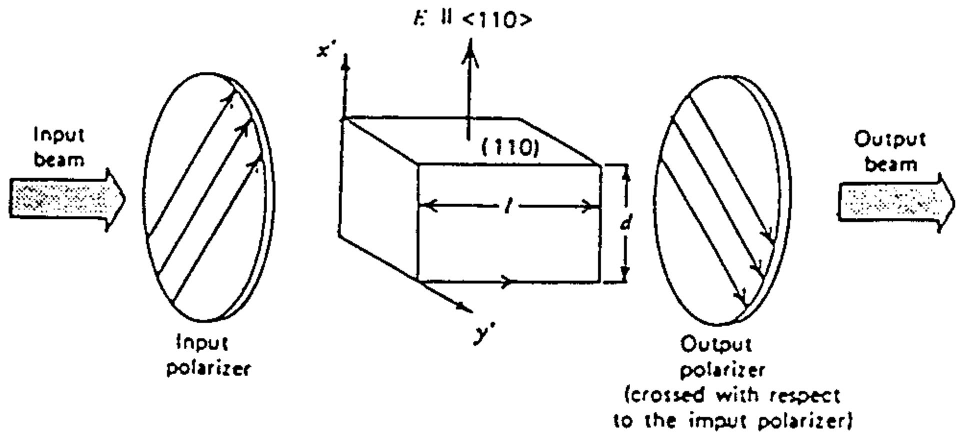

A transverse electro-optic modulator using a zinc-blende-type ($\bar{4}3m$) crystal with E parallel to a cube diagonal ($\langle 110 \rangle$ direction).

The phase retardation is

$$\Gamma = \frac{2\pi}{\lambda} n^3 r_{41} \left(\frac{L}{d}\right) V.$$

The half-wave voltage is

$$V_\pi = \frac{d}{L} \cdot \frac{\lambda}{2n^3 r_{41}}.$$

ELECTRO-OPTIC WAVEGUIDE DEVICES

Guided Wave Phase Modulator

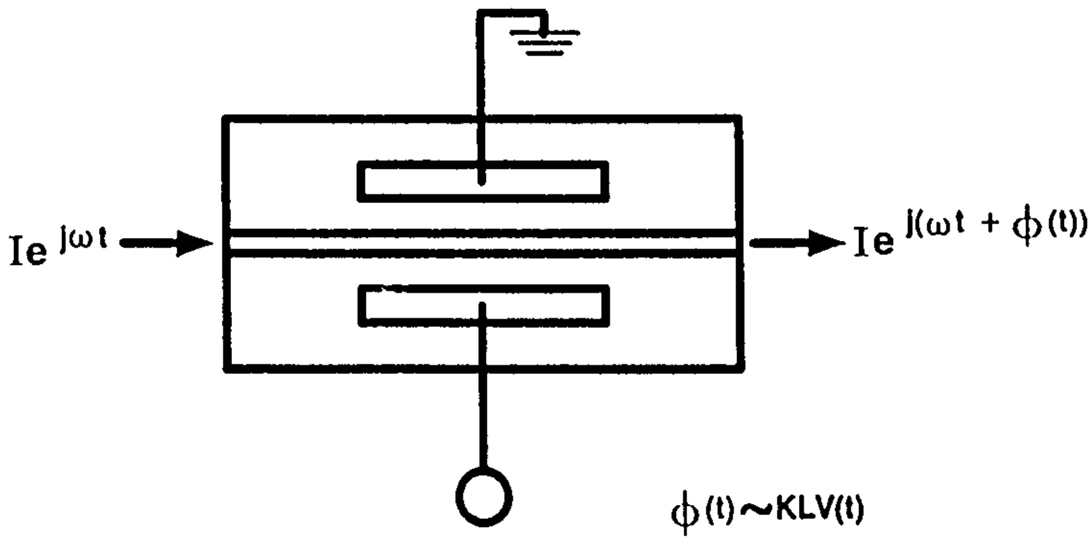

Phase shift: $\phi(t) \doteq \pi \frac{V(t)}{V\pi}; V_\pi$ = Voltage for π – phase shift

ELECTRO-OPTIC EFFECTS IN DIELECTRICS AND SEMICONDUCTORS

Phase shift of optical field after travelling through a length z in optical medium:

$$\Delta\phi = \left(\frac{2\pi}{\lambda}n + i\frac{\alpha}{2}\right)z$$

λ = optical wavelength in vacuum

n = effective refractive index encountered by optical wave

α = optical absorption coefficient

$\Delta\phi$ = associated with static or low frequency electric field:

$\Delta n\ (E_{el})$: field induced changes in refractive index:
electrorefraction
linear (Pockels) and quadratic (Kerr) electrooptic effects

$\Delta\alpha\ (E_{el})$: field induced changes in optical absorption:
electroabsorption
field induced electrorefraction and absorption in bulk material (Franz-Keldysh-effect) and in mutiple-quantum wells (Quantum Confined Stark Effect)

$\Delta\phi$: associated with changes in carrier density:

$\Delta n\ (\Delta N)$: carrier induced refractive index changes

$\alpha\ (\Delta N)$: carrier induced absorption
band filling effect
band-shrinkage effect
free carrier plasma effects

$\Delta\phi$: associated with optical fields E_{opt}
$\Delta n\ (E_{opt})$; $\Delta\alpha\ (E_{opt})$

In order to enhance the magnitude of the opticaly nonlinear effects, resonant enhancements close to optical transitions are exploited.

38

CARRIER INDUCED ELECTRO-OPTIC EFFECTS

- **Plasma Effect**

  Free electrons and holes lower the refractive index in comparison to intrinsic material

  $-\Delta n \sim N_{el}, P_{el}$
  isotropic

- **Bandfilling Effect**

  Filled bands shift absorption edge to higher energies and lower the refractive index at long wavelengths

  $-\Delta n \sim N_{el}, P_{el}$
  isotropic

- **Bandgap Renormalization**

  Bandgap shrinks due to Coulomb interactions at very high carrier densities

  $\Delta n \sim N_{el}, P_{el}$
  isotropic

FREE-CARRIER EFFECTS

Free carriers lower the refractive index and cause absorption beyond the band-edge at infrared wavelengths.

Refractive index change due to free-carrier plasma:

$$\Delta n = -\frac{e^2\lambda^2}{8\pi^2 c^2 \varepsilon_0 n_0}\left(\frac{N}{m_e} + \frac{P}{m_h}\right)$$

λ = Photon wavelength

n_0 = Refractive index of material in absence of free carriers

N, P = Densities of electrons and holes

m_e, m_h = Effective masses of electrons and holes

c = Speed of light

ε_0 = Dielectric Permittivity of vacuum

n-GaAs:

$\Delta n = -3.3 \cdot 10^{-21}\ \mathrm{cm}^3 \cdot N(\mathrm{cm}^{-3})$ at $\lambda = 1.3\ \mu m$

n-InGaAsP/InP-Quarternaries:

$\Delta n \cong -4.3 \cdot 10^{-21}\ \mathrm{cm}^3\ \ N(\mathrm{cm}^{-3})$ at $\lambda = 1.52\ \mu m$

ETH Eidgenössische Technische Hochschule Zürich

FREE CARRIERS ABSORPTION AND REFRACTIVE INDEX CHANGES

Refractive Index Control by Free Carriers

$$\Delta n = -\frac{e^2}{8\pi^2 \varepsilon_0 c^2} \cdot \frac{N\lambda^2}{n \cdot m_{eff}}$$

Δn = refractive index change

n = refractive index

λ = optical wavelength

N = free carrier density

m_{eff} = effective mass of free carriers

ε_0 = dielectric permittivity of vacuum

c = speed of light in vacuum

Free Carrier Absorption

$$\alpha = \frac{e^2}{4\pi^2 \varepsilon_0 c^3} \cdot \frac{N\lambda^2}{n \cdot m_{eff}^2 \mu}$$

μ = mobility of free carriers

ETH Eidgenössische Technische Hochschule Zürich

CARRIER INDUCED REFRACTIVE INDEX CHANGES DUE TO BAND-FILLING (BURSTEIN-MOSS EFFECT)

Depending on the carrier densities and the proximity of the light to the absorption edge, pronounced changes in refractive index are observed in semiconductors, especially in cases with low effective electron or hole mosses. This effect is due to the filling of the conduction or valence bands at high carrier densities. As the Fermi level moves into the conduction or value band at high carrier densities, the photons have to overcome slightly higher energy barriers to excite electrons from the valence band into empty stacks of the conduction band.

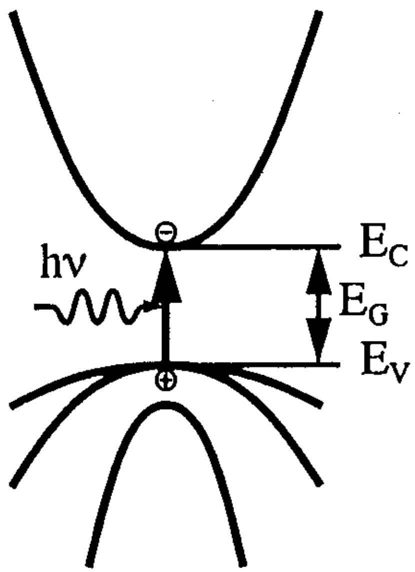

Band-to-band absorption at low carrier densities:

$h\nu \geq E_c - E_v$

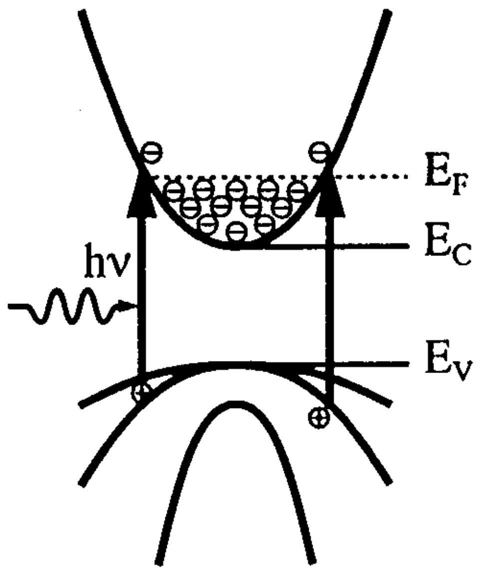

Band-to-band absorption at high carrier densities in highly doped n-type semiconductor. Photons have to overcome higher energy:

$h\nu \geq E_F - E_v$

BAND-FILLING (BURSTEIN-MOSS) EFFECT

Mobile carriers in the conduction and valence band lower the band-to-band absorption and the refractive index for photon energies slightly higher than the bandgap.

In the transparent region, band-filling lowers the refractive index:

$$\Delta n_{BF} = -NB(h\upsilon)$$

Δn_{BF} = Refractive index change in transparent region caused by band-filling

$B(h\nu)$ = Photon energy ($h\nu$) dependent normalized refractive index change (cm^{-3})

N = Carrier density (cm^{-3})

n-$Ga_{1-x}Al_xAs$:

$$B(h\nu) = \frac{S_{BF}}{2n_0\left(E_{FB}^2 - (h\nu)^2\right)}$$

S_{BF} = $1.4 \cdot 10^{-20} (eV)^2\, cm^3$

n_0 = Refractive index

E_{BF} = $(1.45 + 1.247\,x)$ (eV)

At high carrier densities ($>10^{17}\ cm^{-3}$) band shrinkage effects counteract band-filling.

Eidgenössische Technische Hochschule Zürich

CARRIER INDUCED REFRACTIVE INDEX CHANGES DUE TO BAND-FILLING (BURSTEIN-MOSS EFFECT)

Band-filling at high carrier densities leads to a lowering of the optical absorption at photon energies slightly higher than the bandgap.

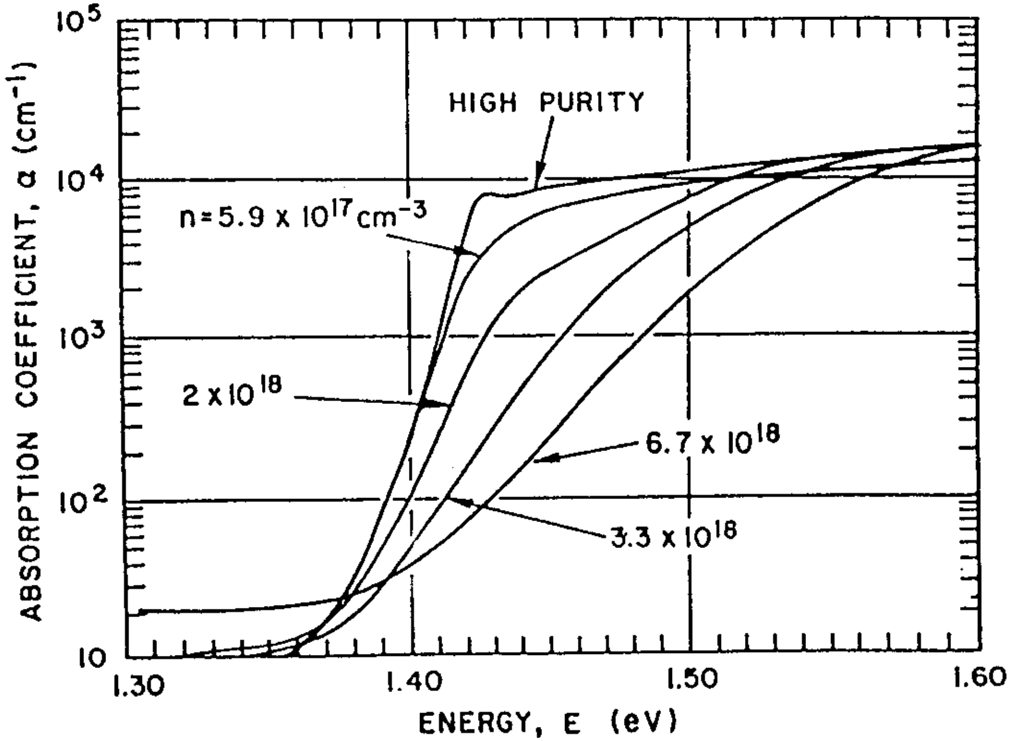

Absorption coefficient of high purity and n-type GaAs of different doping densities in the vicinity of the band-to-band absorption edge.

These band-filling related differences in absorption coefficients are related via the Kramers-Kronig relations to corresponding refractive index changes.

ETH Eidgenössische Technische Hochschule Zürich

REFRACTIVE INDEX CHANCE DUE TO BAND-FILLING IN InP AND InGaAsP QUARTERNARIES

Δn_{BF} = $-N\,B(h\nu)$

Δn_{BF} = Band-filling induced refractive index change in transparent region

N = Carrier density (cm^{-3})

$B(h\nu)$ = Photon energy ($h\nu$) dependent normalized refractive index change

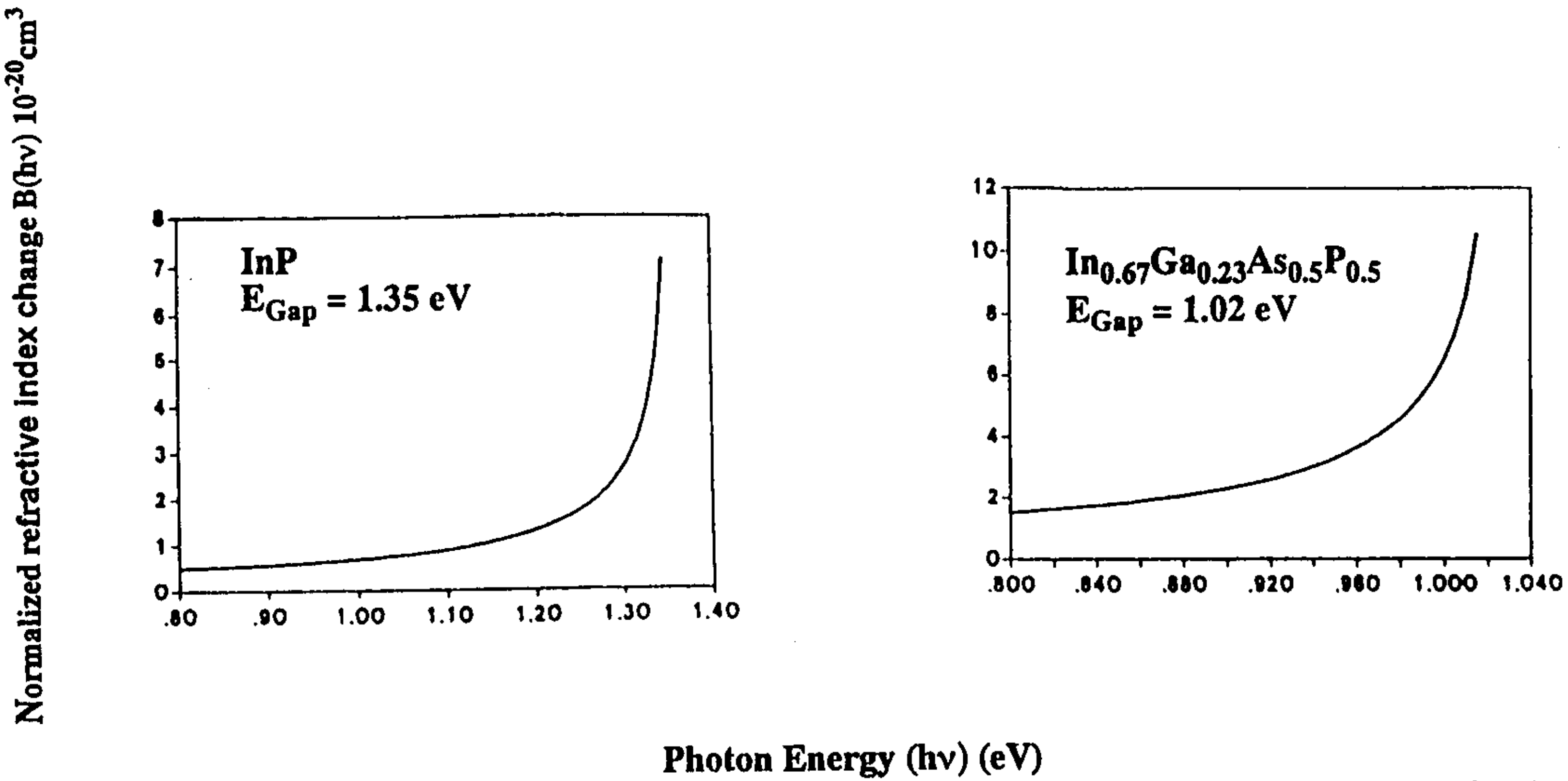

Eidgenössische Technische Hochschule Zürich

ELECTROREFRACTION AND ABSORPTION DUE TO FRANZ-KELDISH EFFECT AT HIGH ELECTRIC FIELDS

In semiconductors, high electric fields induce pronounced increases in optical absorption and large refractive index changes for photon energies corresponding to the transparent region close to the bandedges. These electro absorption and refraction processes are due to photon-assisted tunneling from the valence into the conduction band that becomes possible at high electric fields.

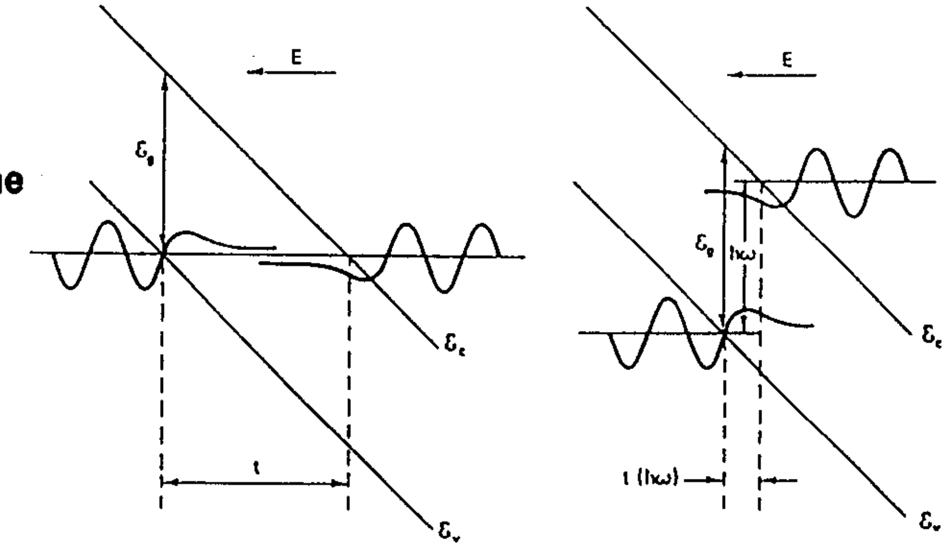

Photon-assisted tunneling from valence (E_V) into conduction band E_c at $h\omega \leq E_G$ exploits overlap of wave functions within narrow tunneling region t at high electric fields E.

FRANZ-KELDYSH ELECTROABSORPTION AT HIGH ELECTRIC FIELDS IN GaAs AND InGaAsP

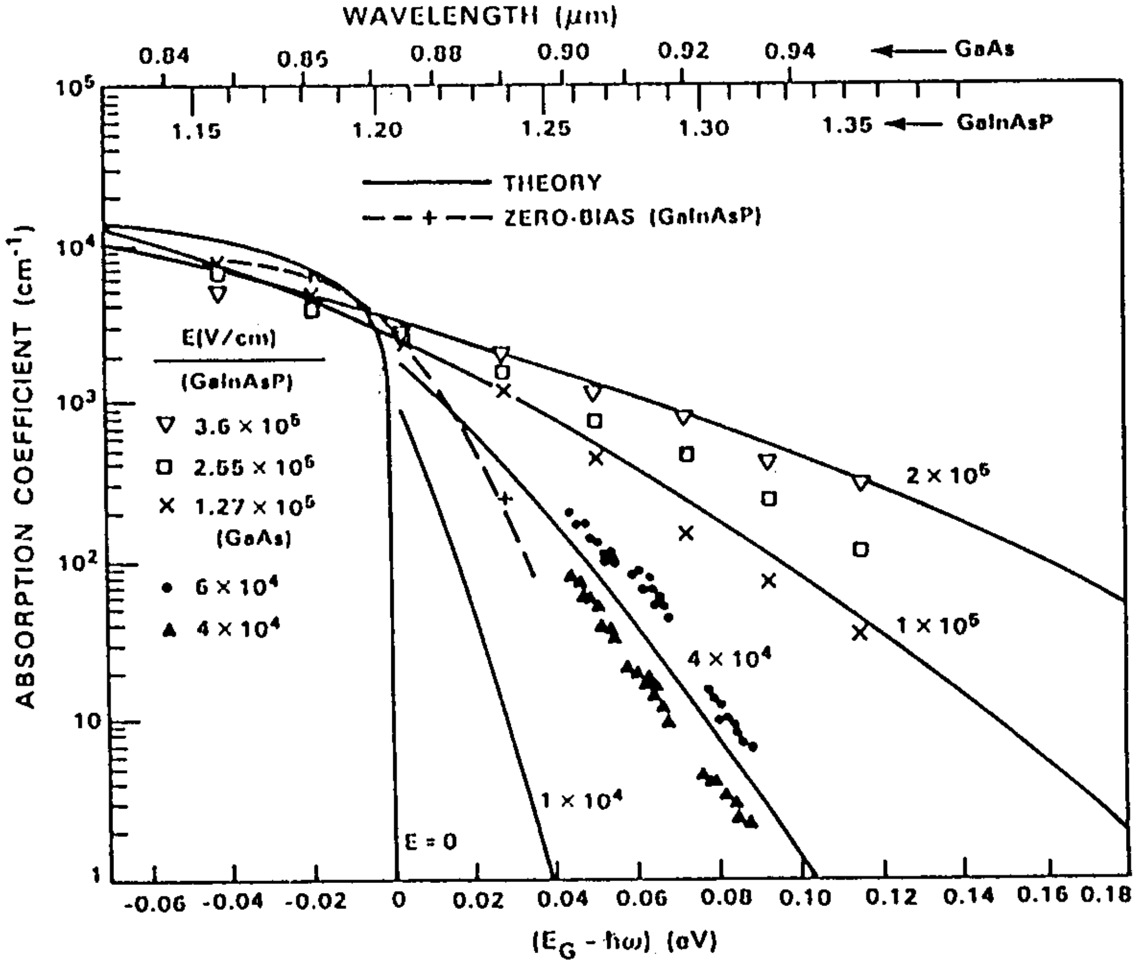

Electric field E(cmV^{-1}) and photon energy (hω) dependence of band-to-band absorption (cm^{-1}) for GaAs and $In_{09}Ga_{01}As_{0.22}P_{0.78}$/InP ($\lambda_{Gap}$ = 1.2 μm).

ETH Eidgenössische Technische Hochschule Zürich

FRANZ-KELDYSH ELECTROREFRACTION AT PHOTON ENERGIES IN THE TRANSPARENT REGION

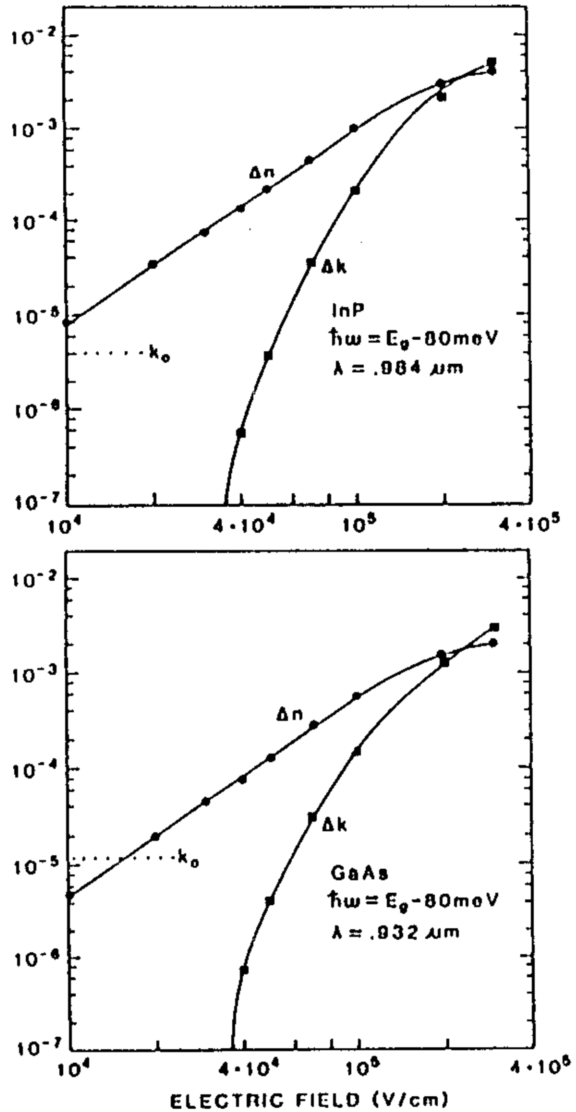

Electrorefraction Δn and Electroabsorption $\Delta\kappa = \frac{\lambda}{4\pi}\Delta\alpha$ of GaAs and InP as a function of electric field for photons with an energy $h\nu = E_{Gap}$ - 80 meV below the bandgap E_G

Electrorefraction is an isotropic polarization independent and more or less quadratic electro-optic effect:

$$\Delta n = \frac{n_0^3}{2} R_{FK} E_{el}^2$$

with the Kerr coefficient approximately obeying the empirical relation

$$R_{FK} = 1.5e^{-15} \exp\left(-\frac{E_G - \hbar\omega}{112\,\text{meV}}\right) \frac{\text{cm}^2}{\text{V}^2}$$

in InP and InGaAsP-Quarternaries

Eidgenössische Technische Hochschule Zürich

Optoelectronic Switches Modulators and Semiconductor Amplifier Gates for High Speed Fiber-Transmission Systems

⇒ Motivation for Optical Switching in High Speed Fiber Optical Communication Networks

⇒ Basic Concepts of Optical Switches, Modulators and Semiconductor Optical Amplifier Gates

⇒ Physical Effects exploited in Waveguide Type Optical Switches, Modulators and Semiconductor Optical Amplifier Gates

➡ **Implementations of High Speed Optical Modulators**

⇒ Implementations of High Speed Waveguide Type Space Switches

⇒ Semiconductor Optical Amplifier Gates and Wavelength Converters

⇒ Summary and Conclusions

ETH Eidgenössische Technische Hochschule Zürich

Guided Wave Mach-Zehnder Interferometric Modulator

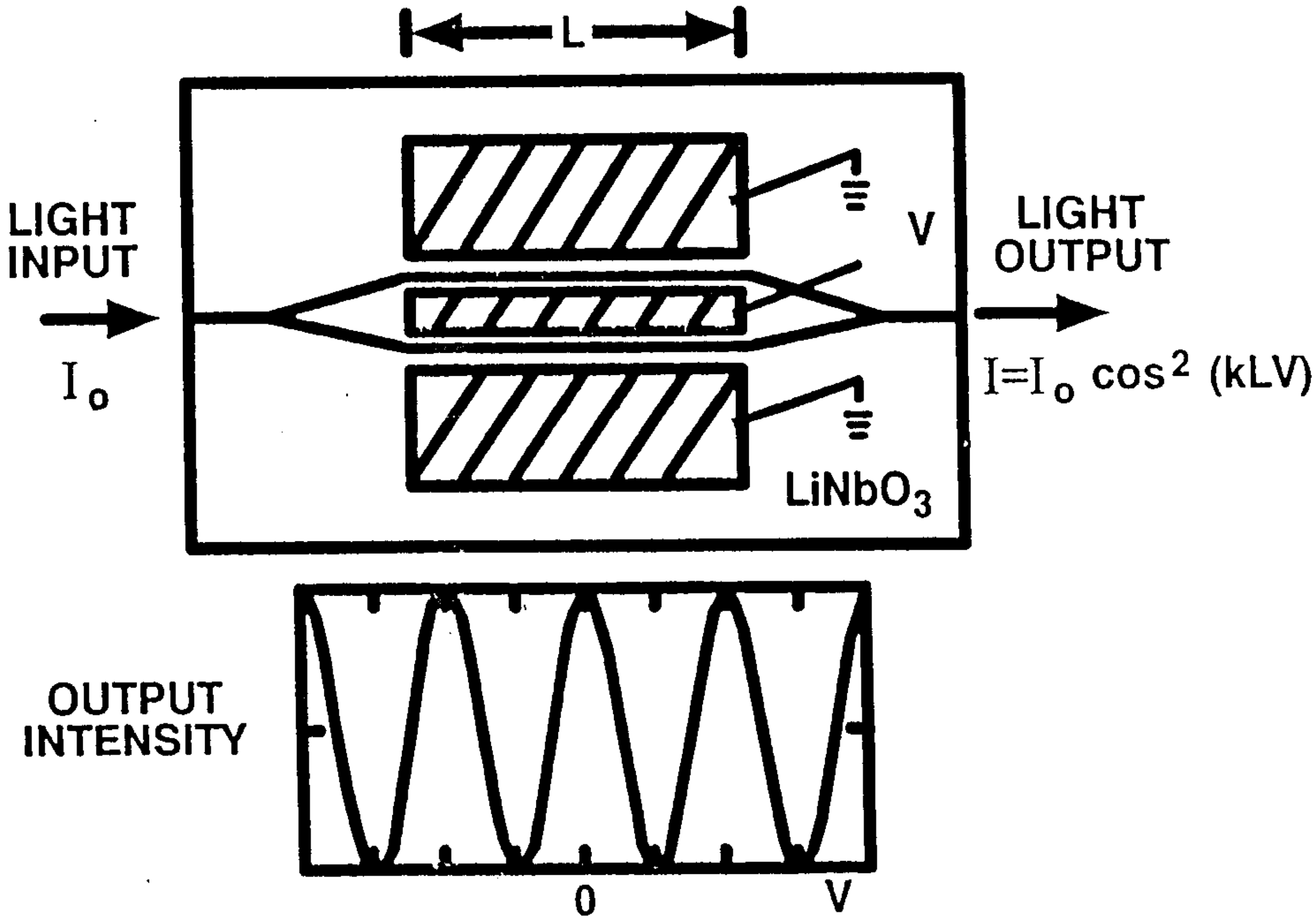

PACKAGED $LiNbO_3$-WAVEGUIDE OPTICAL MODULATOR/SWITCH SHOWING ALIGNMENT TECHNIQUE FOR FIBER COUPLING AND ELECTRICAL BIASING

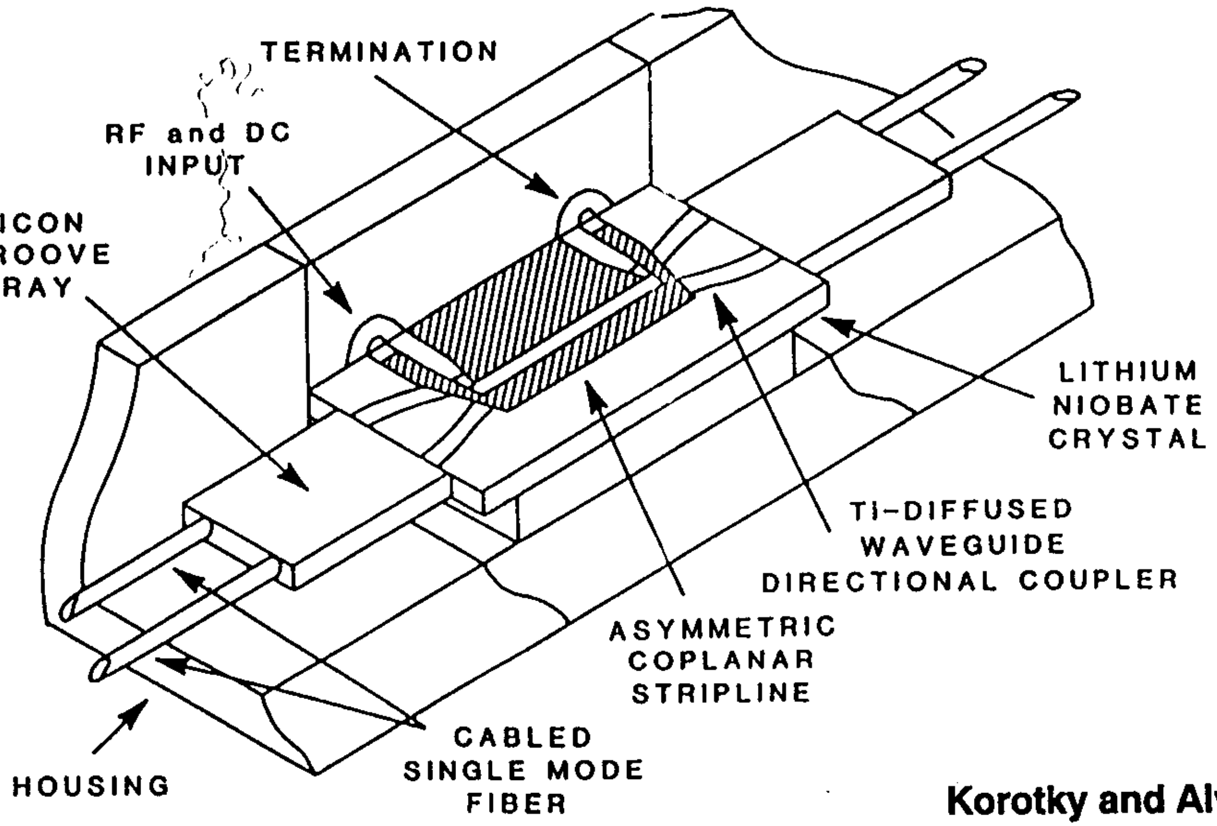

Korotky and Alverness, 1988

ETH Eidgenössische Technische Hochschule Zürich

INTEGRATED OPTIC MACH-ZEHNDER WAVEGUIDE INTERFEROMETER

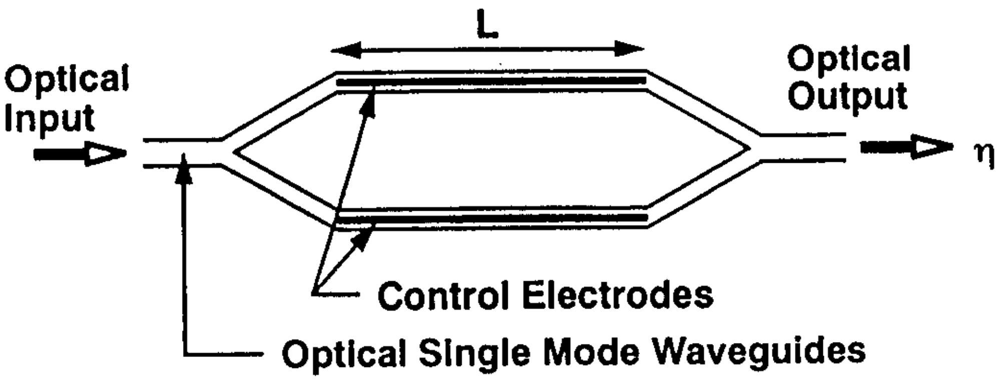

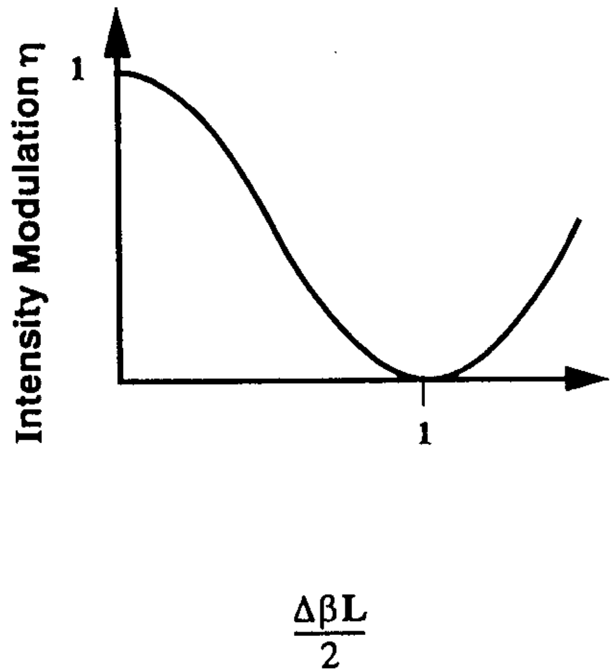

Optical Power Transfer:

$$\eta = \frac{P_{out}}{P_{out,max}} = \cos^2\left(\frac{\Delta\beta L}{2}\right)$$

L Length of phase-shift regions

$\Delta\beta$ = Difference in optical propagation constants between the two waveguide arms

Normalized Phase Shift

Control of Optical Transfer η is by means of electric field or current induced asymmetries in the optical propagation constants of the waveguide arms

Eidgenössische Technische Hochschule Zürich

OPERATIONAL PRINCIPLE OF Y-BRANCH MONOMODE WAVEGUIDE SPLITTER/COMBINER

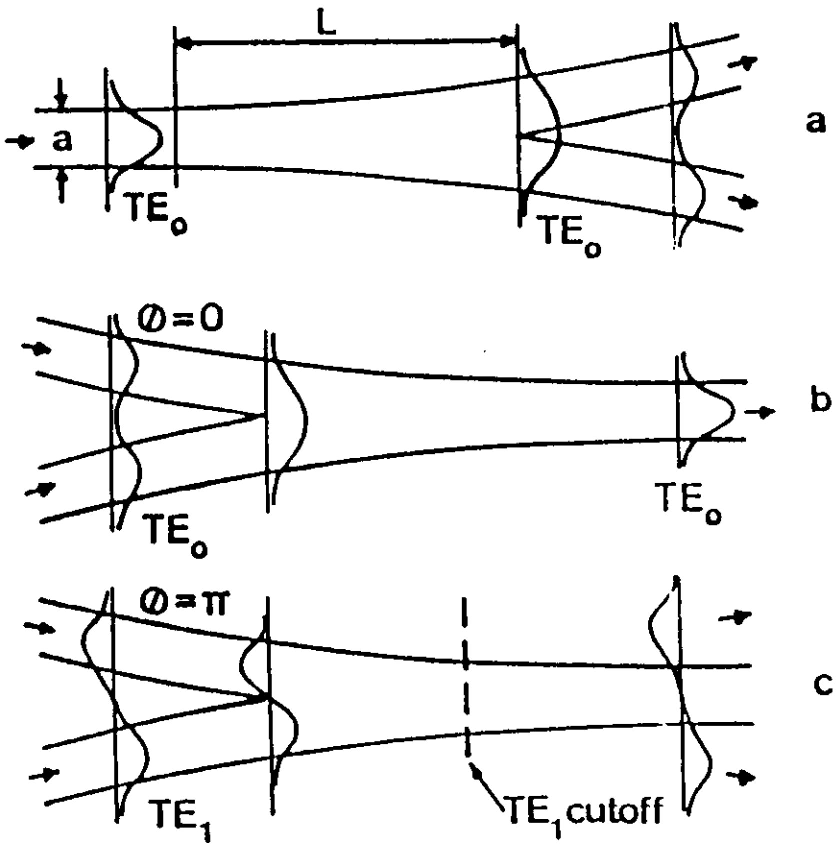

a) TE_0-Mode is split into two TE_0 outputs

b) In-phase combination of two TE_0-Mode inputs in y-coupler leads to TE_0-Mode in output-branch

c) Out-of-phase combination of two TE_0-Mode inputs leads to higher order TE_1-Mode which is not transmitted in output waveguide. The higher order mode is radiated out of the waveguide

Eidgenössische Technische Hochschule Zürich

53

MODELING INTEGRATED OPTICAL COMPONENTS

Mach-Zehnder Interferometer Modulator

A. One State -Througput = 99.8%

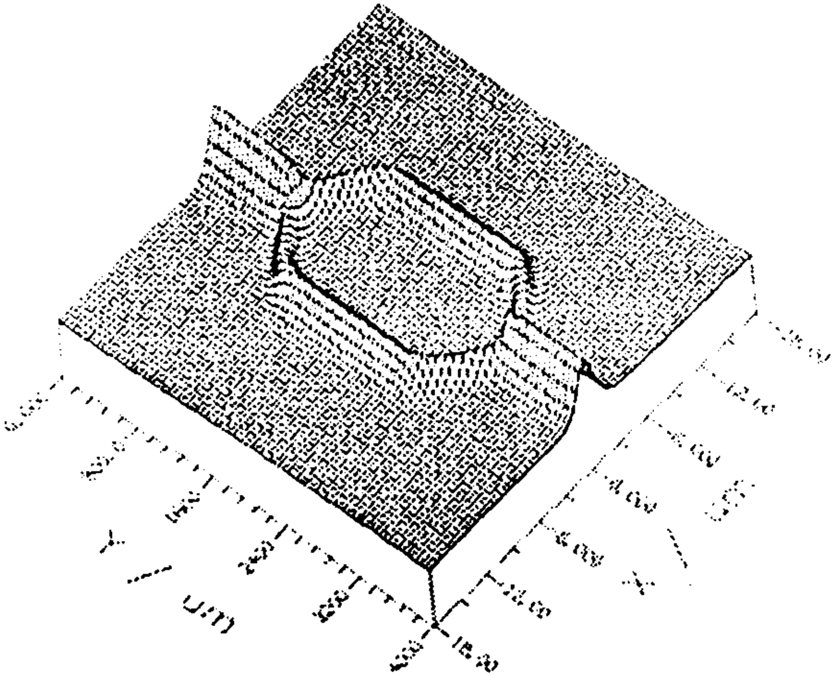

B. Off State - Throughput = 1.8%

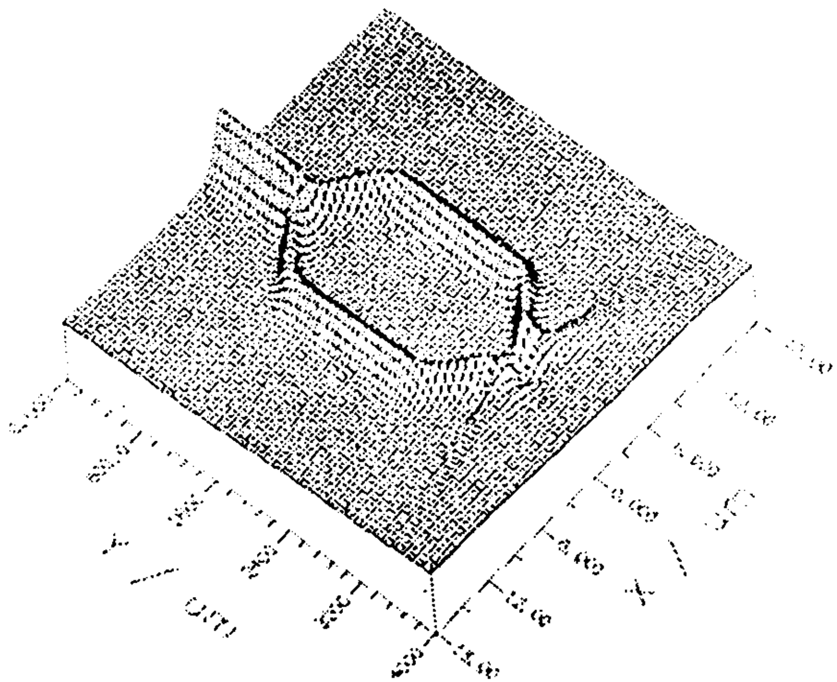

ETH Eidgenössische Technische Hochschule Zürich

MULTIPLE - QUANTUM - WELL ELECTROABSORPTIVE OPTICAL MODULATOR

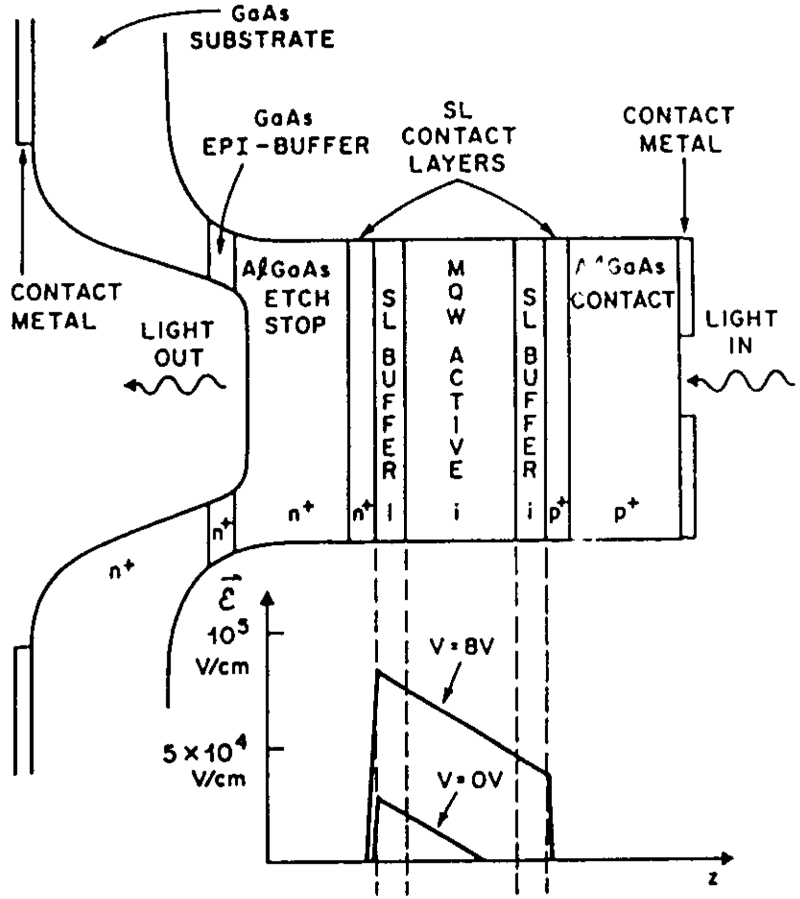

With changes in absorption coefficient of ~ 5000 to 10'000cm^{-1} due to Quantum Stark Effect induced at high reverse bias fields, light transmission is altered significantly in p-i-n MQW layers, already for overall thicknesses of only one micron. (The thickness of the p-i-n region of the drawn MQW-modulator in exaggerated for clarity). Typical diameters are 600 mm and thickness 4 mm for these AlGaAs/GaAs devices.

ETH Eidgenössische Technische Hochschule Zürich

55

trieste1995/10

QUANTUM WELL MODULATORS

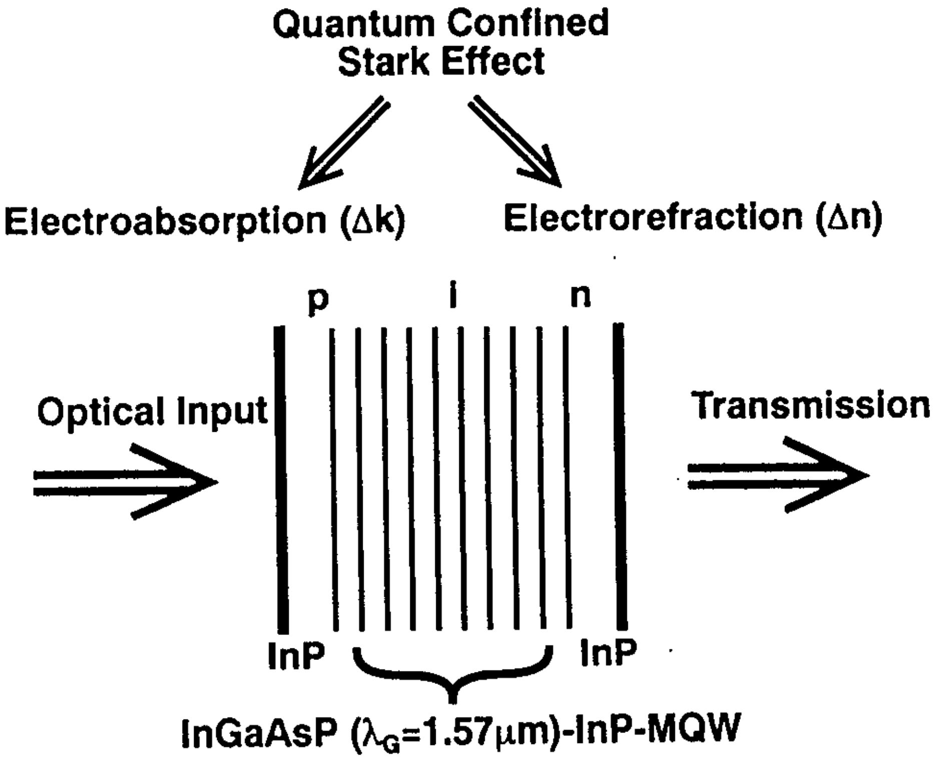

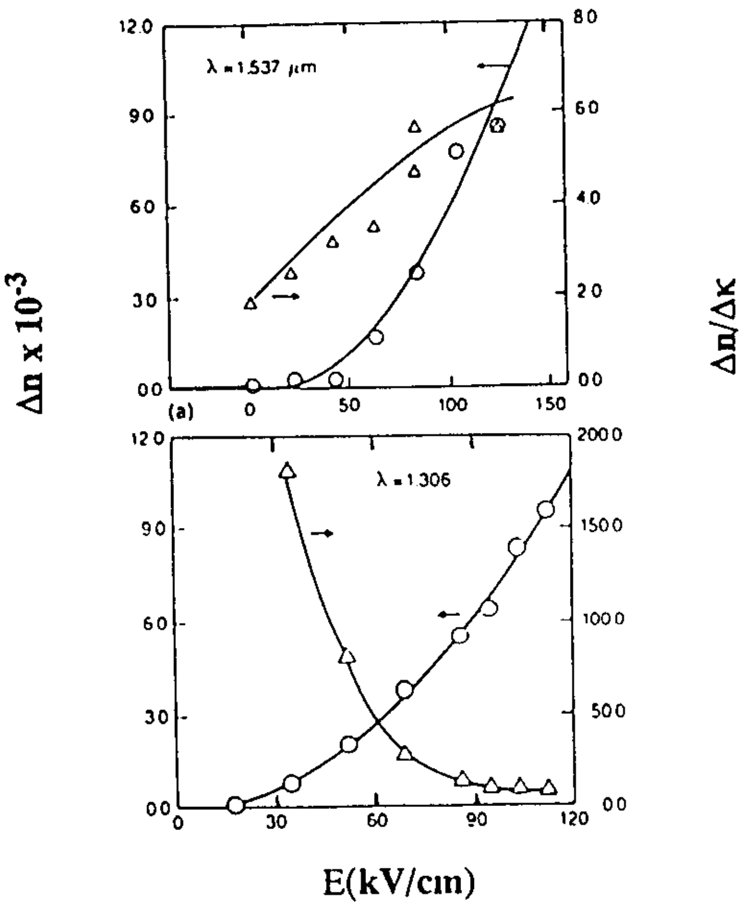

STARK EFFECT

Frequency shifts of optical spectra of atoms under the influence of electric fields

Eidgenössische Technische Hochschule Zürich

ELECTRO-OPTIC EFFECTS AT HIGH ELECTRIC FIELDS

- **Franz-Keldish Effect in Bulk III-V Semiconductors**

  Photon assisted tunneling at high electric fields leads to increased refractive indices at long wavelengths

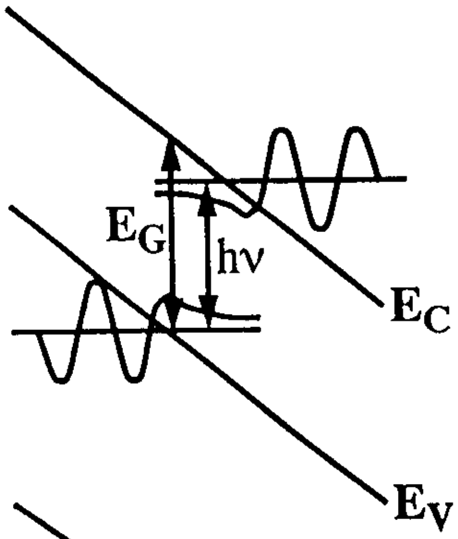

$$\Delta n = \frac{n^3}{2} R \cdot E_{el}^2$$

nearly isotropic in $\bar{4}3$m-crystals

- **Stark Effect in Quantum Well Structures High electric fields lead to pronounced changes in absorption and refractive indices at wavelengths close to band edge**

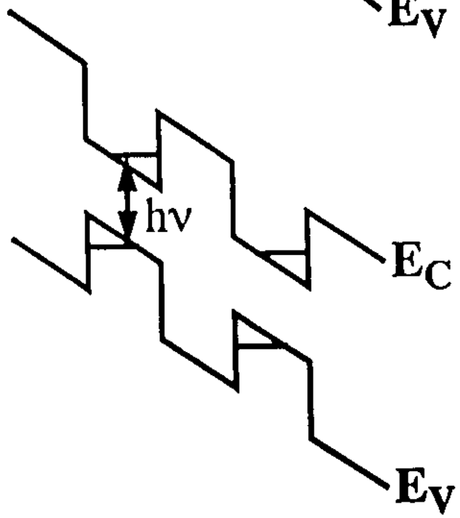

Can be made polarization insensitive by proper choice of quantum wells with tensile and compressive strain

Eidgenössische Technische Hochschule Zürich

HIGH SPEED QUANTUM WELL OPTICAL WAVEGUIDE SWITCHES

Ultracompact Quantum Well Directional Coupler Switch

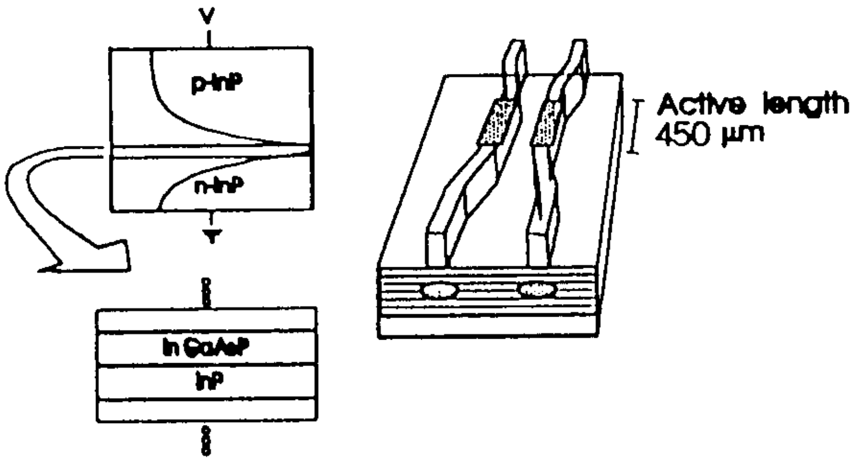

- Based on quantum Stark effect in multi-quantum well p-i-n structures
- Voltage-length product 2V-mm
- Composition of InGaAsP quantum wells allows operation at 1.3 or 1.55 µm wavelength

Polarization Independent Strained Quantum Well Waveguide Switch

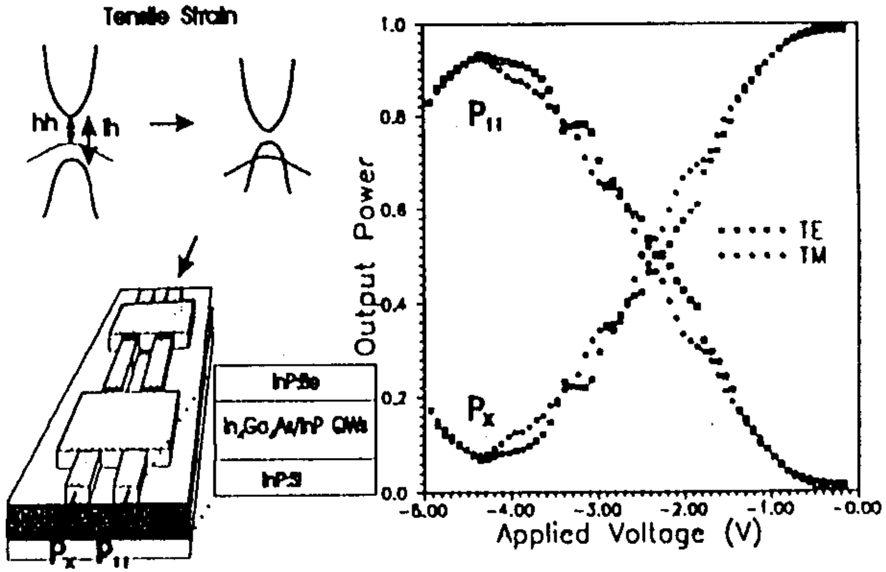

- Bandgap-engineers the quantum well material by means of tensile strain to adjust the relative energy of the light hole (lh) and heavy (hh) valence bands to achieve polarization independence

Jane Zucker

ETH Eidgenössische Technische Hochschule Zürich

DEPLETION LAYER SWITCH WITH QUANTUM WELL ENHANCED REFRACTIVE INDEX CHANGES

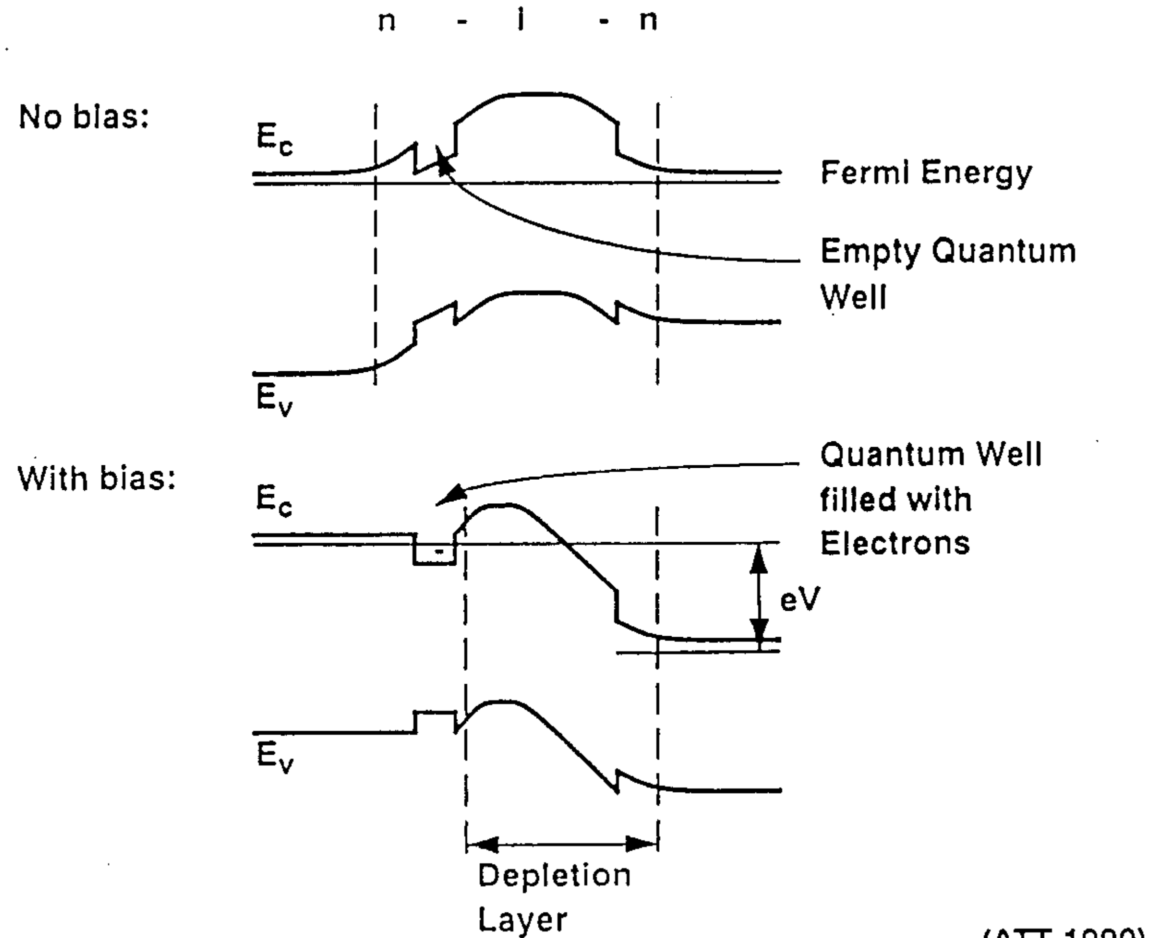

(ATT 1990)

Optoelectronic Switches Modulators and Semiconductor Amplifier Gates for High Speed Fiber-Transmission Systems

- ⇒ Motivation for Optical Switching in High Speed Fiber Optical Communication Networks
- ⇒ Basic Concepts of Optical Switches, Modulators and Semiconductor Optical Amplifier Gates
- ⇒ Physical Effects exploited in Waveguide Type Optical Switches, Modulators and Semiconductor Optical Amplifier Gates
- ⇒ Implementations of High Speed Optical Modulators
- ➡ Implementations of High Speed Waveguide Type Space Switches
- ⇒ Semiconductor Optical Amplifier Gates and Wavelength Converters
- ⇒ Summary and Conclusions

ETH Eidgenössische Technische Hochschule Zürich

SWITCH ARRAYS

Structure:	Crossbar	Lattice	Tree
	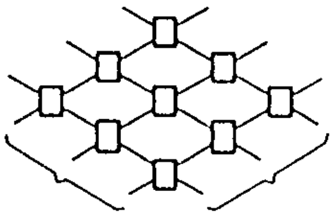	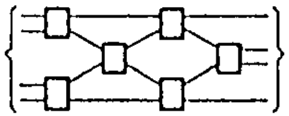	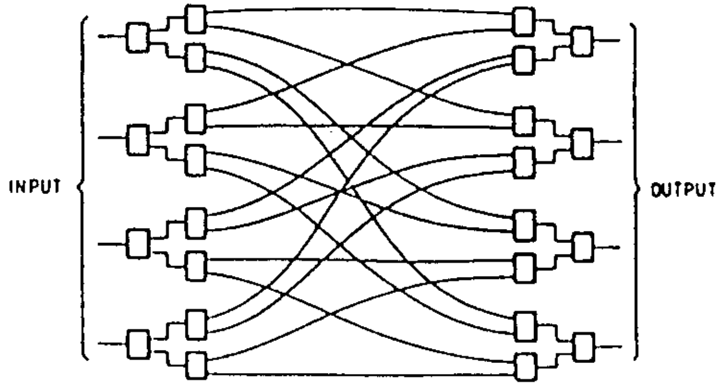
Number of Levels/switches	2 N-1/N^2	N/½N(N-1)	2 ldN/2N(N-1)
Non blocking	Strictly	If rearranging is permitted	Strictly Convenient for broadcasting

OPTOELECTRONIC WAVEGUIDES MODULATORS AND SWITCHING ARRAYS IN InGaAsP/InP AND IN GaAs

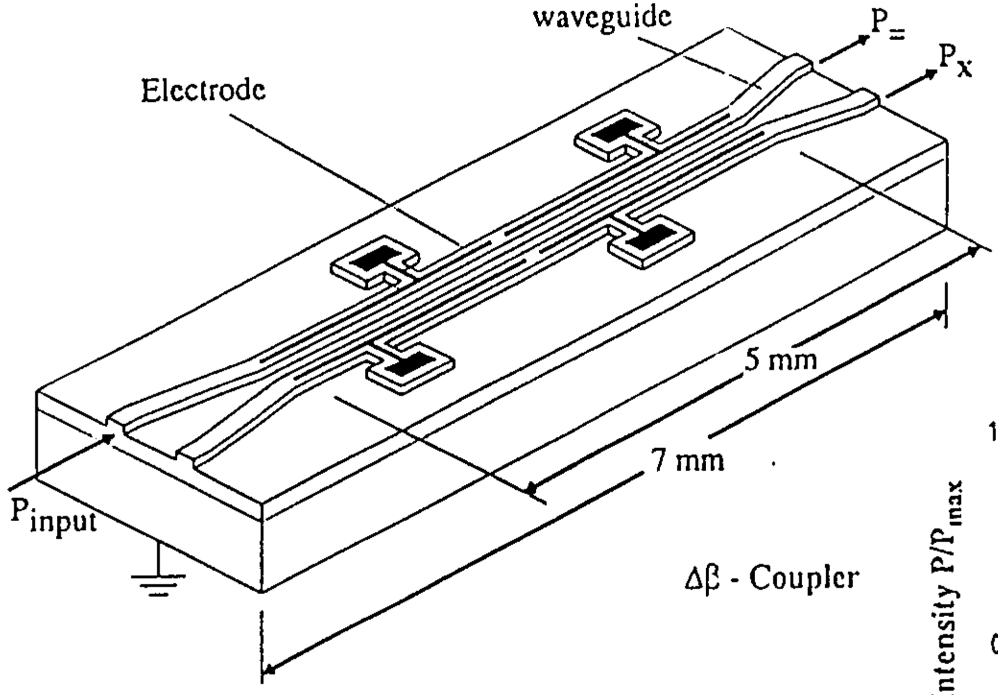

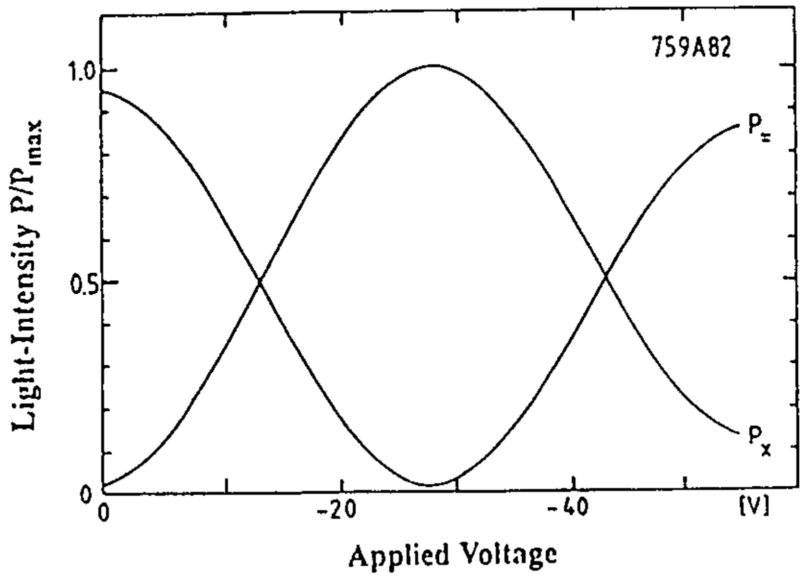

INTEGRATED OPTICAL DIRECTIONAL WAVEGUIDE COUPLER

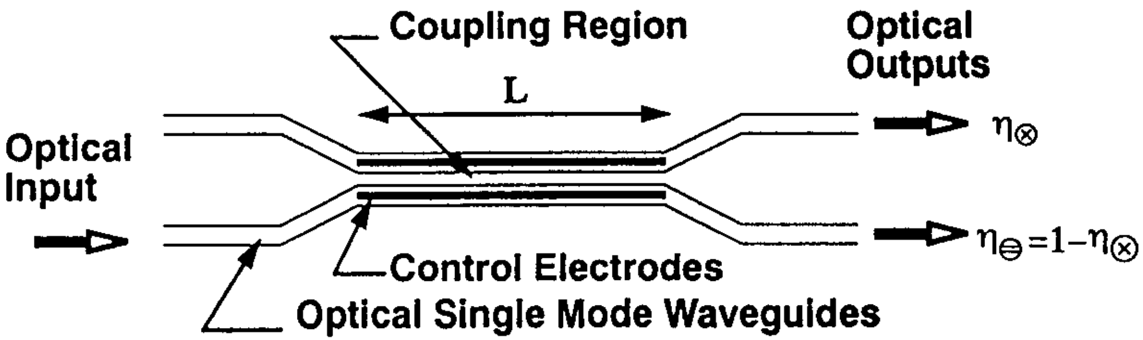

Optical Power Transfer:

$$\eta_{\otimes} = \frac{P_{out\otimes}}{P_{out\otimes} + P_{out\ominus}} = \frac{\text{Output power in crossed output}}{\text{Output power in both outputs}}$$

$$\eta_{\ominus} = 1-\eta_{\otimes} = \frac{P_{out\ominus}}{P_{out\otimes} + P_{out\ominus}}$$

$$\eta_{\otimes} = \frac{1}{\left(1+\left(\frac{\Delta\beta}{2\kappa}\right)^2\right)}\sin^2\left\{\kappa L\left(1+\left(\frac{\Delta\beta}{2\kappa}\right)^2\right)^{1/2}\right\}$$

L = Interaction Length

κ = Coupling per unit length, depends on waveguide parameters, guided wavelength l and inter- waveguide gap

$\Delta\beta$ = $\frac{2\pi}{\lambda}\Delta n$ = difference in propagation constants between the two waveguides

Δn = difference in effective refractive index between the two waveguides

Control of optical Power Transfer $\eta_{\otimes}$ and $\eta_{\ominus}$ is by means of electric fields or currents that alter the refractive index Δn and asymmetries of the waveguide propagation constants, i.e. of $\Delta\beta$

ETH Eidgenössische Technische Hochschule Zürich

OPTICAL TRANSFER FUNCTION OF DIRECTIONAL WAVEGUIDE COUPLER

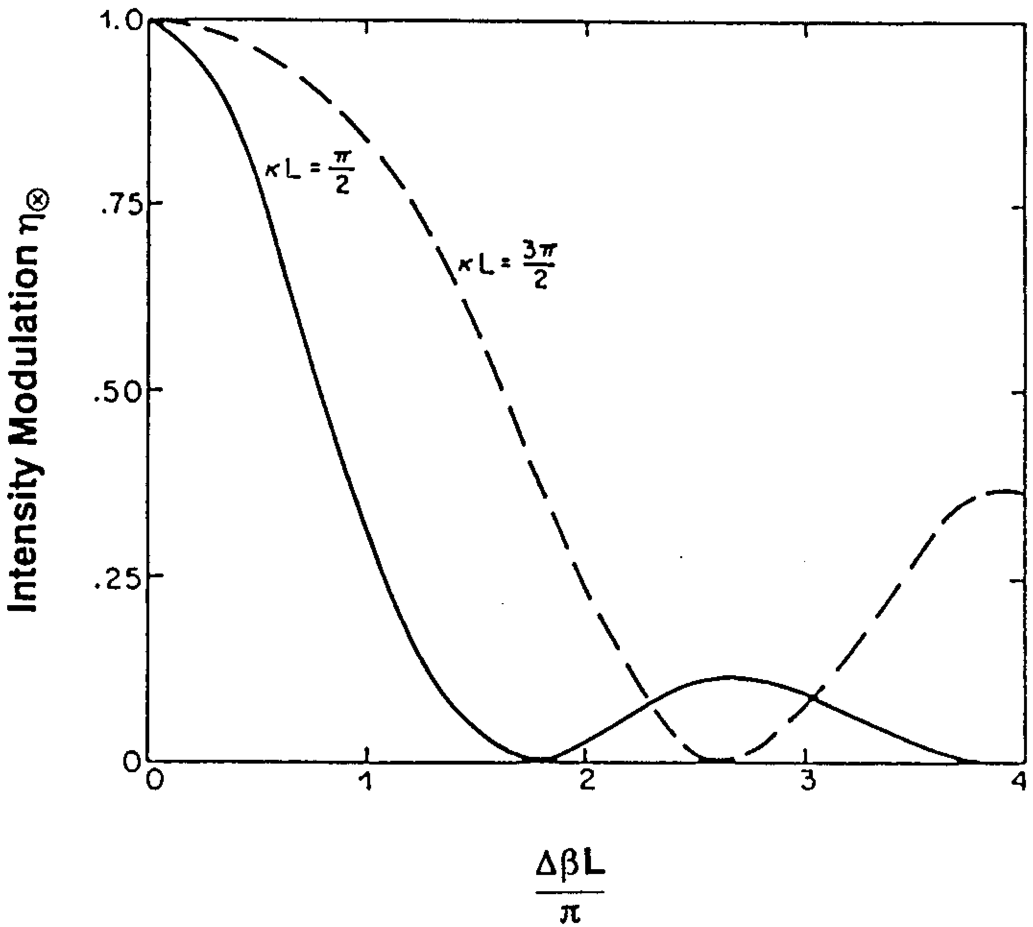

Normalized difference of waveguide propagation constants

For identical waveguides

$$\Delta\beta = 0 \text{ and } \eta_{\otimes} = \sin^2(\kappa L)$$

complete crossover, i.e. $\eta_{\otimes} = 1$ occurs for

$$\frac{\kappa L}{2} = \frac{\pi}{2}; \frac{3\pi}{2}; \text{etc.}$$

The above figure gives the $\Delta\beta$ changes needed for modulation

and complete switching in the case of
$L_c = \frac{\pi}{2\kappa}$ and $\frac{3\pi}{2\kappa}$.

ETH Eidgenössische Technische Hochschule Zürich

DIRECTIONAL COUPLER SWITCH/MODULATOR

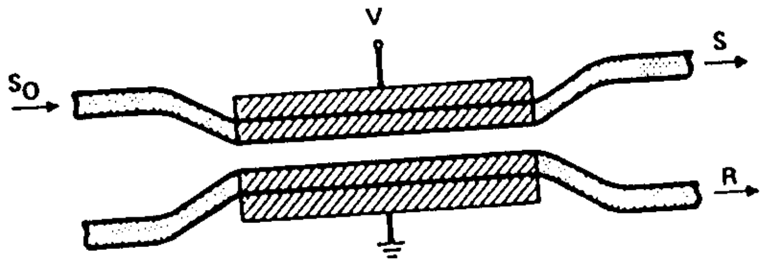

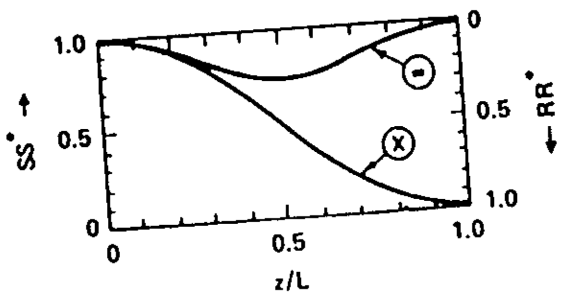

Top view of a directional coupler switch with uniform electrodes placed over the waveguides in the coupling region. Also shown are the intensity distributions along the coupler in crossover ⓧ and straight-through ⊜ switching states.

ETH Eidgenössische Technische Hochschule Zürich

DIRECTIONAL COUPLER SWITCH/MODULATOR

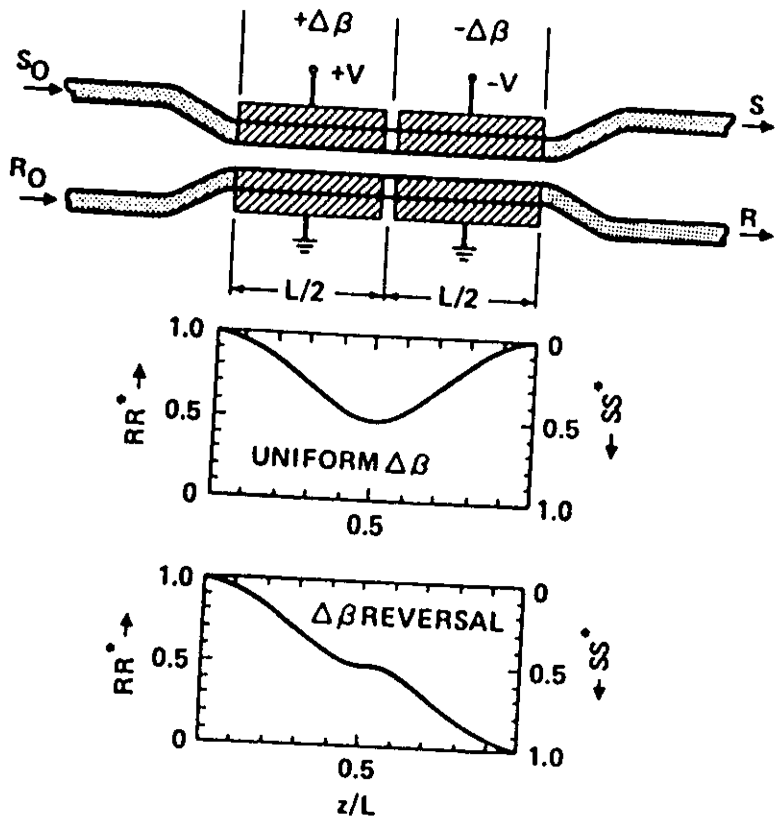

Top view of stepped Δβ reversal switch requiring two sets of electrodes. Also shown are the intensity distributions along the coupler for a coupler of length $L/\ell = \sqrt{2}$.

COUPLED MODE THEORY

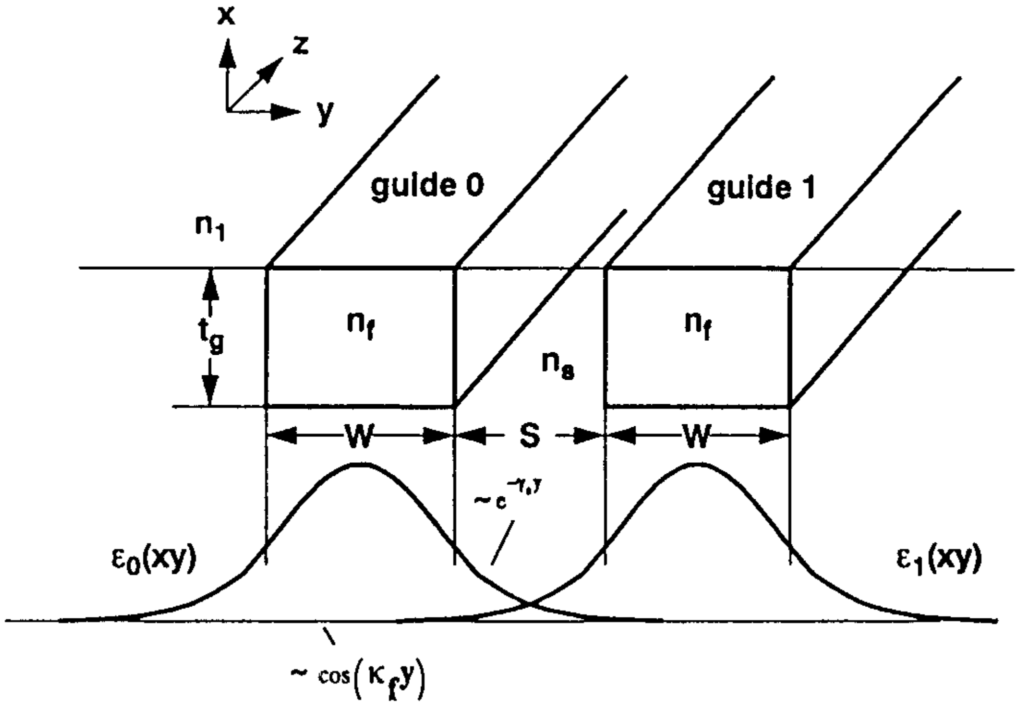

Mode coupling between optical waveguides takes place when they are so closely spaced that the evanescent fields of one guide penetrate the other guide. A wave which propagates initially in one waveguide is then transferred into the other guide. The coupling length L_C for maximum power transfer depends on the spacing and the refractive index and geometry of the waveguides. For long ($L \gg L_C$) coupled waveguides the optical power which propagates shifts forth and back between the two waveguides.

ETH Eidgenössische Technische Hochschule Zürich

8 x 8 DIRECTIONAL COUPLER OPTICAL MATRIX SWITCH

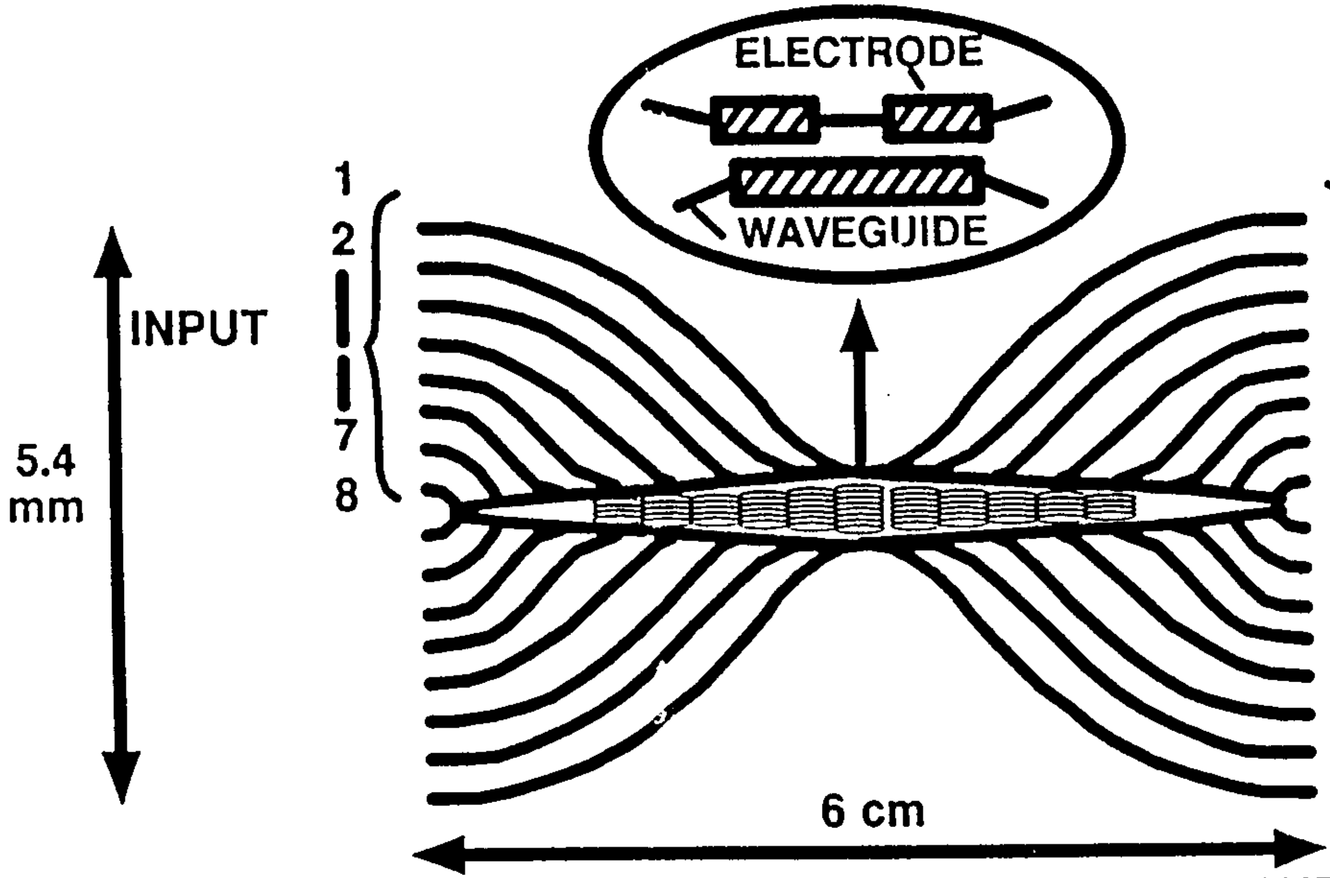

- GRANESTRAND, ET. AL.
ELECT LETT 22, 816 (1986)

8 x 8 SWITCHING MATRIX IN $LiNbO_3$

(Granestrand, Stoltz, Thylén, 1987)

Strictly nonblocking. Each switch element can be individually addressed. Any nonoccupied input port can be connected to any nonoccupied output port, without rearranging previously established signal ports.

Experimental Results:

Overall length	60 mm
Waveguide Spacing	360 μm
Insertion Loss per Switch Element	4.5 ± 0.12 dB
Switching Voltage for x State	26.4 ± 1.6 V
Switching Voltage for = State	18.6 ± 3.6 V
Crosstalk	-30 ± 4 dB

Compact and Polarization Independent Directional Coupler Type Optical Switch on InGaAsP/InP

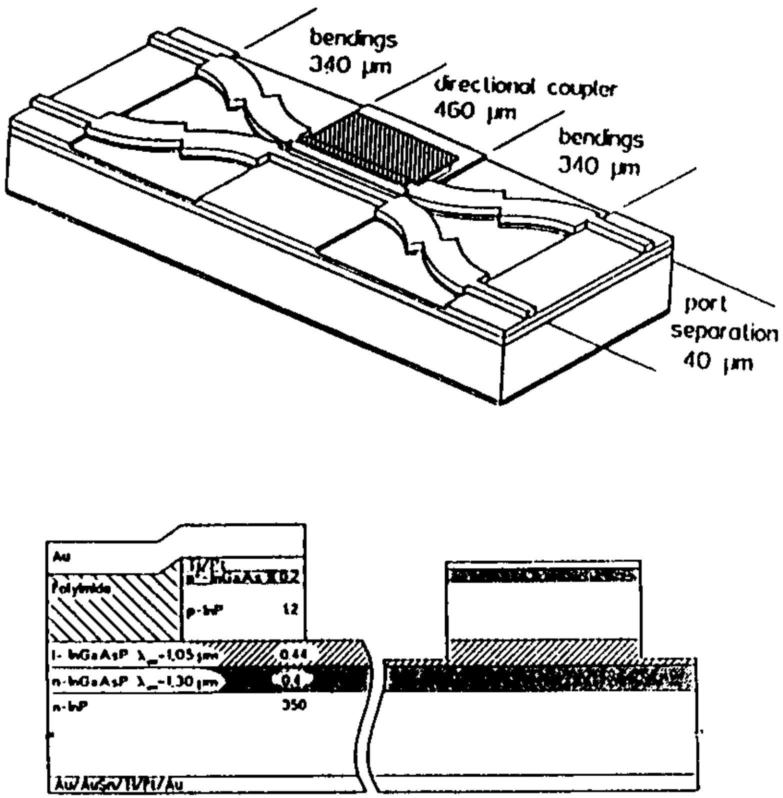

Schematic view and cross section of directional coupler switch

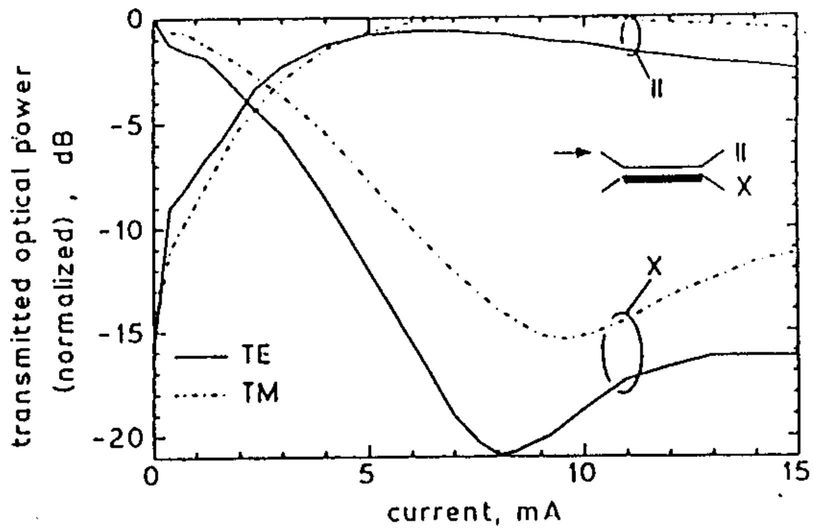

Optical transmission for TE and TM polarization as function of bias current at 1.5 micrometer

Siemens

OPTICAL WAVEGUIDE SWITCH

Experimental Opto-Hybrid Assembly conbining Optical Waveguide switch-chip with Four Optical Inputs and Outputs, Fiber Alignment Fixheres and Electrical Connections

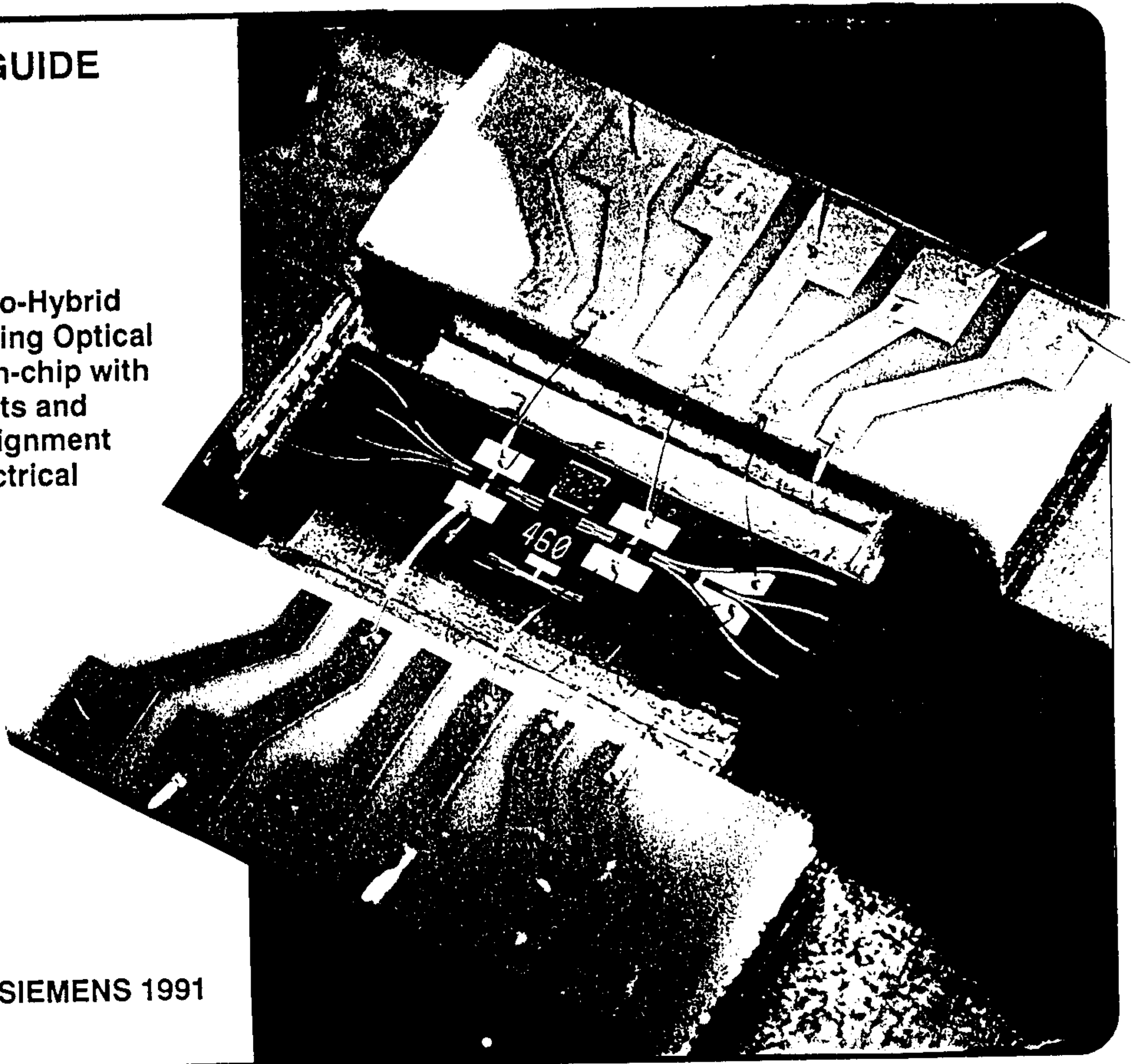

SIEMENS 1991

DIRECTIONAL COUPLER GaAs-AlGaAs WAVEGUIDE ELECTROOPTIC SWITCH MATRICES

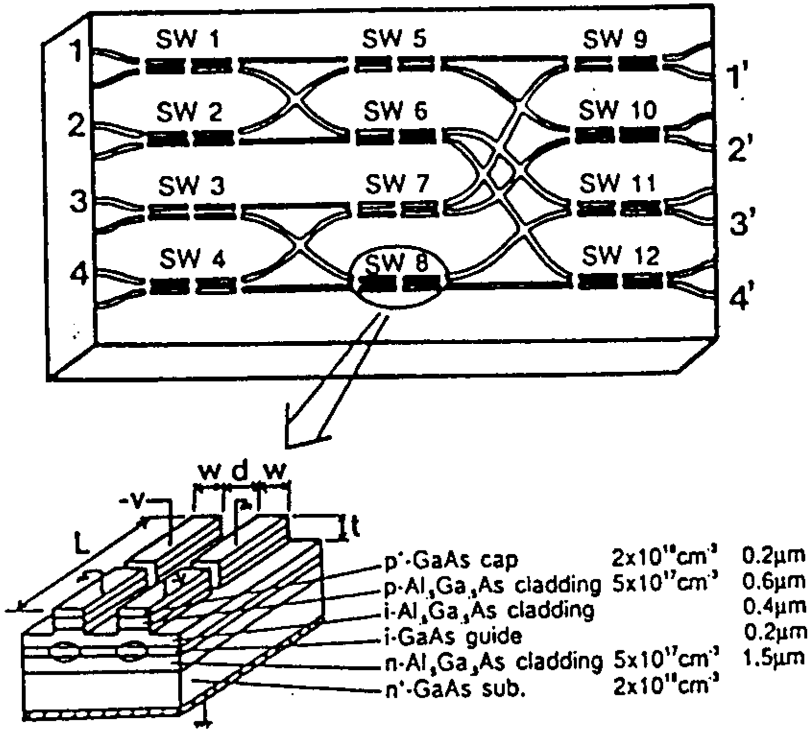

4 x 4 GaAs-AlGaAs Optical matrix Switch using Simplified-Tree Architecture

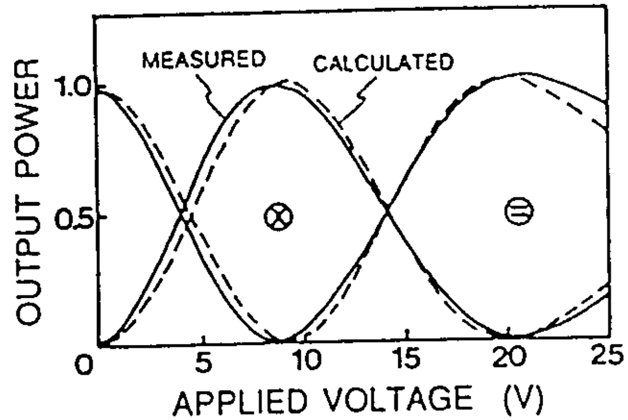

Typical Switching Characteristics

Operational Wavelength 1.3 µm

Switching Response Speed 1 GHz

Propagation Loss 11 dB

Crosstalk -30 dB

NEC

Eidgenössische Technische Hochschule Zürich

suematsu 7

8x8 GaAs/AlGaAs Semiconductor Optical Waveguide Switch Matrix using Electro-Optic Guided-Wave Directional Couplers

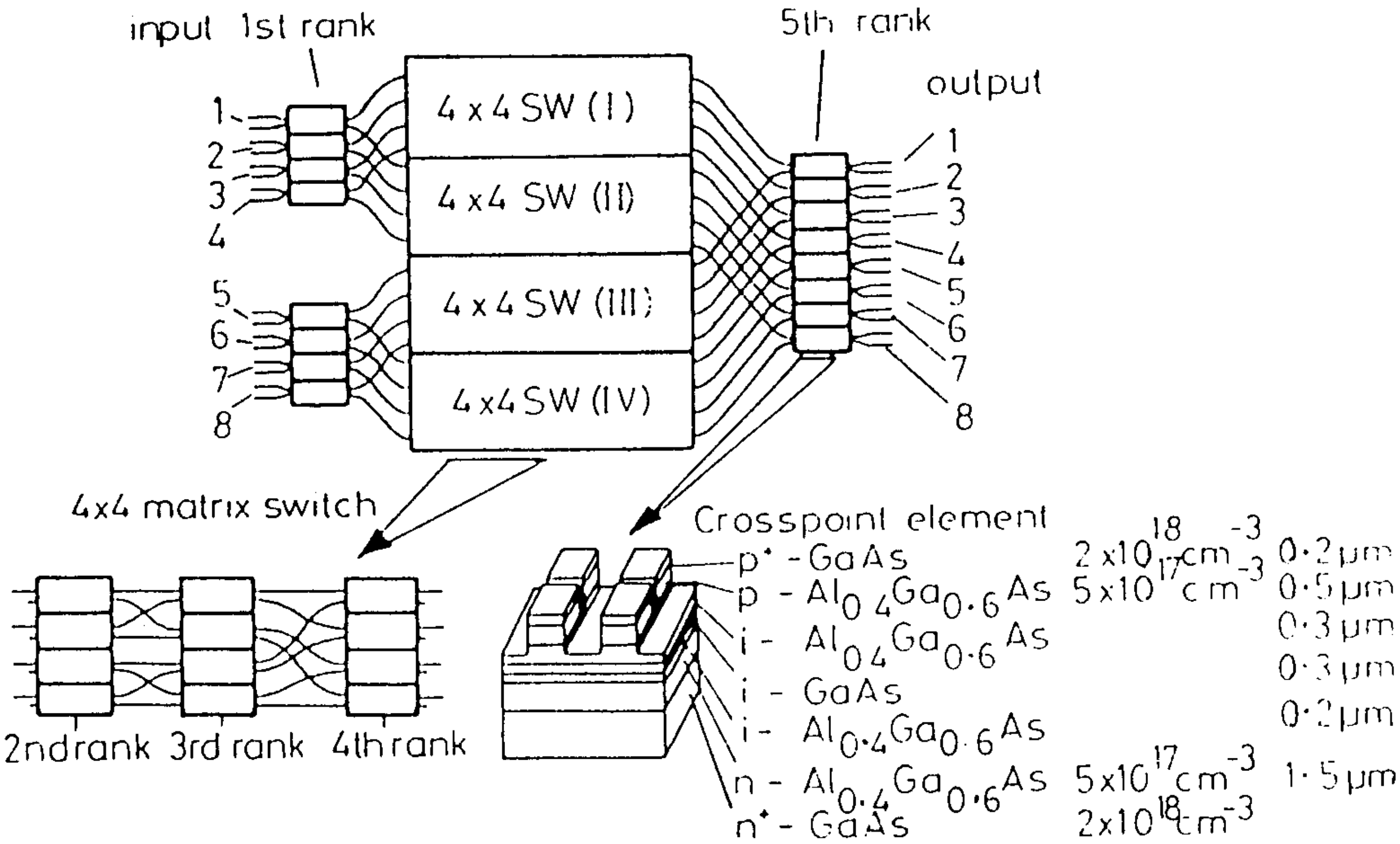

Switching Voltages: **Cross State 12 ± 1 V**
Bar State 25.5 ± 1 V

Crosstalk < -21 dB; **Minimum on-chip loss < 9 dB**

NEC 1992

ETH Eidgenössische Technische Hochschule Zürich

DIGITAL OPTICAL SWITCH

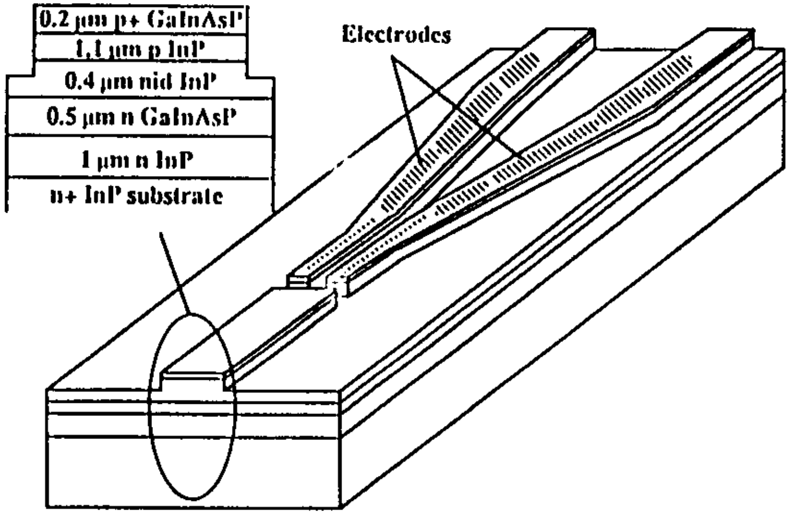

Switch Structure and Epitaxial Layers (GaInAsP: l_{Gap} = 1.3 µm; Waveguide Width: 3 µm; Overall Length: 6 mm)

Eidgenössische Technische Hochschule Zürich

75

DIGITAL OPTICAL SWITCH

Truly digital optical switches maintain their on- and off-states independent of voltage below and above a transition range.

Low drive current InP digital optical TM mode switch

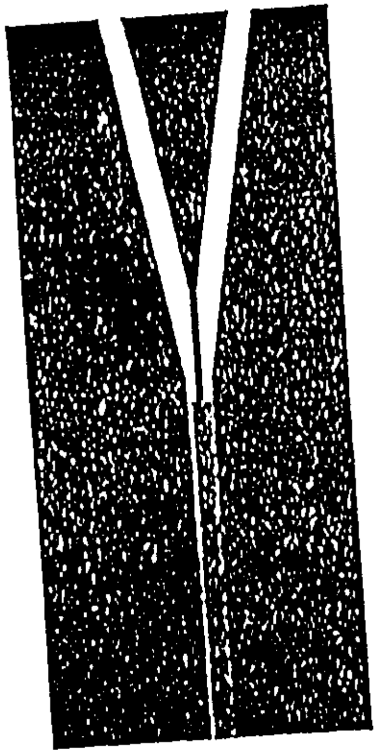

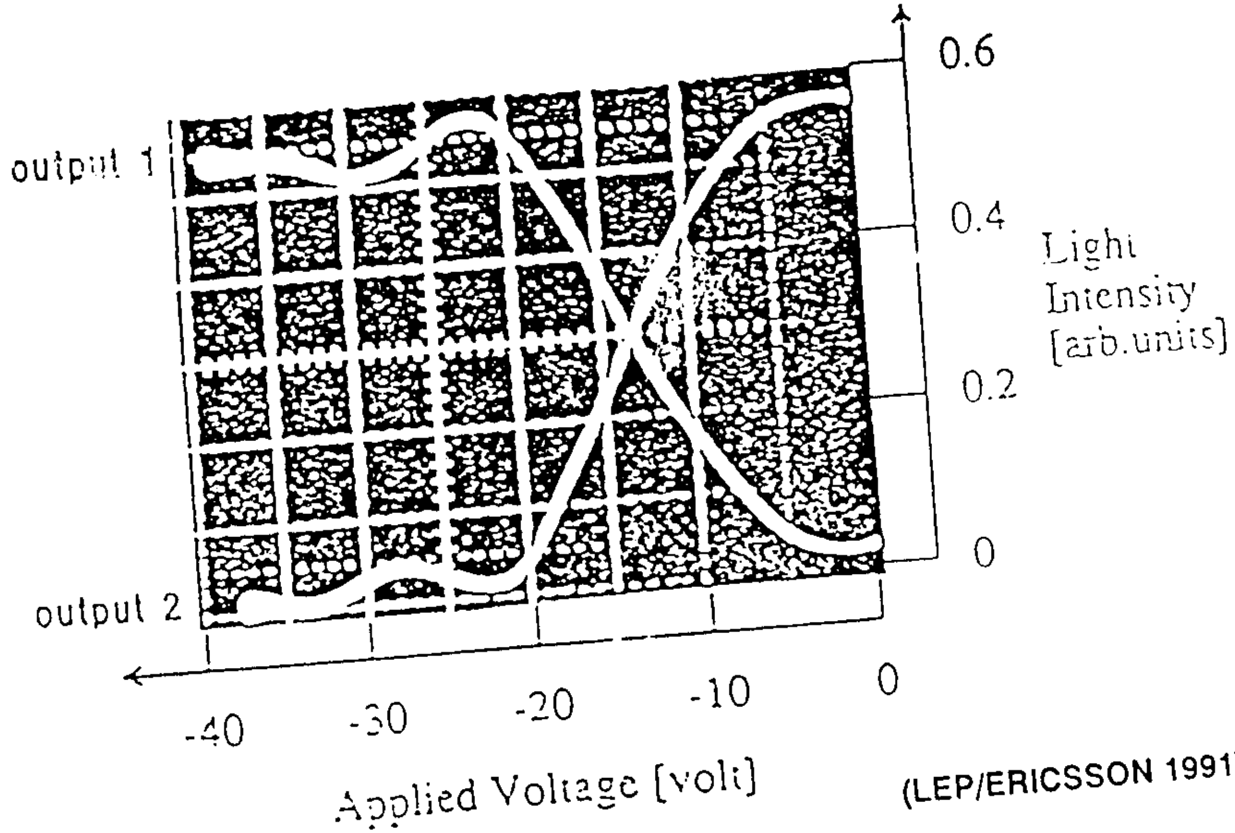

(LEP/ERICSSON 1991)

ETH Eidgenössische Technische Hochschule Zürich

DIGITAL OPTICAL SWITCH

Original Version: LiNbO3 by Silverstein
Current Versions: InP by Ericsson & AAR

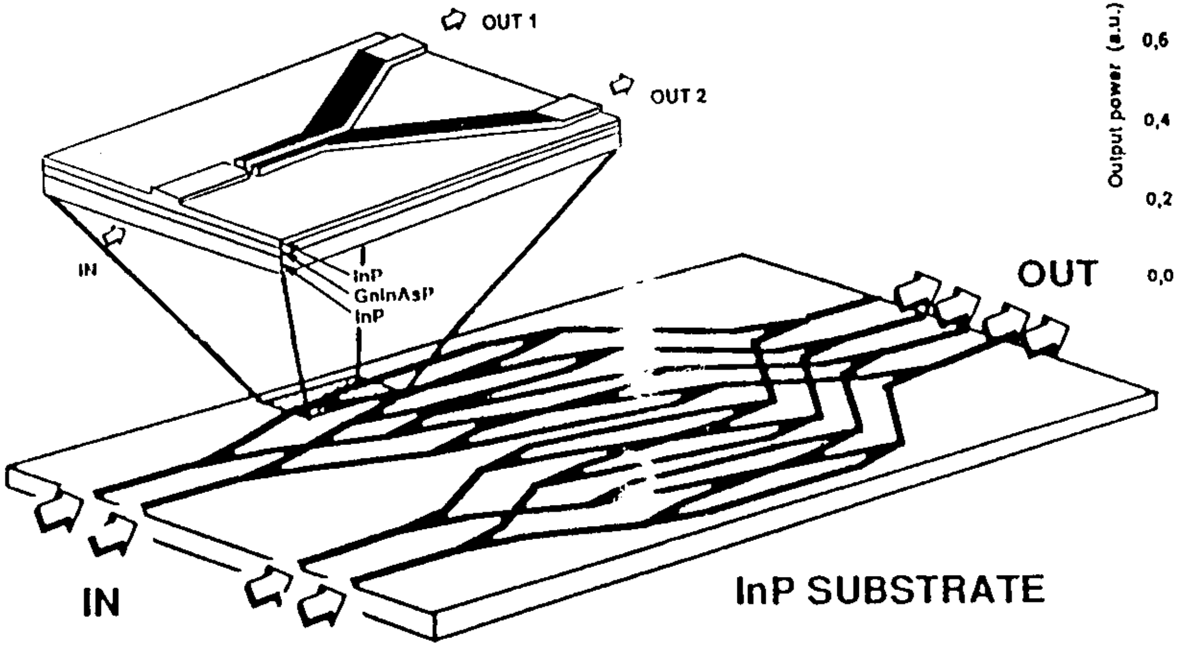

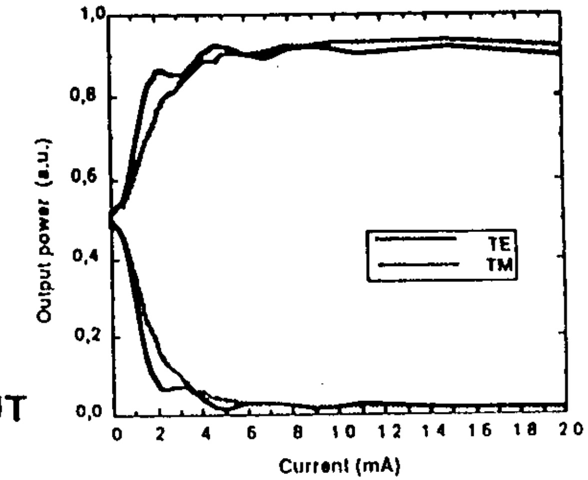

- Polarization Insensitive
- Truly digital operation

ETH Eidgenössische Technische Hochschule Zürich

suematsu 3

4x4 InP WAVEGUIDE DIGITAL OPTICAL SWITCH

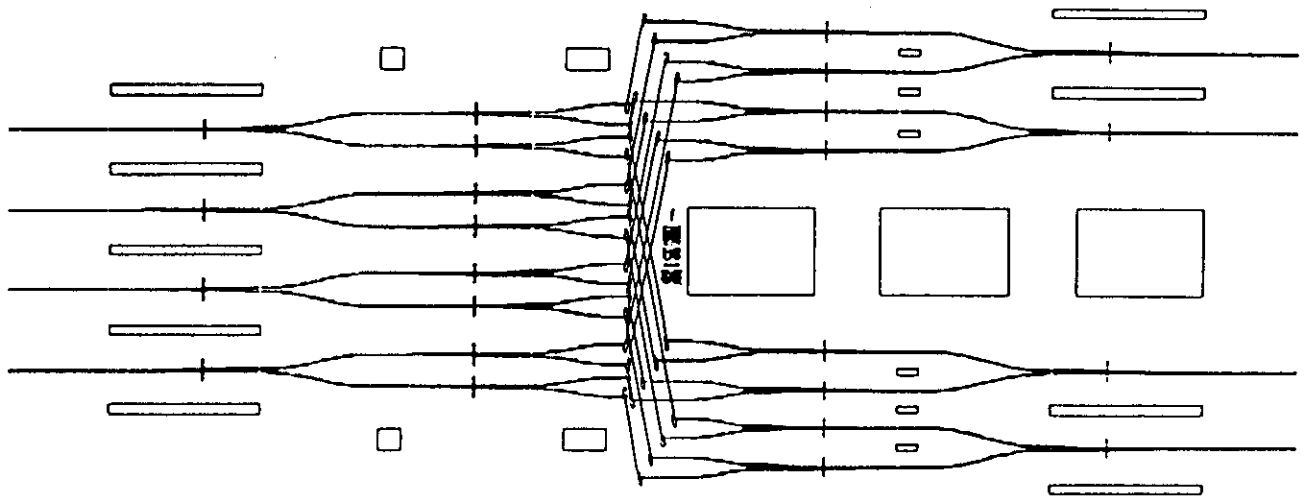

- Compact 4x4 switch is polarization insensitive, combines 24 digital optical switches and 32 waveguide mirrors
- Thick (>2 μm) waveguide structure allows low (<1 dB) waveguide to fiber coupling losses

Vinchant, AAR 93

Digital Optical Switches based on InP/InGaAsP
X and Y Junctions

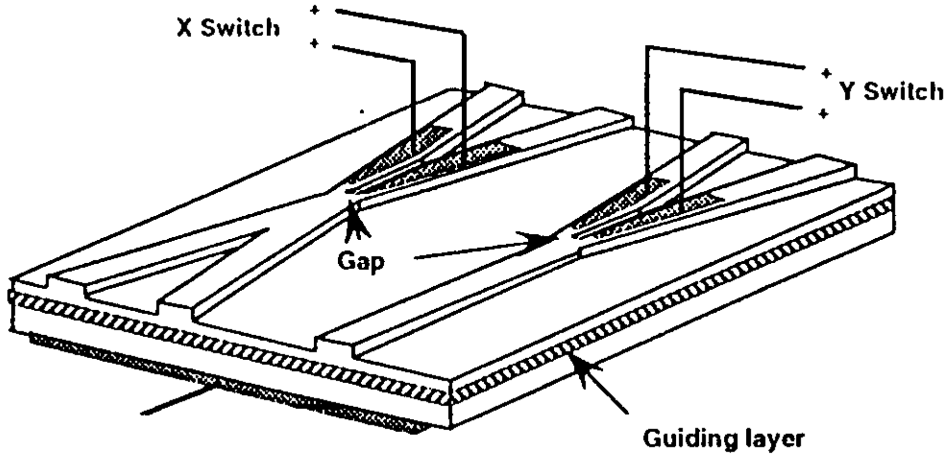

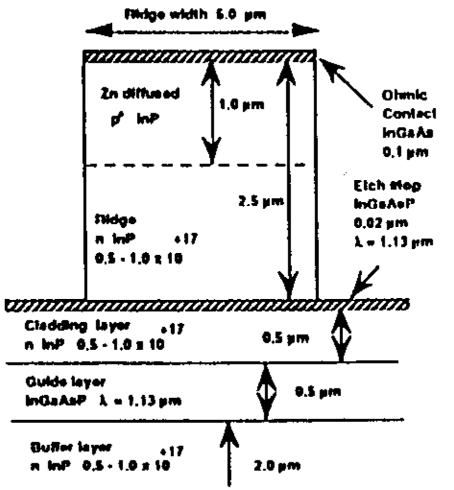

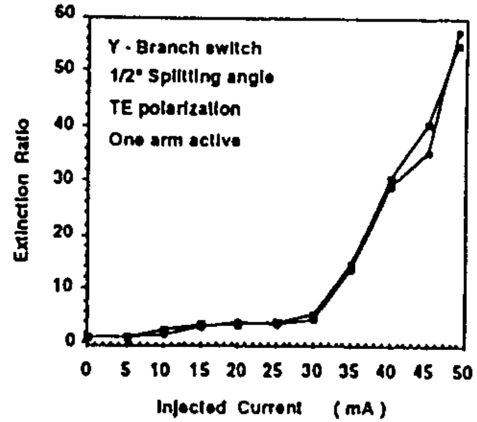

GTE 1992

Eidgenössische Technische Hochschule Zürich

DIGITAL OPTICAL SWITCH

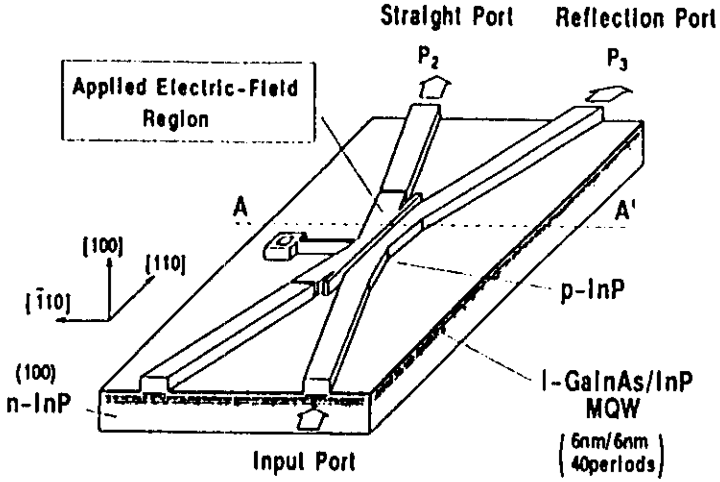

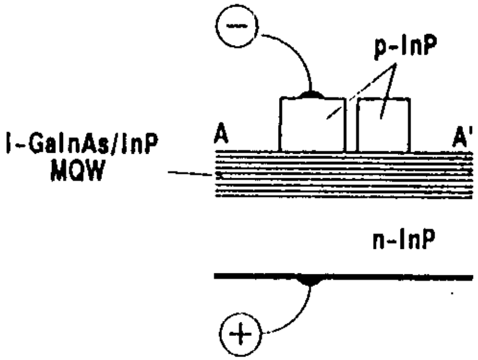

Carrier Injection Mode.
Y-Junctions with 2 mrd angles
Crosstalk at 6 mA:
15.7 dB in TE
15.2 dB in TM
with negligible extra losses
up to 100 mA

Reverse Bias Operation
at 1.52-1.57 μm Wavelengths.
Y-Junctions with 3mrd angles
Optical Losses:
1.1 dB/cm in TE
2 dB/cm in TM
Crosstalk at -10V:
13.8 dB in TE
12.1 dB in TM

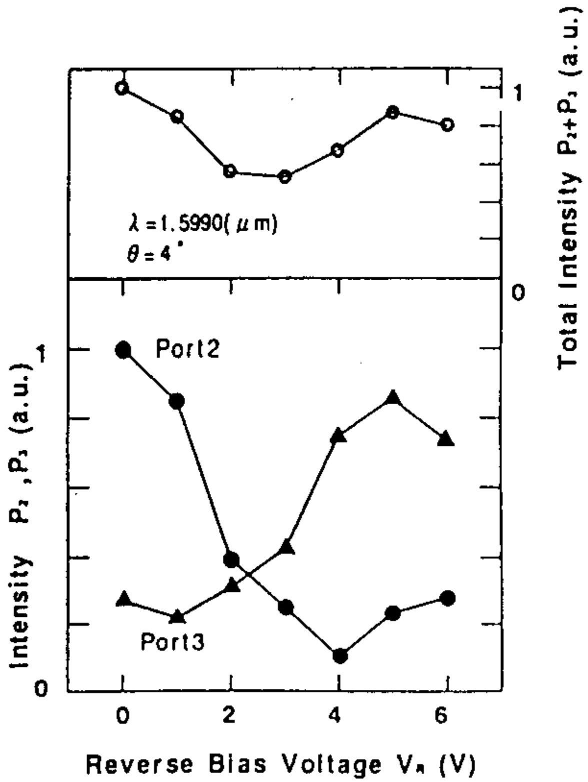

ETH Eidgenössische Technische Hochschule Zürich

CARRIER DEPLETION InGaAsP/InP DIRECTIONAL COUPLER SWITCH

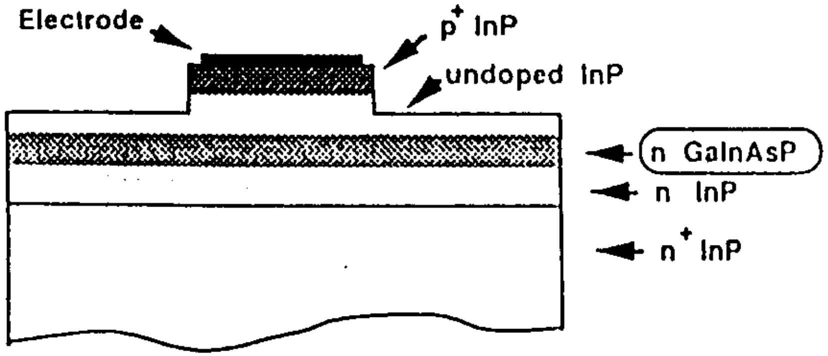

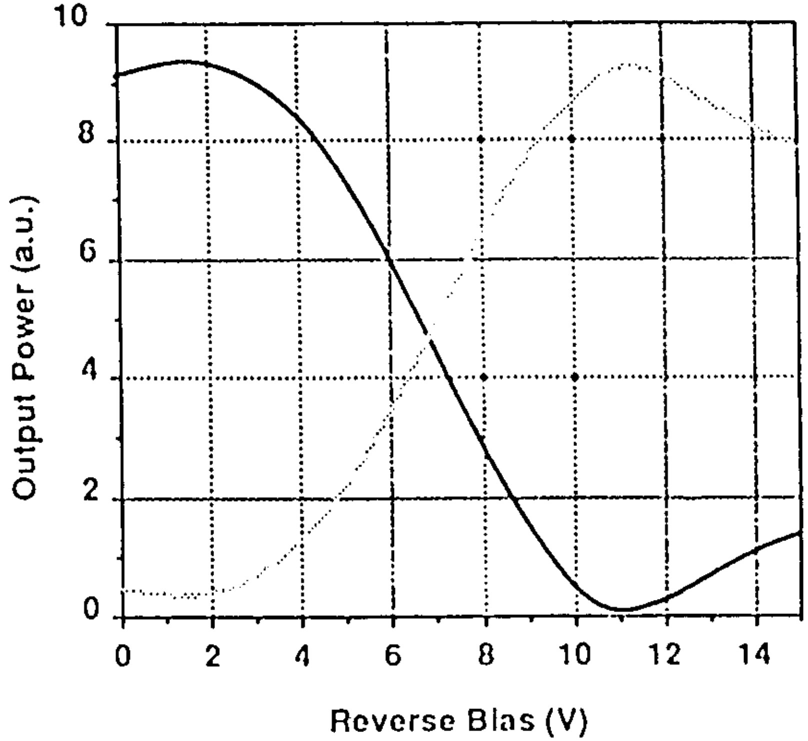

- Waveguide losses 1 dB/cm
- Modulation efficiency 15°/V mm
- Electrical bandwidth > 1 GHz

AAR

ETH Eidgenössische Technische Hochschule Zürich

OPTICAL SWITCHES BASED ON ADIABATIC WAVEGUIDE TRANSITIONS

Waveguide transitions are adiabatic, when their changes in the waveguide geometry are sufficiently slow, that the optical modes of the system remain constant.

Adiabatic waveguide transistions, such as directional couplers and Y-junctions have the property that all power stays in the mode initially excited at the input of the device, with no power coupled to other modes or lost by radiation.

Adiabatic structures have the advantage that there is no critical length that has to be adjusted to achieve high performance.

If the refractive indices of these structures are altered by an applied electric field or by carrier injection, digital optical switches, that is switches that switch from one drive independent state to the other, can be realized.

ETH Eidgenössische Technische Hochschule Zürich

INTEGRATED OPTIC ADIABATIC DIRECTIONAL WAVEGUIDE COUPLERS

Simulation of light propagation through monomode waveguide couplers.

Asymmetric adiabatic directional coupler in which light input from wide guide is coupled as ground mode through interaction region and to wide output guide

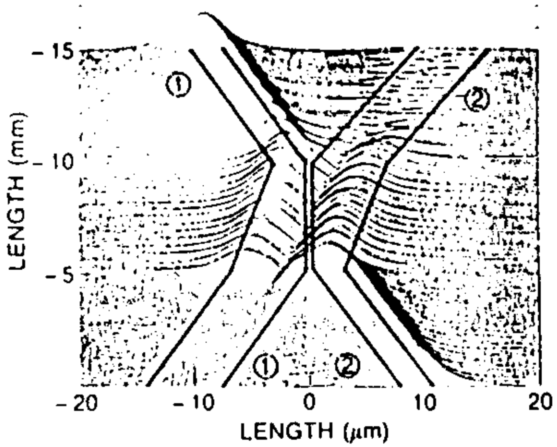

Asymmetric adiabatic directional coupler in which light input from narrower guide excites first order mode in interaction region which couples to narrow output guide

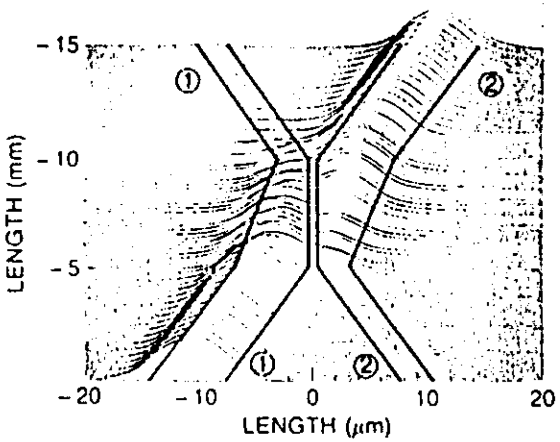

Symmetric directional coupler of comparable length shows many crossings of power forth and back from waveguide to waveguide

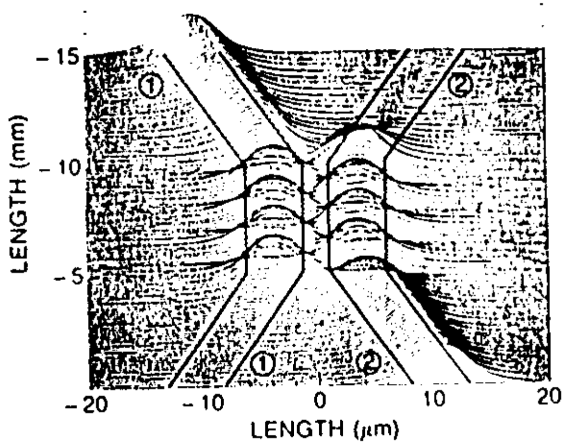

While the lengths of symmetric directional couplers have to be precisely controlled, asymmetric adiabatic couplers, albeit much larger, do not need tight length control. In addition their operation is polarization independent

ATT

ETH Eidgenössische Technische Hochschule Zürich

Polarization-Insensitive InP/InGaAsP 2x2 Switch

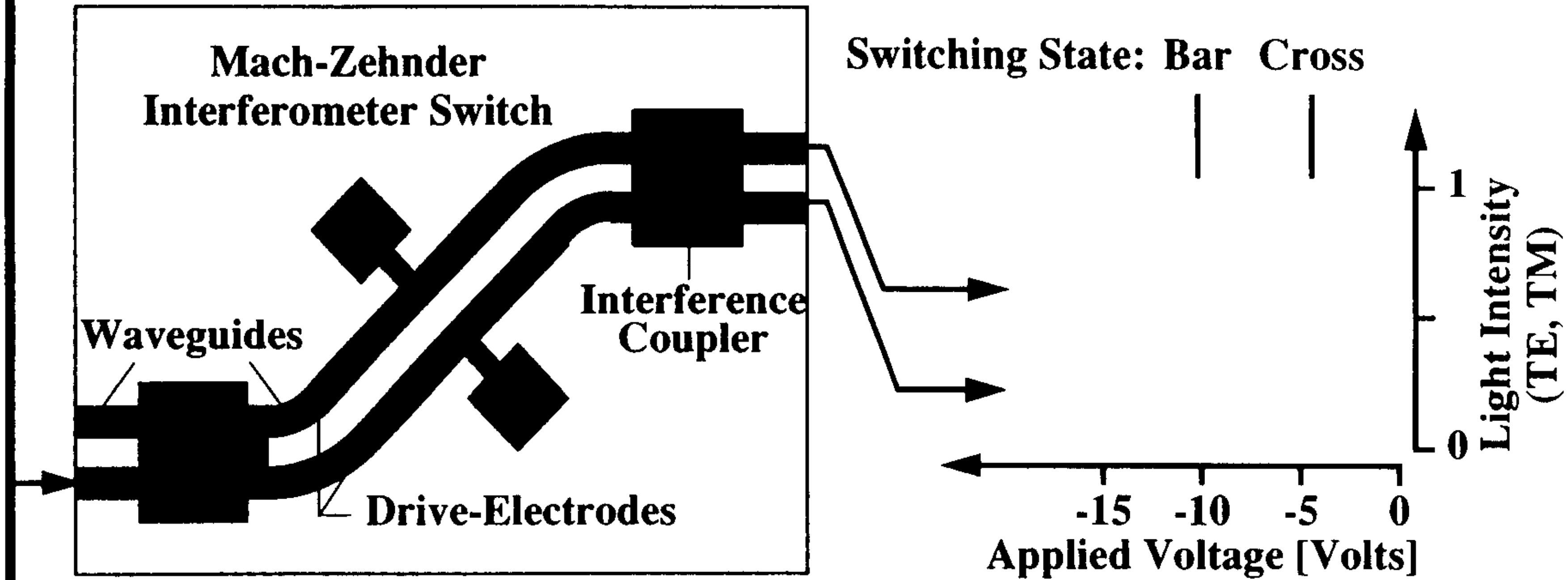

V_{switch}: 6 Volts On/off: 16 dB Loss: 2.5-3.2 dB

Eidgenössische Technische Hochschule Zürich

MMI: Intensity Distribution according to Beam Propagation Method

1xN-MMI: Input at W/2

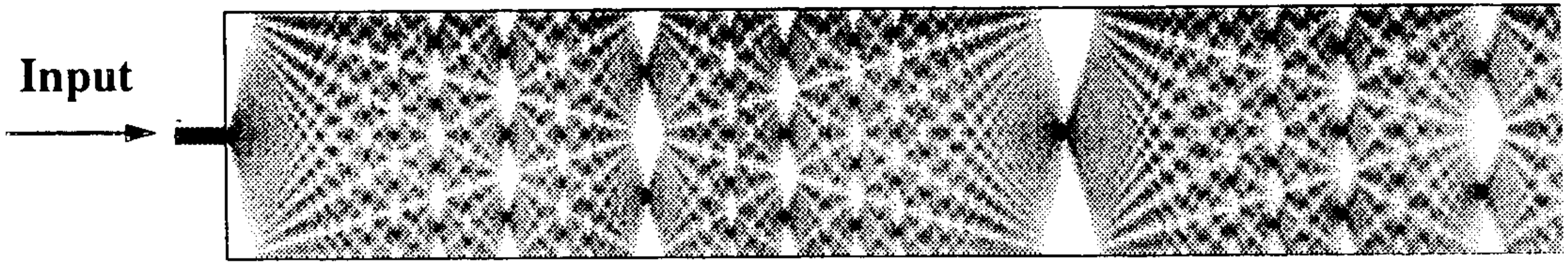

2xN-MMI: Input at W/3

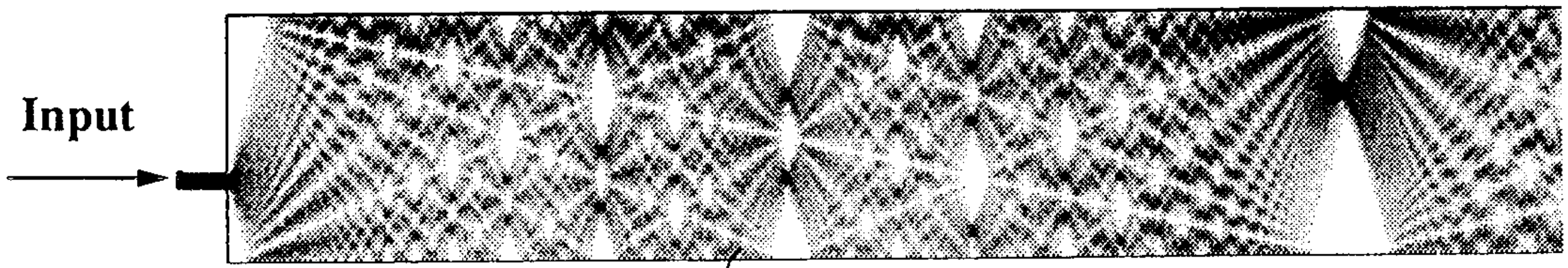

6 mm

Multi-Mode Interference Couplers

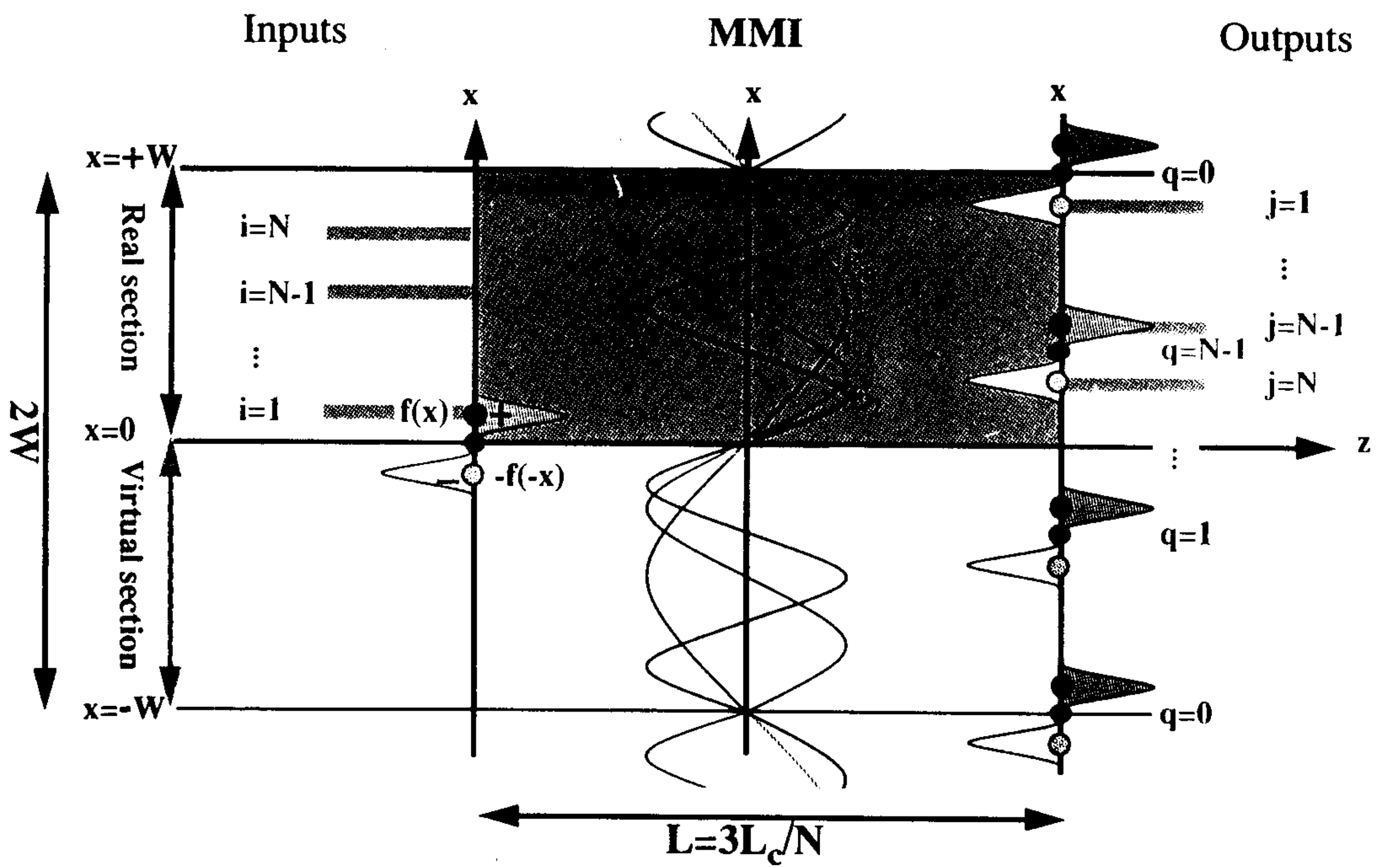

ETH Eidgenössische Technische Hochschule Zürich

High Speed Optical Space Switch Module

Array with 4 Switches, 4 Input and 4 Output Fibers, and High Speed Electronic Drivers

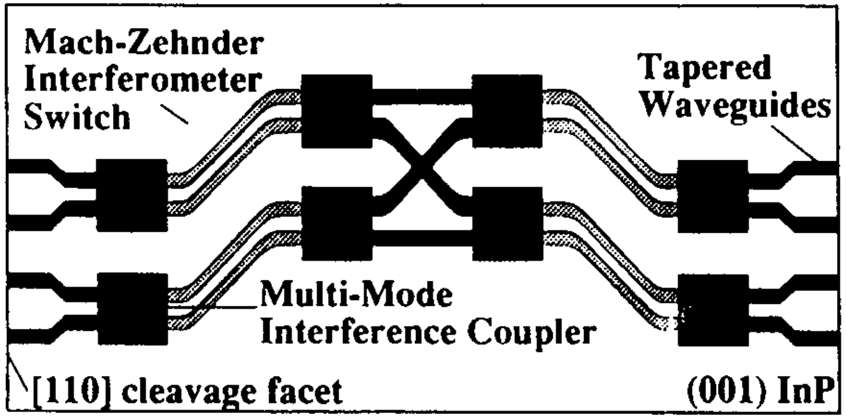

Wavelength of Operation	1.55 μm
Spectral Bandwidth (>10dB on-off)	50 nm
Fiber-to-Fiber Insertion Loss	≤ 10 dB
Optical On-Off Ratios	≥ 20 dB
Polarization Insensitivity	±1 dB
Switch Rearrangement Time	≤ 300 ps
Operational Voltage	5 Volt

Switch Transmission as Function of Bias

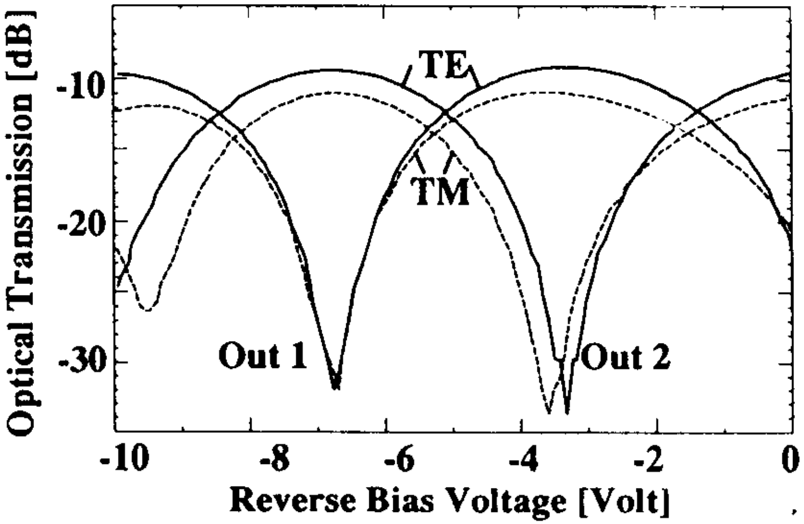

Switch Turn-on Characteristic

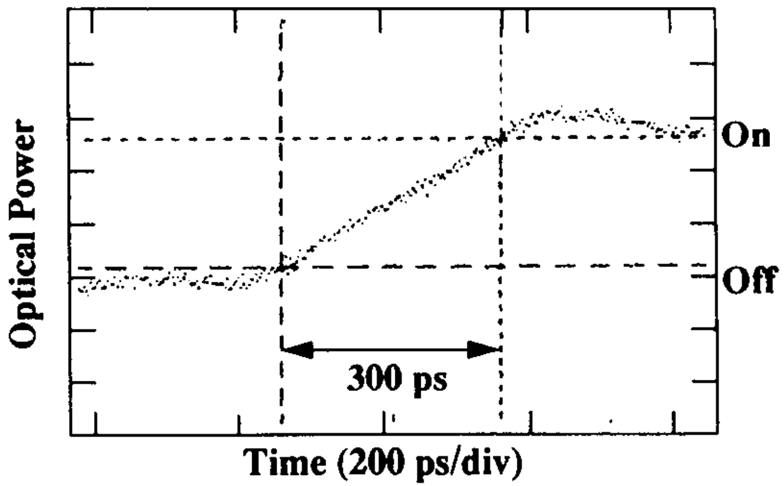

Eidgenössische Technische Hochschule Zürich

Integrated Waveguide Mode Adapters for Low-Loss OEIC to Fiber Coupling

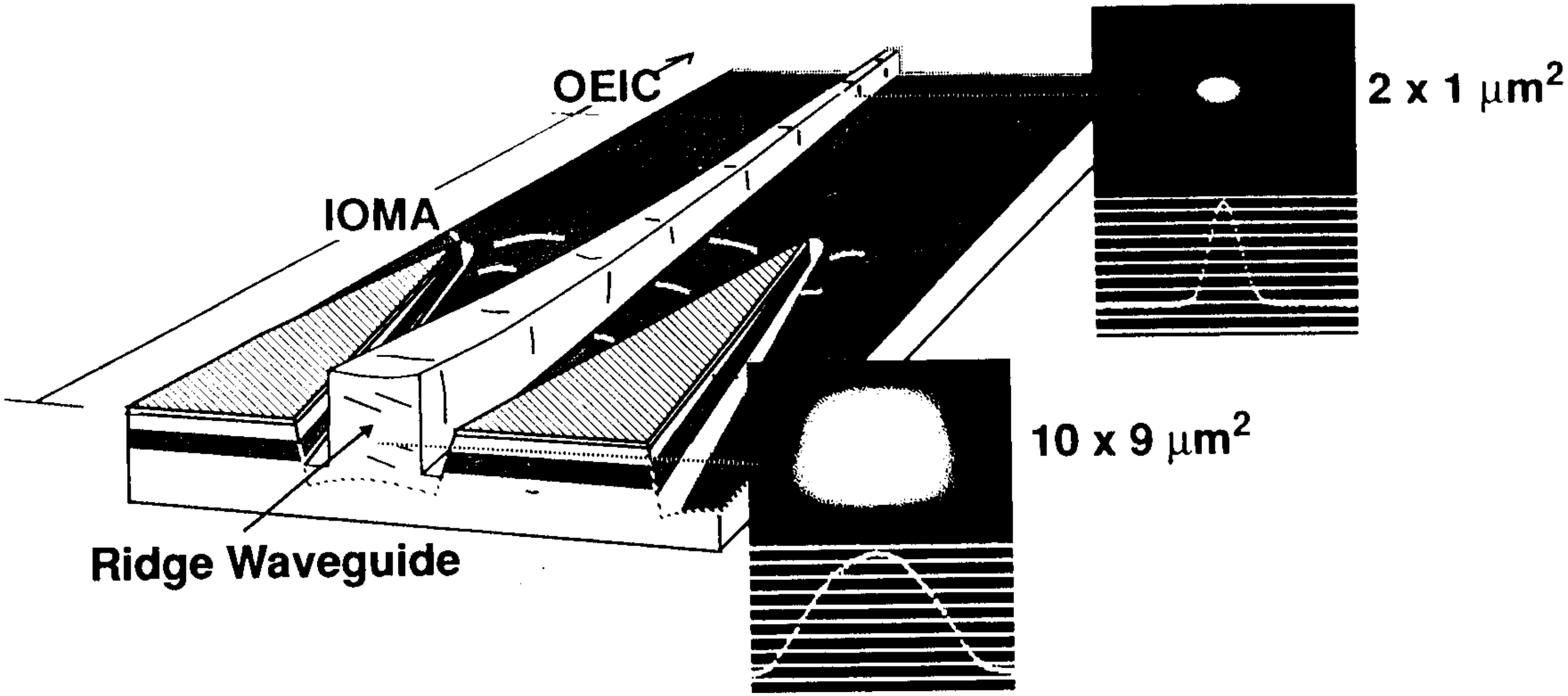

- Taper formation by means of selective area etching and InP - cladding regrowth
- InP waveguide component to optical fiber coupling losses < 1 dB, and lateral alignment tolerances of ± 2.5 µm.

ATMOS R2039

POLARIZATION INSENSITIVE WAVEGUIDE SWITCH

4 InP

Eidgenössische
Technische Hochschule
Zürich

OPTICAL WAVEGUIDE SWITCH AND OEIC MOUNTING AND FIBER TO WAVEGUIDE ALIGNMENT TECHNIQUE

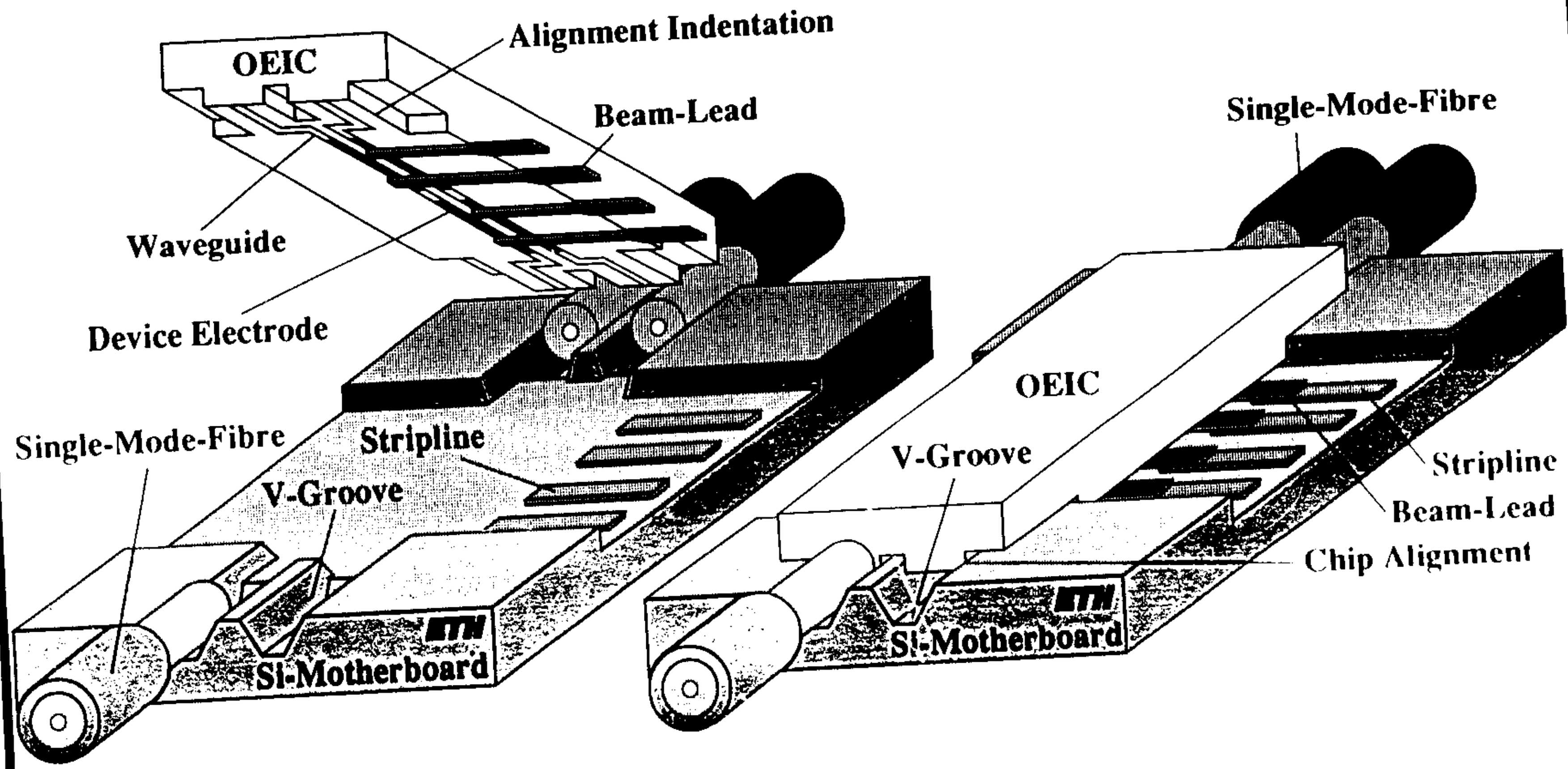

ETH Eidgenössische Technische Hochschule Zürich

Si V-GROOVES FOR OPTICAL ALIGNMENT OF SMF AND OEIC

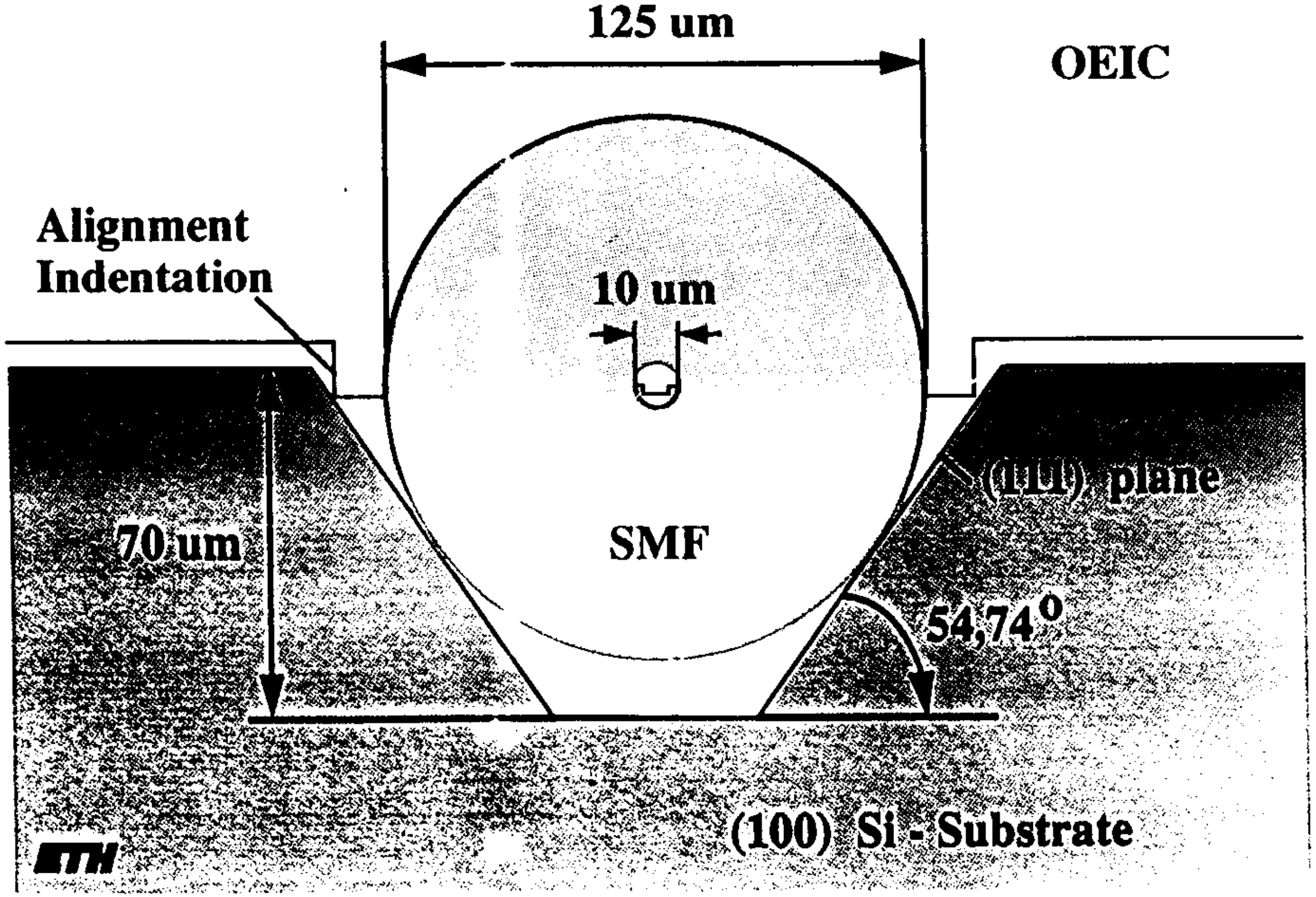

Package for Semiconductor Optical Switch Array

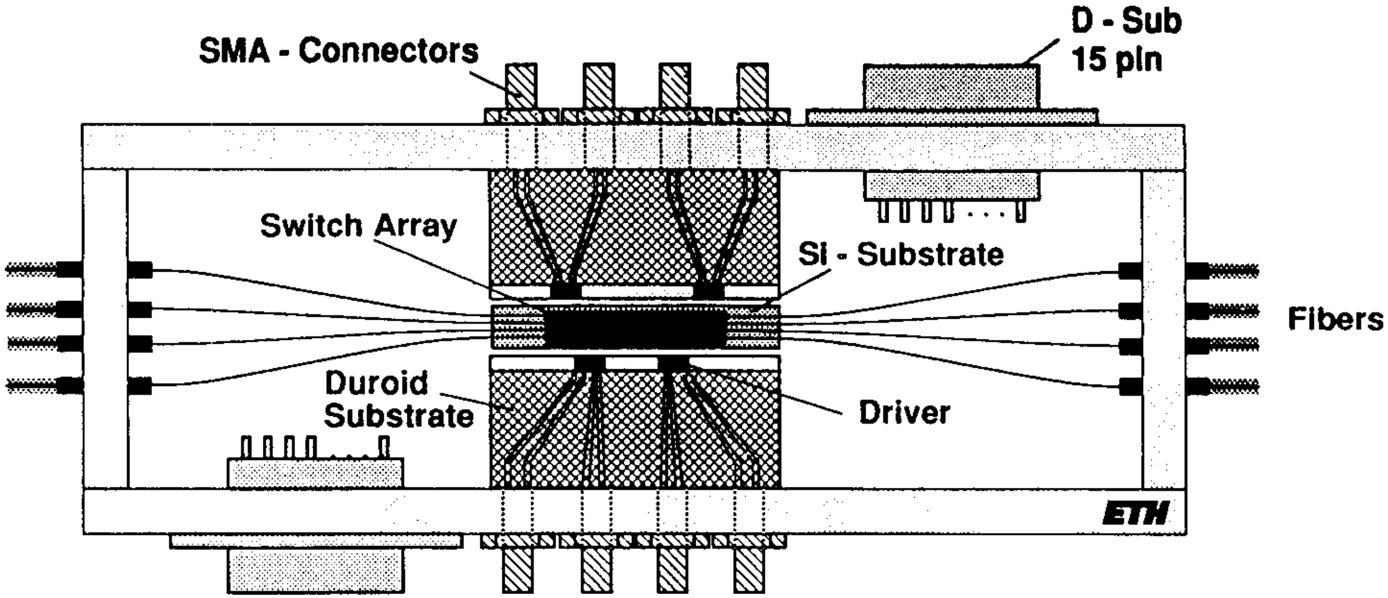

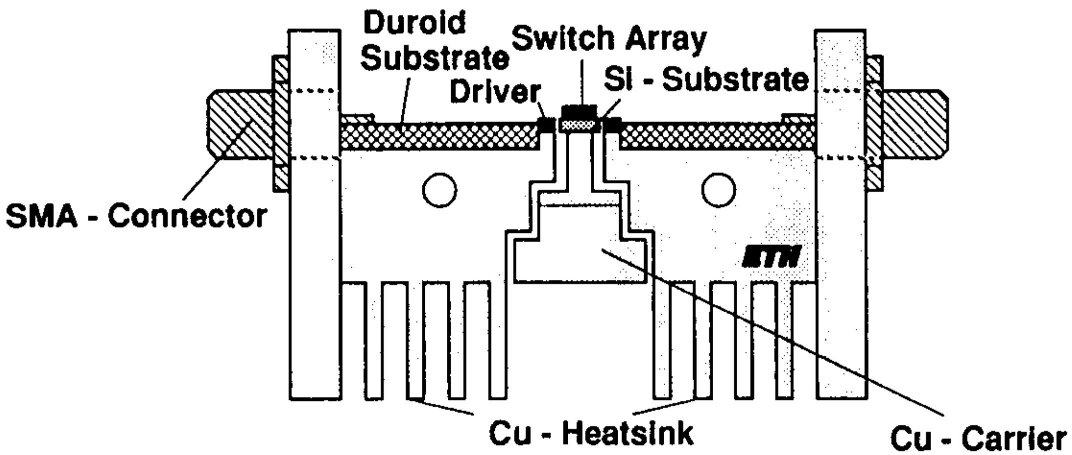

ATMOS R2039

POLARIZATION INSENSITIVE 2X4 InP WAVEGUIDE SWITCH

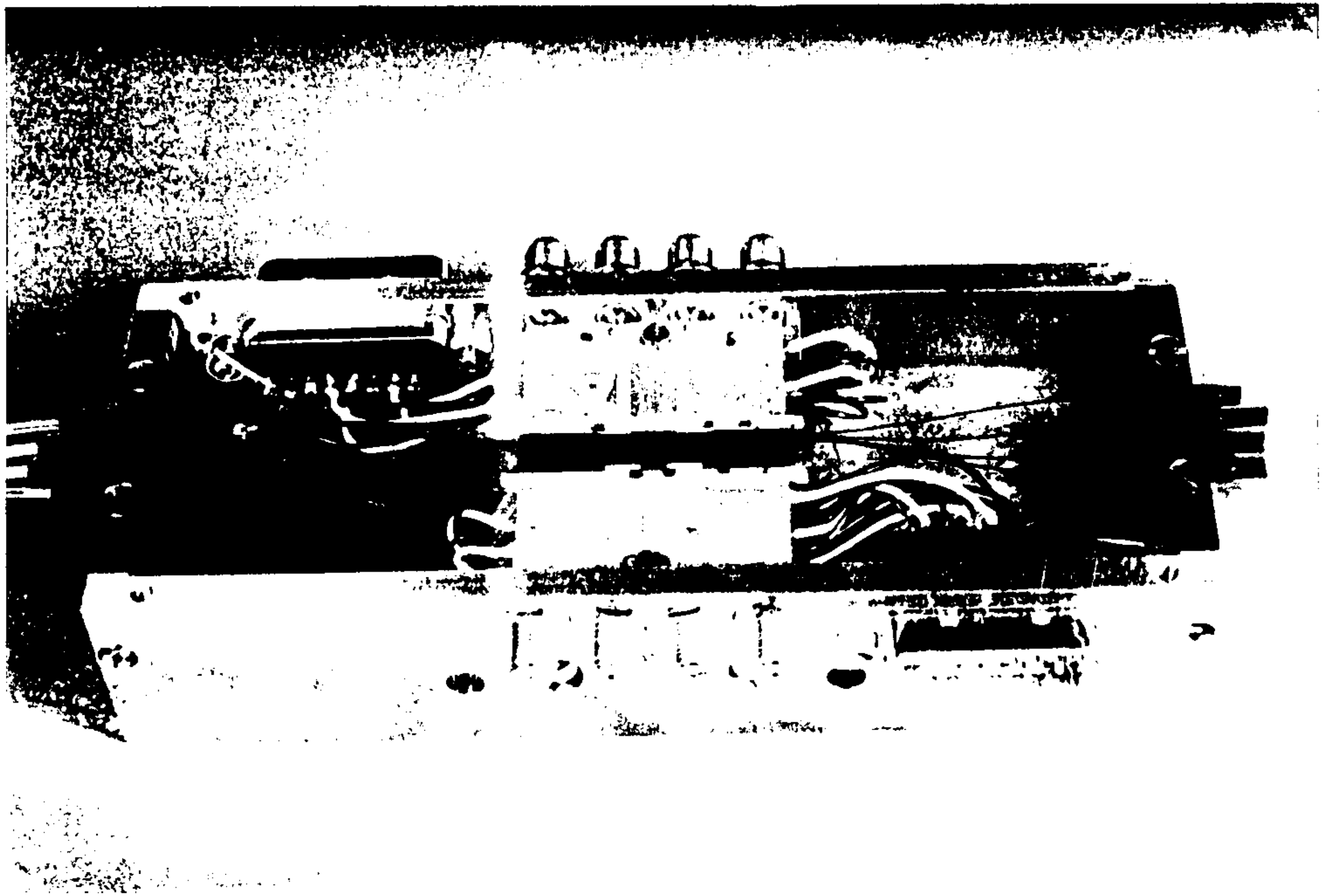

Eidgenössische
Technische Hochschule
Zürich

Optical ATM switching in the evolving B-ISDN

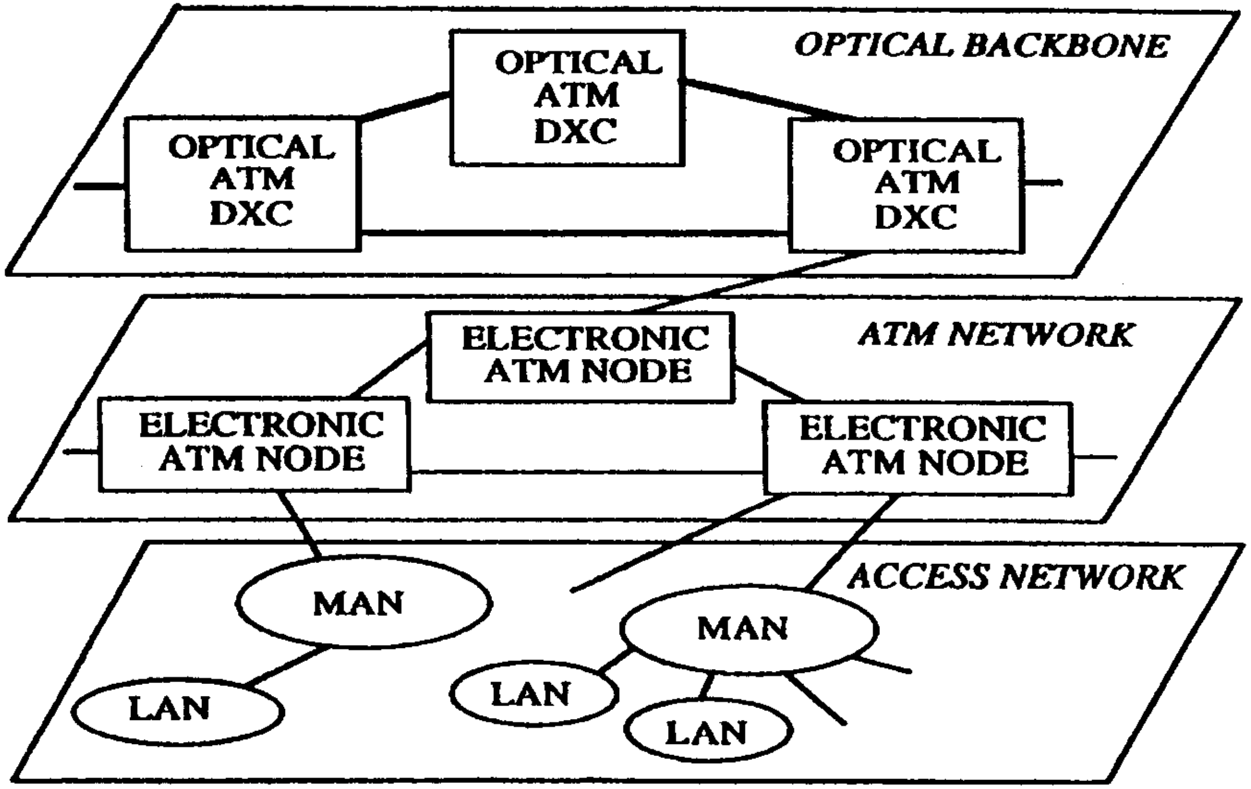

94

ATMOS R2039

MAN Node schematic block diagram.

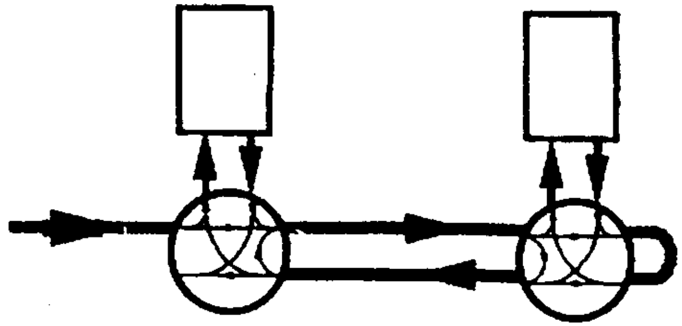

MAN node testbed

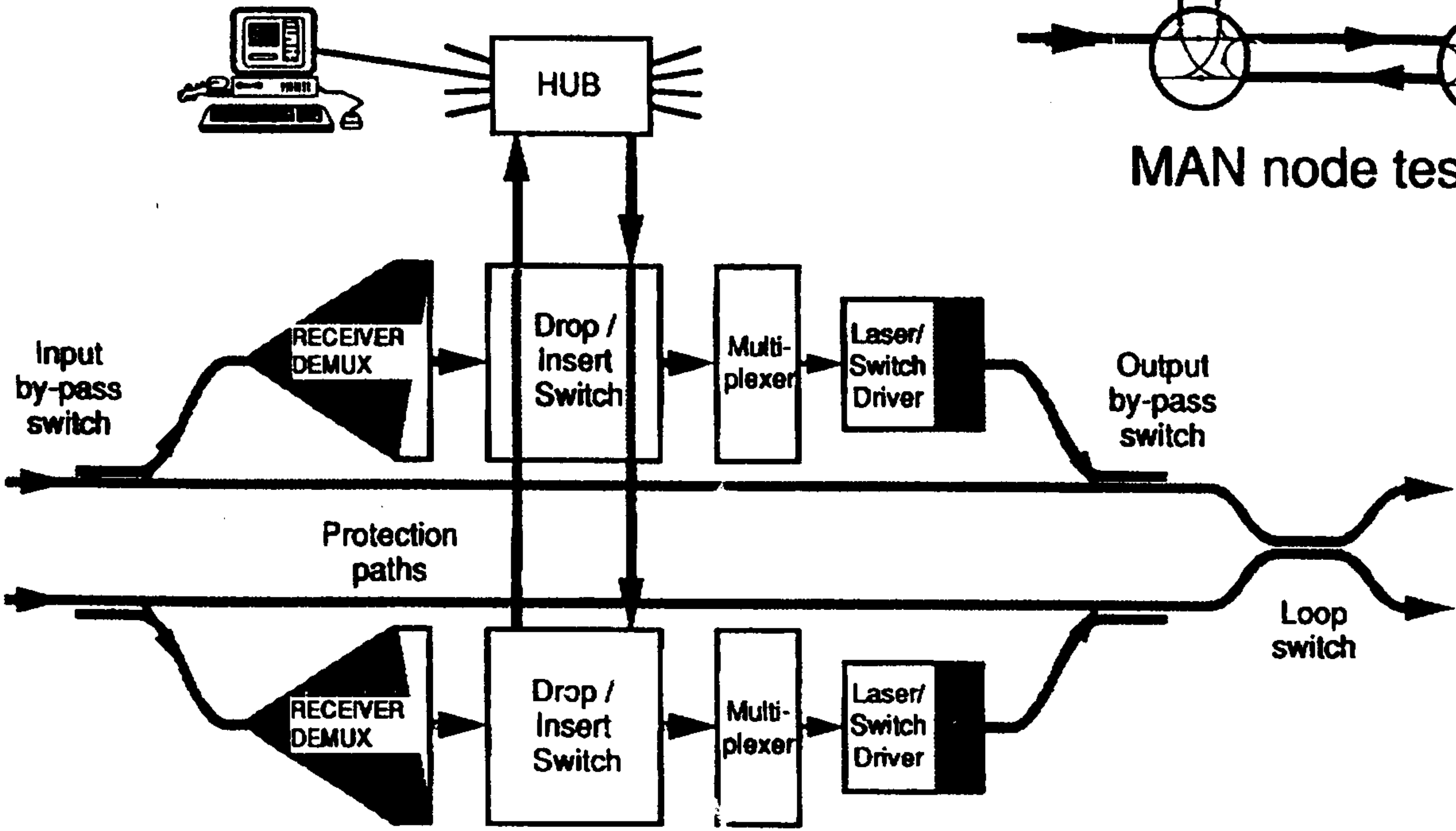

ATMOS R2039

Bidirectional Access Node Switch Module

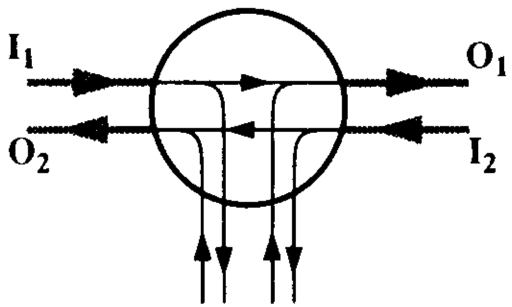

Access Node

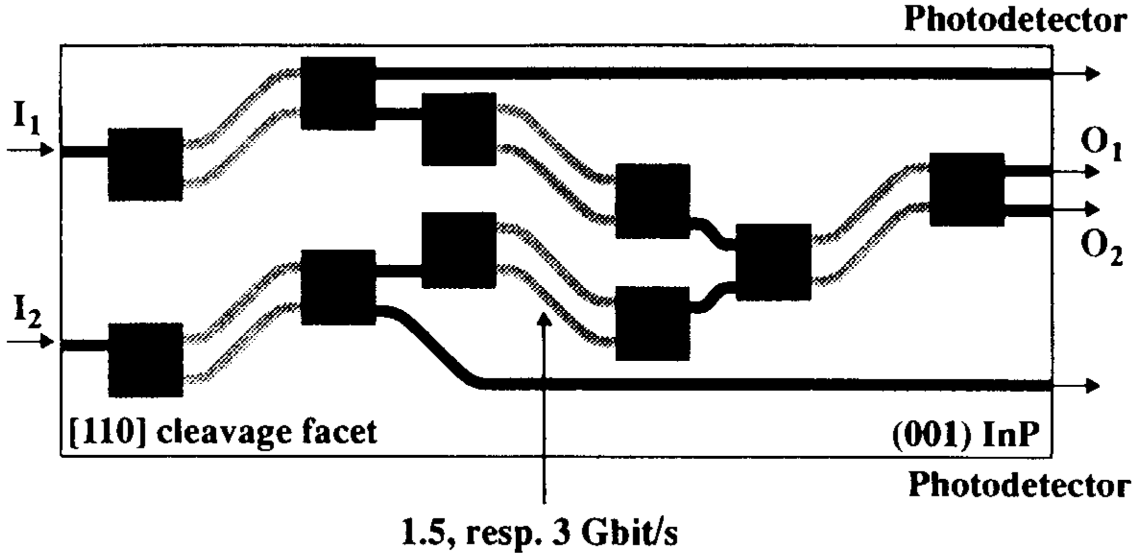

Mach Zehnder Interferometer switches with Multimode Interference Coupler realized as fabrication tolerant InP-Quaternary rib-waveguides on (001) substrates. Switches are oriented at an angle to the [110] cleavage facets to exploit Franz-Keldysh electrooptic effect for polarization insensitive switching.

Wavelength Range	1.52 to 1.57 µm
Polarization Insensitivity	±1 dB
Input to Output Fiber to Fiber Loss	12 dB
Input to Photodetector Loss	10 dB
Switch On-Off Ratios	≥ 10 dB
Switch Rearrangement Time (Including HBT Driver)	≤ 190 ps

ETH Eidgenössische Technische Hochschule Zürich

Multifunctional InP switch for optical processing

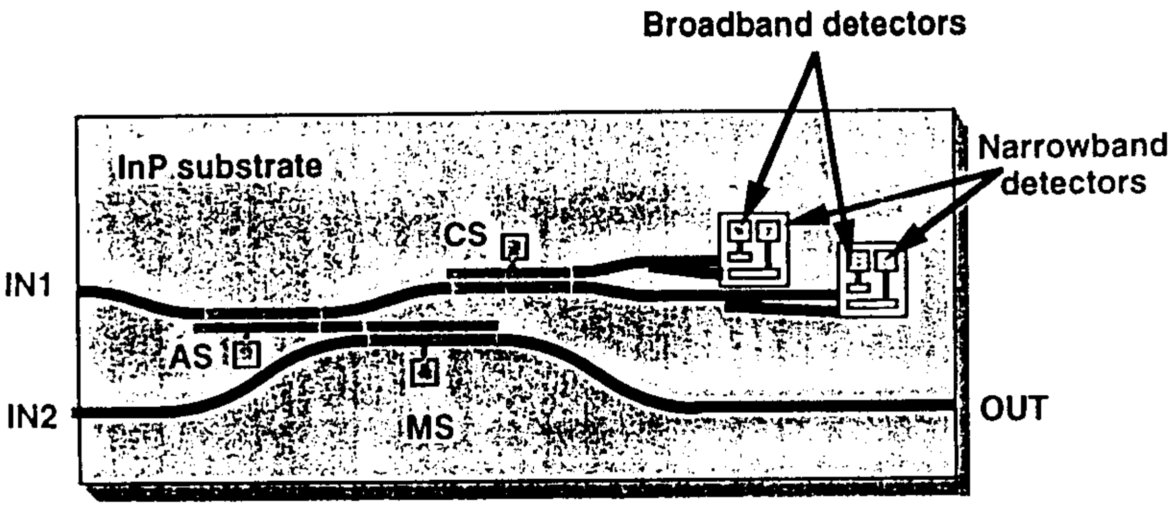

AS: Access switch   CS: Correlation switch   MS: Modulation switch

- Two epitaxial steps process
- Carrier depletion directional couplers
- Evanescent field coupled detectors
- Semi-insulating InP substrate
- Compatibility with GaAs ELO integration

- Switching voltage ~-10 V
- Crosstalk ≤ -15 dB
- Propagation losses ~1.5 dB/cm
- High electrical isolation between switches & detectors ~ -60 dB

1 Gb/s eye diagrammes with hybrid switch drivers

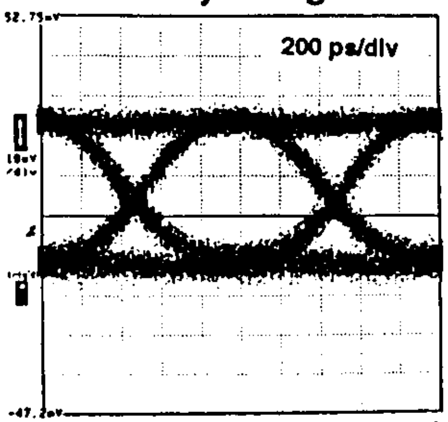

Optical output channel

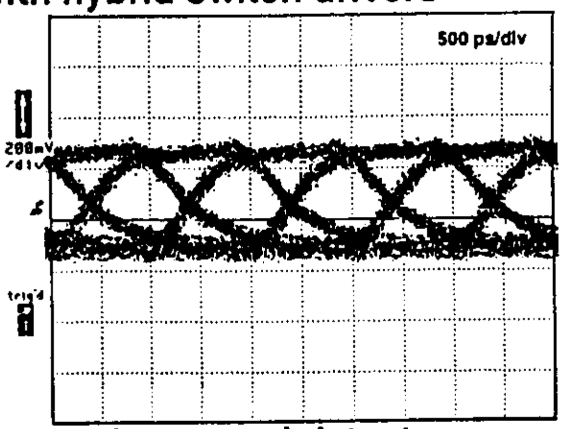

Integrated detector

2.5 Gb/s eye diagramme
with InP HBT switch drivers

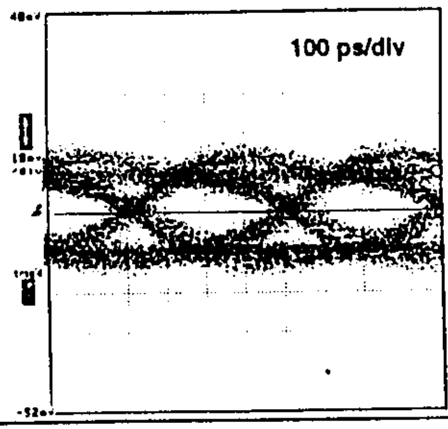

ATMOS R2039

Optoelectronic Switches Modulators and Semiconductor Amplifier Gates for High Speed Fiber-Transmission Systems

- ⇒ Motivation for Optical Switching in High Speed Fiber Optical Communication Networks
- ⇒ Basic Concepts of Optical Switches, Modulators and Semiconductor Optical Amplifier Gates
- ⇒ Physical Effects exploited in Waveguide Type Optical Switches, Modulators and Semiconductor Optical Amplifier Gates
- ⇒ Implementations of High Speed Optical Modulators
- ⇒ Implementations of High Speed Waveguide Type Space Switches
- ➡ Semiconductor Optical Amplifier Gates and Wavelength Converters
- ⇒ Summary and Conclusions

ETH Eidgenössische Technische Hochschule Zürich

Optical Amplifier Switches Integrated with Waveguides

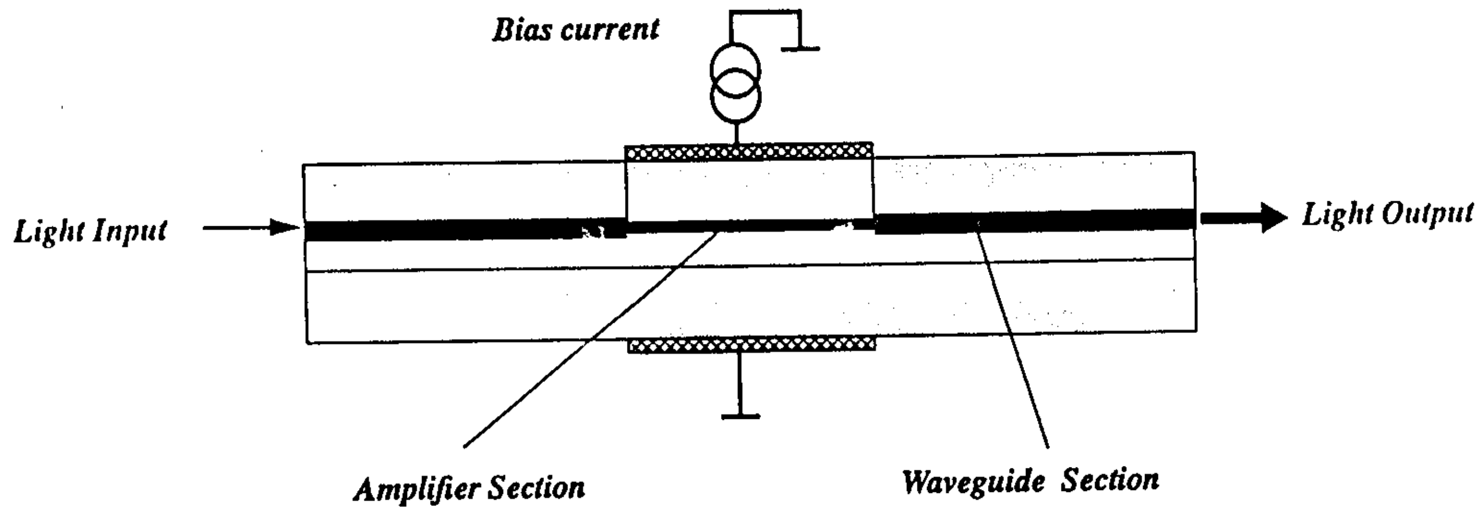

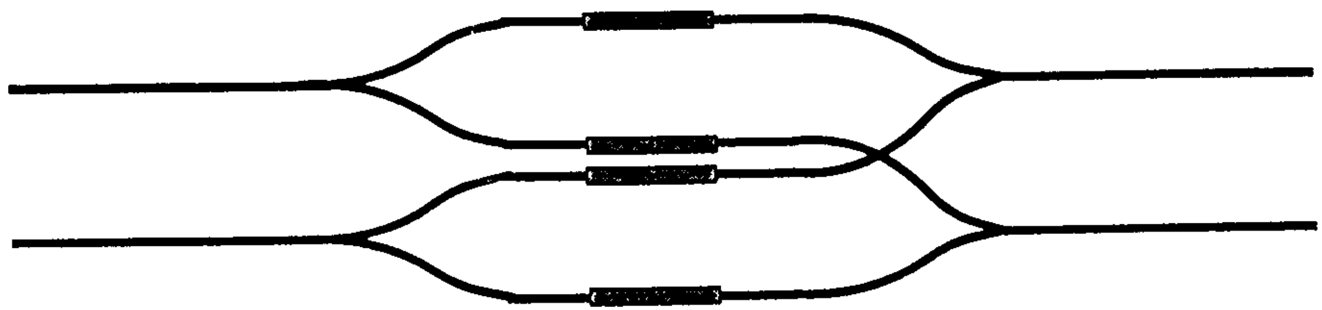

Two-by-Two Optical Amplifier Switch

Semiconductor Optical Amplifiers for 1.3μm Wavelengths with Low Polarization Dependence

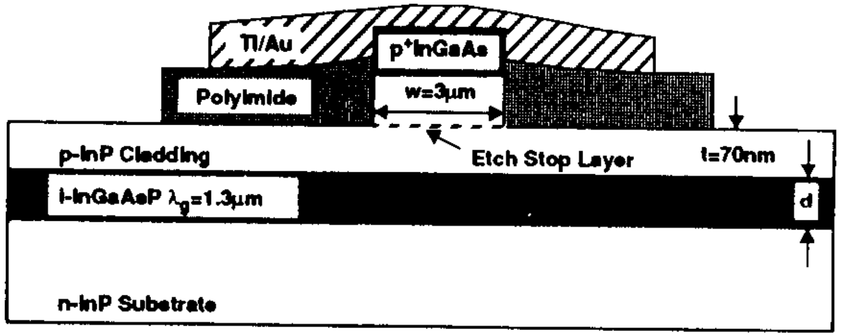

Result: d = { 150nm → Enhanced TE; 250nm → Equal TE and TM; 400nm → Enhanced TM } Optical Gain

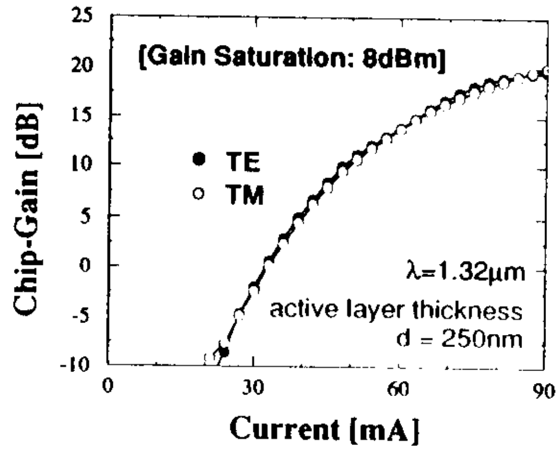

Bulk Ridge-Type Construction
for Polarization Insensitive Gain

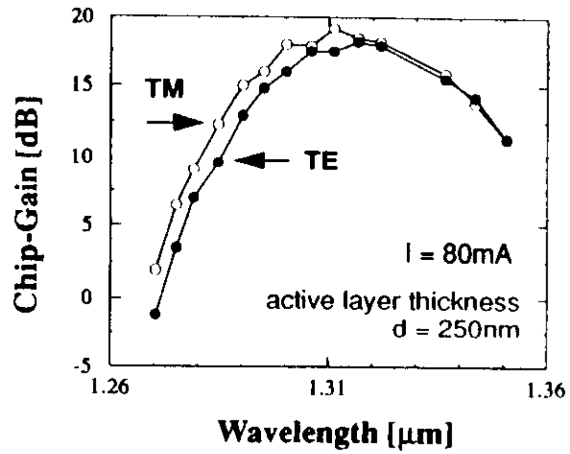

Eidgenössische Technische Hochschule Zürich

Integrated Semiconductor Optical Amplifier with Tilted Mirrors

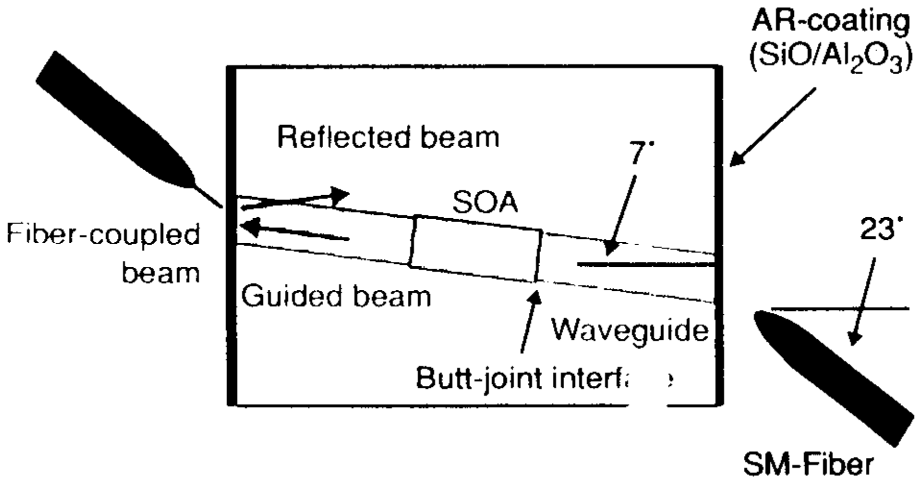

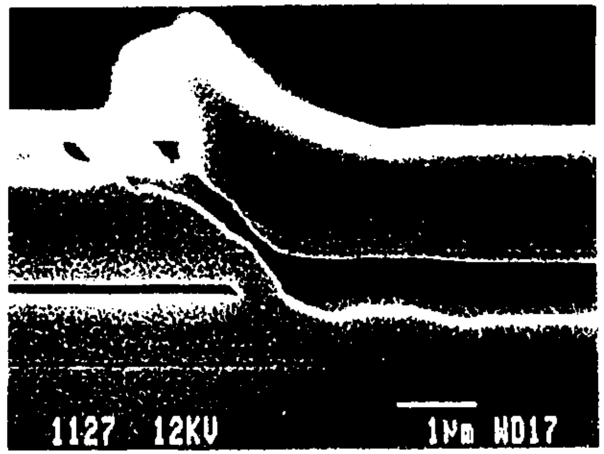

Butt-joint interface

Eidgenössische
Technische Hochschule
Zürich

2x2 Semiconductor Optical Amplifier Switch for 1.3µm Wavelengths

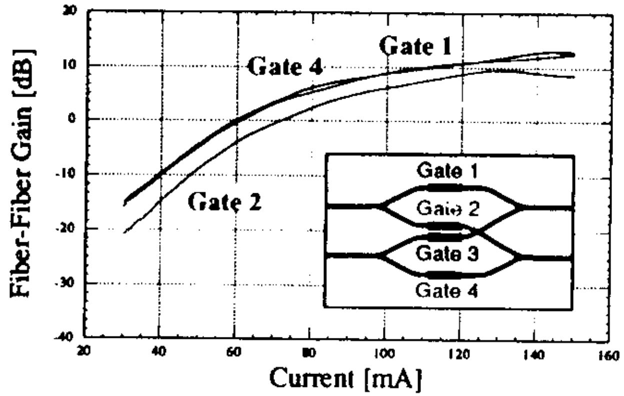

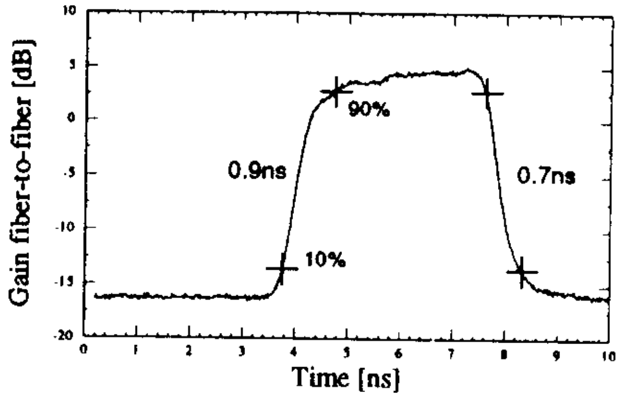

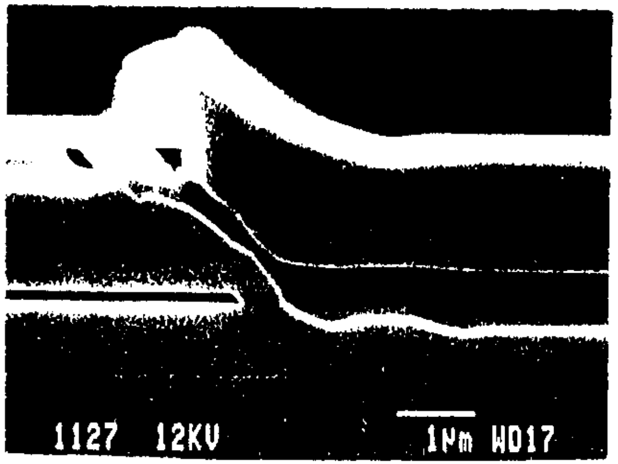

Amplifier Waveguide

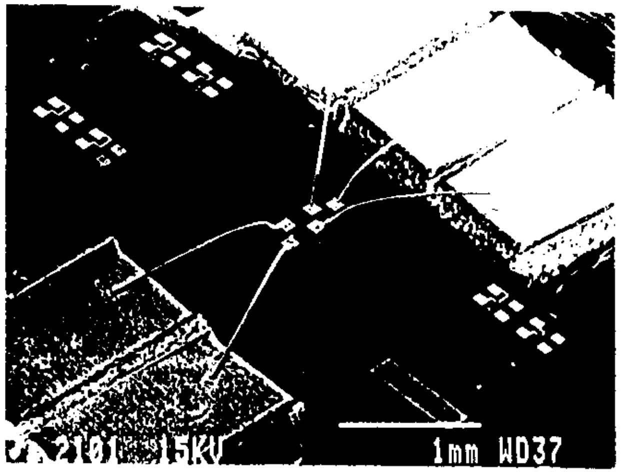

Eidgenössische Technische Hochschule Zürich

Amplified Spontaneous Emission Spectra

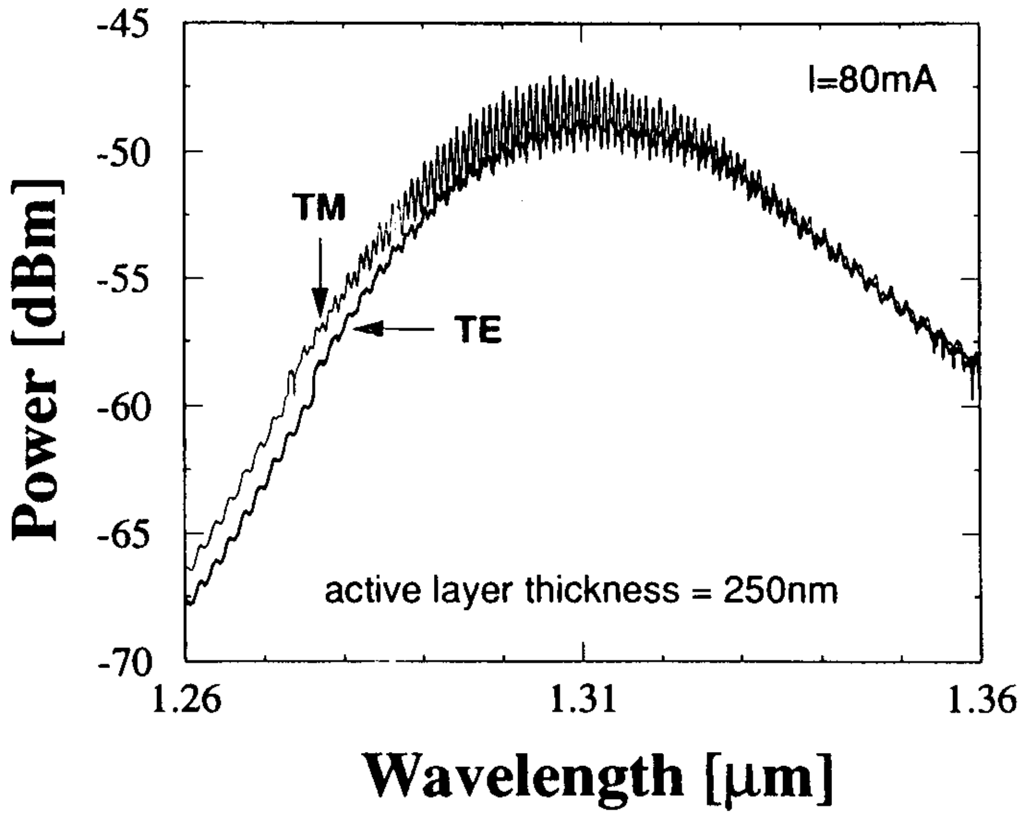

ETH Eidgenössische Technische Hochschule Zürich

Saturation Output Powers

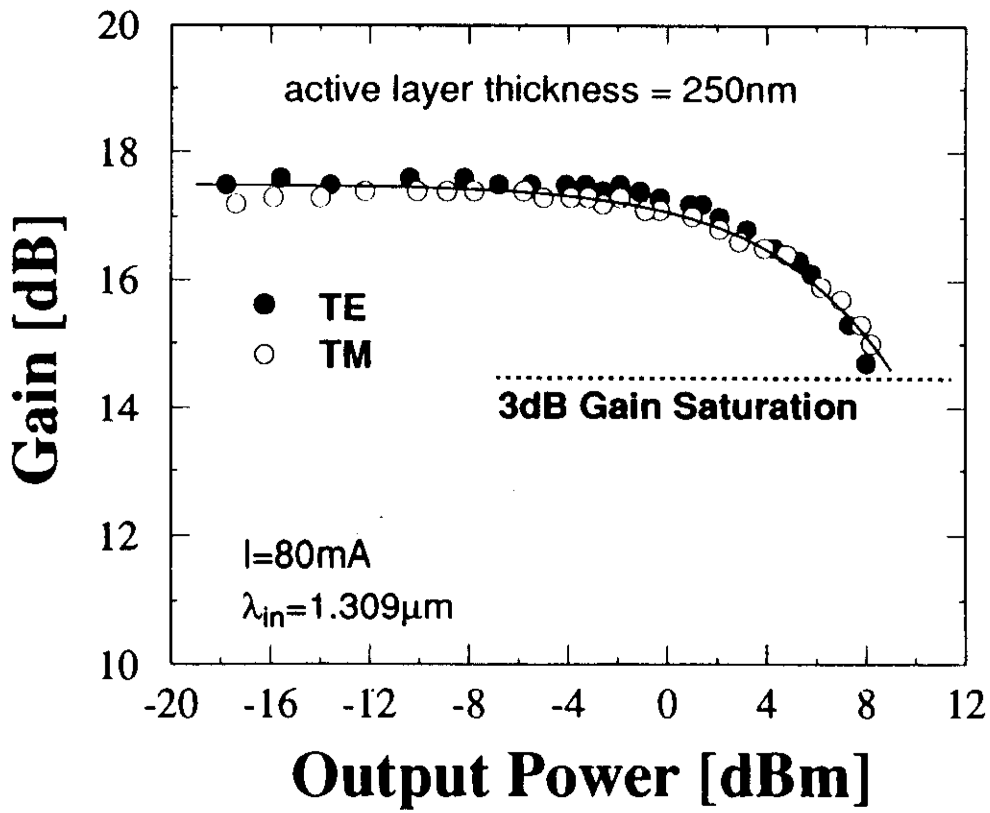

Eidgenössische Technische Hochschule Zürich

ZERO-LOSS OPTICAL AMPLIFIER SWITCH MATRIX FOR 1.5 - 1.55 μm WAVELENGTHS

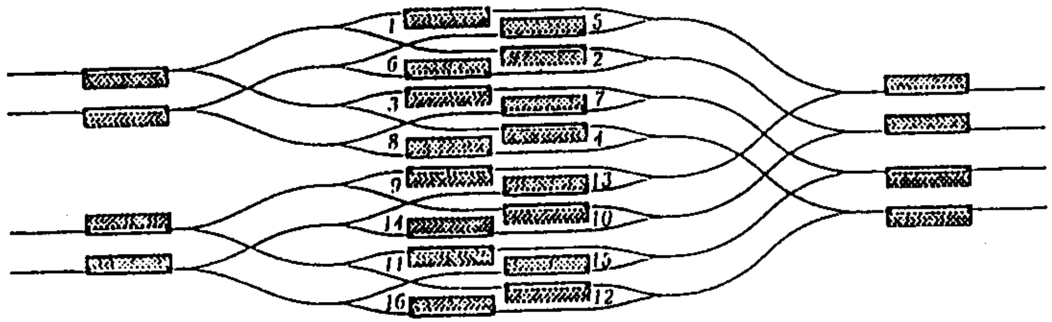

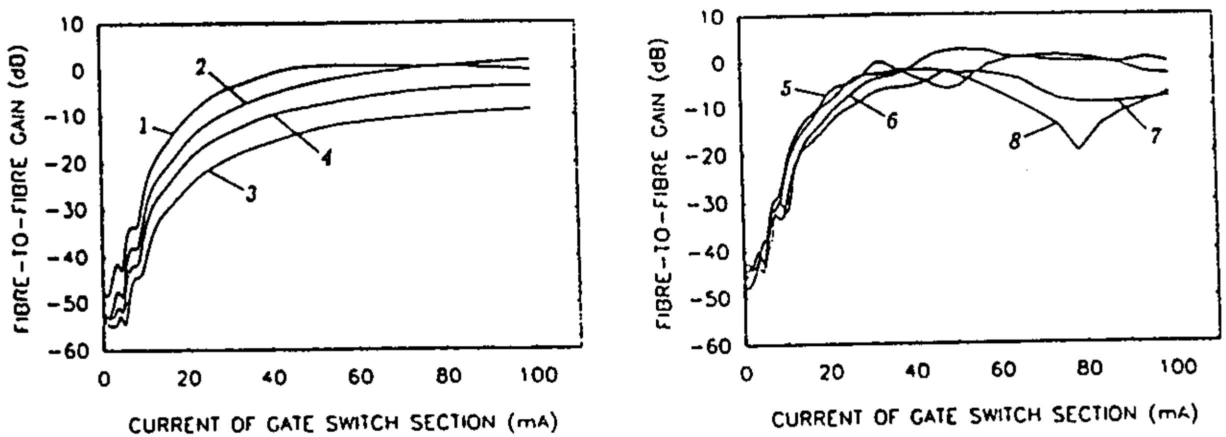

4x4 Laser amplifier gate switch comprising 24 integrated laser amplifiers **Ericsson**

Eidgenössische Technische Hochschule Zürich

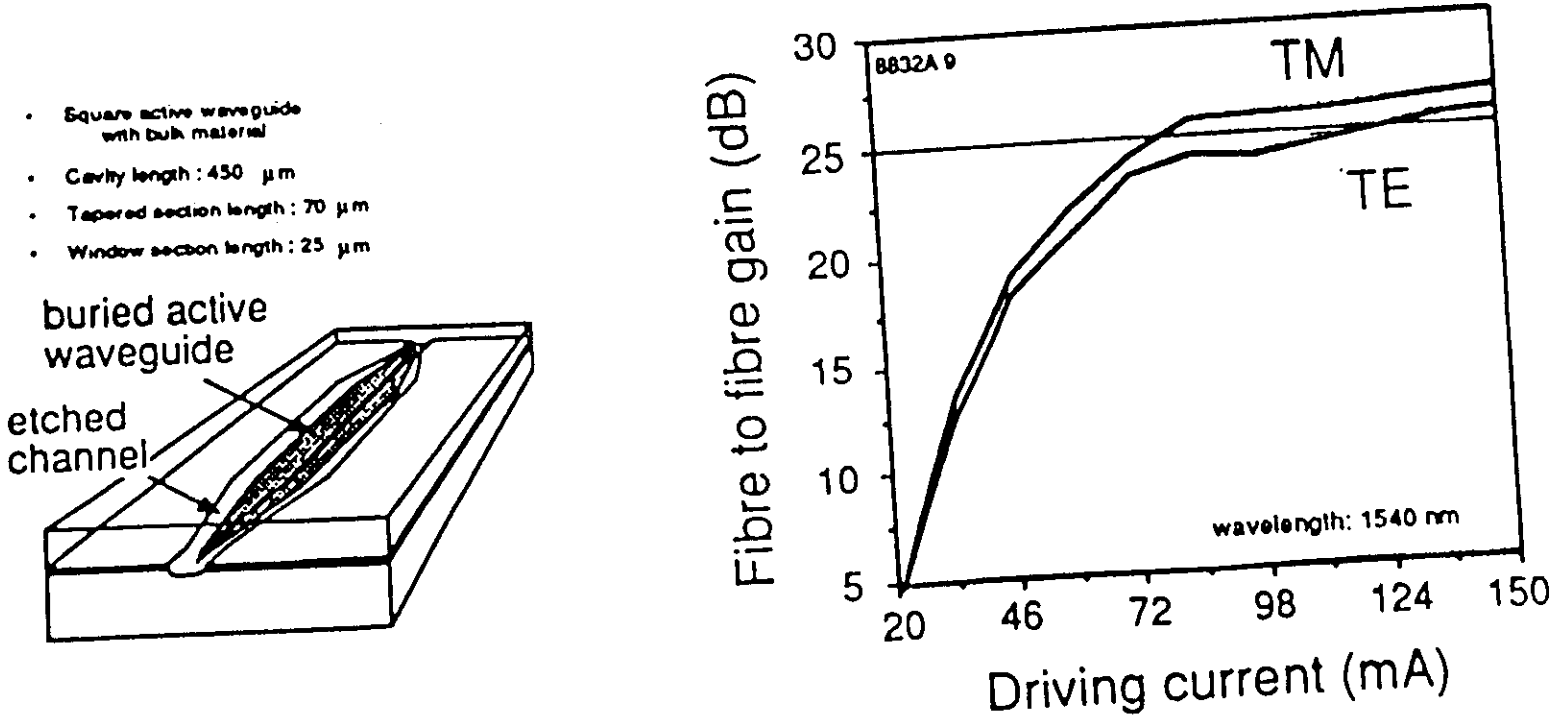

SOA gate structure and an example of the fibre-to-fibre gain.

P. Doussiere et al., *IEEE Photon. Technol. Lett.*, 1994, 6, pp. 170-172

LOSSLESS LOW-CROSSTALK InP-2X2 OPTICAL SWITCH

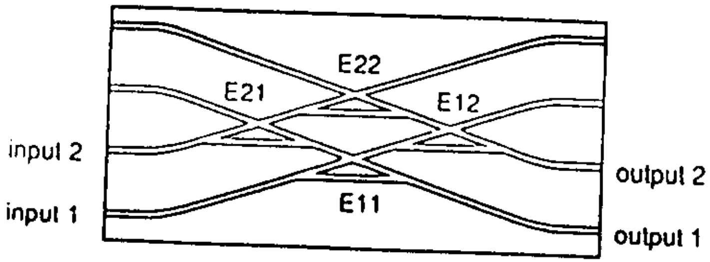

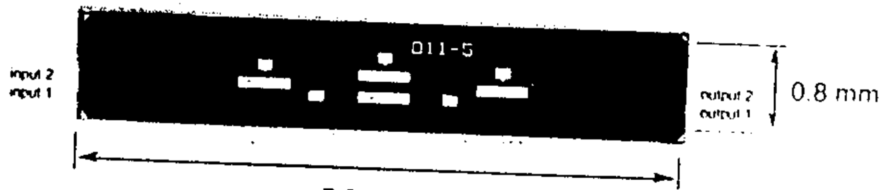

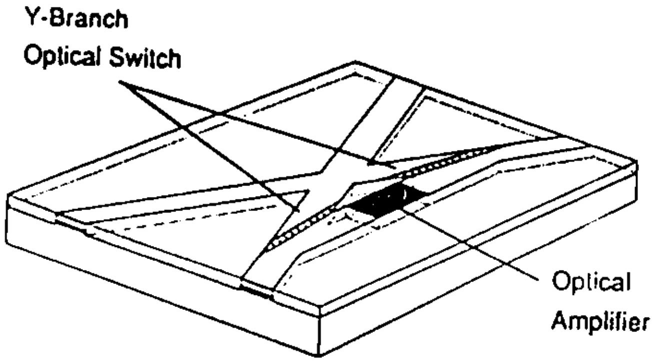

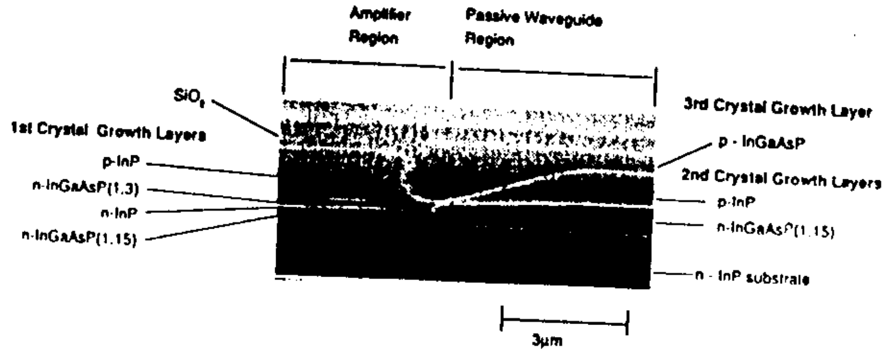

- **Carrier injection type switches combined with traveling-wave optical amplifier**
- **Loss-less fiber-to-fiber operation with on/off ratios of 40 dB**

Hitachi 1993

suematsu 8

Eidgenössische Technische Hochschule Zürich

ALL OPTICAL WAVELENGTH CONVERTER WITH SEMICONDUCTOR AMPLIFIERS

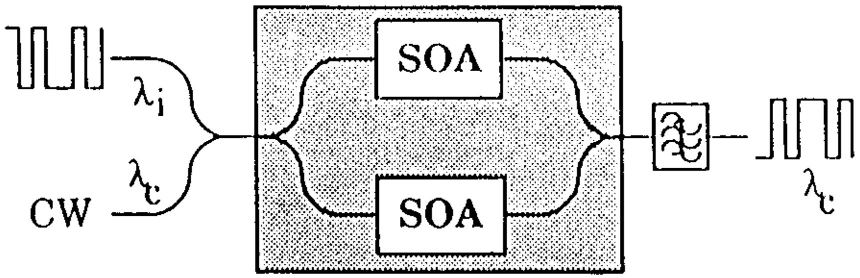

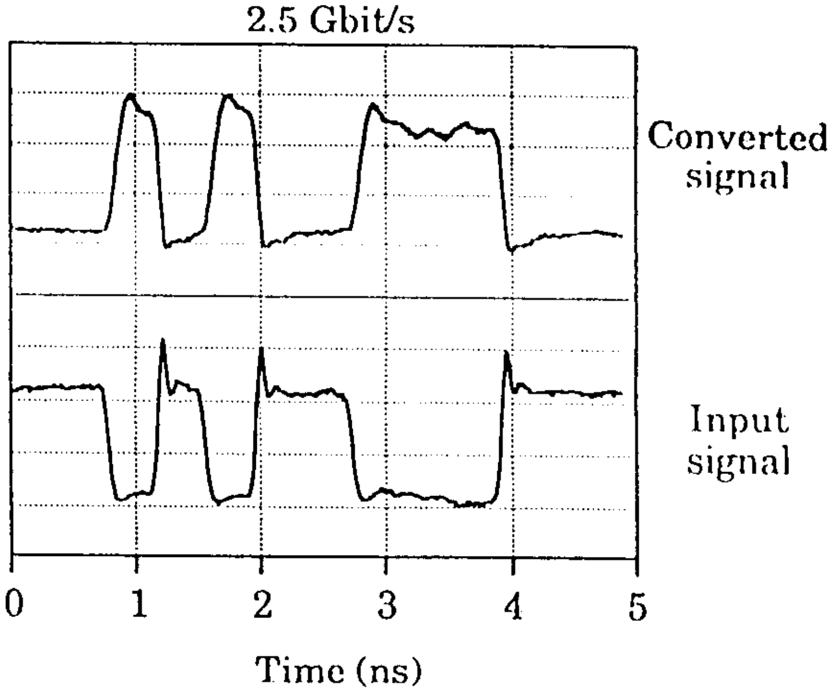

Wavelength Converter with Semiconductor Optical Amplifiers in Mach-Zehnder Configuration

Penalty Free Conversion of 2.5 Gb/s Signals from 1531 nm Input Wavelength to 1543 nm Output Wavelength

TUD

ETH Eidgenössische Technische Hochschule Zürich

suematsu 15

OPTICAL SPACE, TIME AND WAVELENGTH SWITCHING

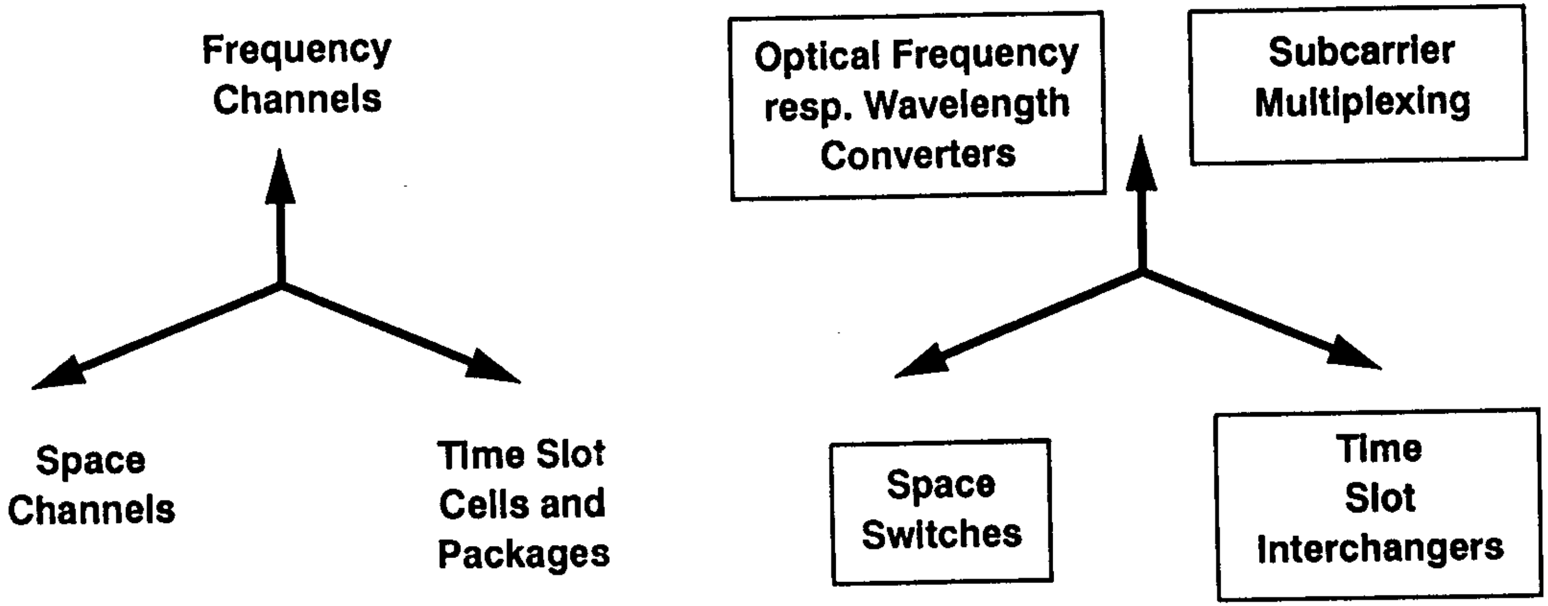

ETH Eidgenössische Technische Hochschule Zürich

ALL-OPTICAL WAVELENGTH CONVERTERS (AWOC's)

.DBR based AOWC :

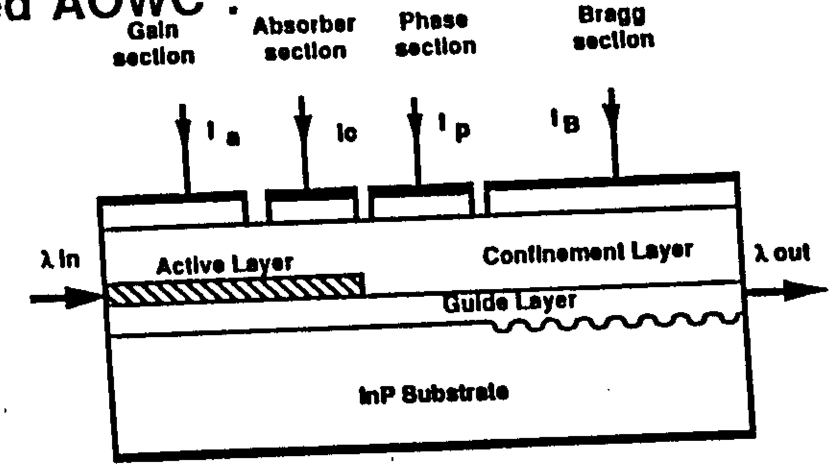

Absorption Saturation	Gain Saturation
Optical triggering at 2.5 Gb/s with 10-9 BER	Optical triggering at 5 Gb/s with 10-9 BER

.Y-laser AOWC :

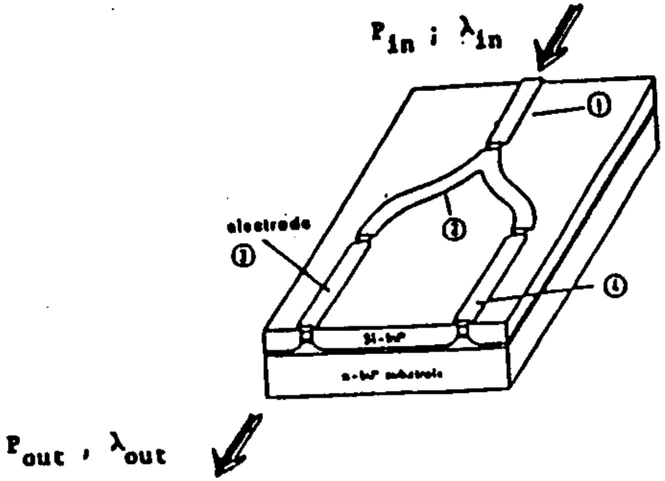

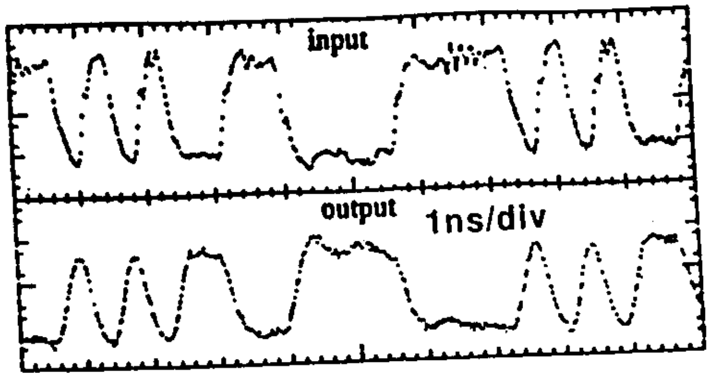

Eidgenössische Technische Hochschule Zürich

ALL OPTICAL WAVELENGTH CONVERTER WITH SEMICONDUCTOR AMPLIFIERS

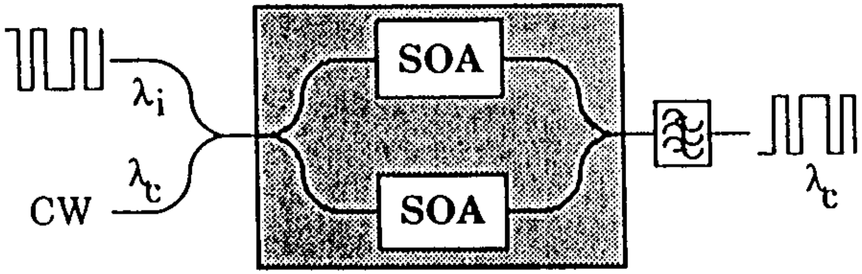

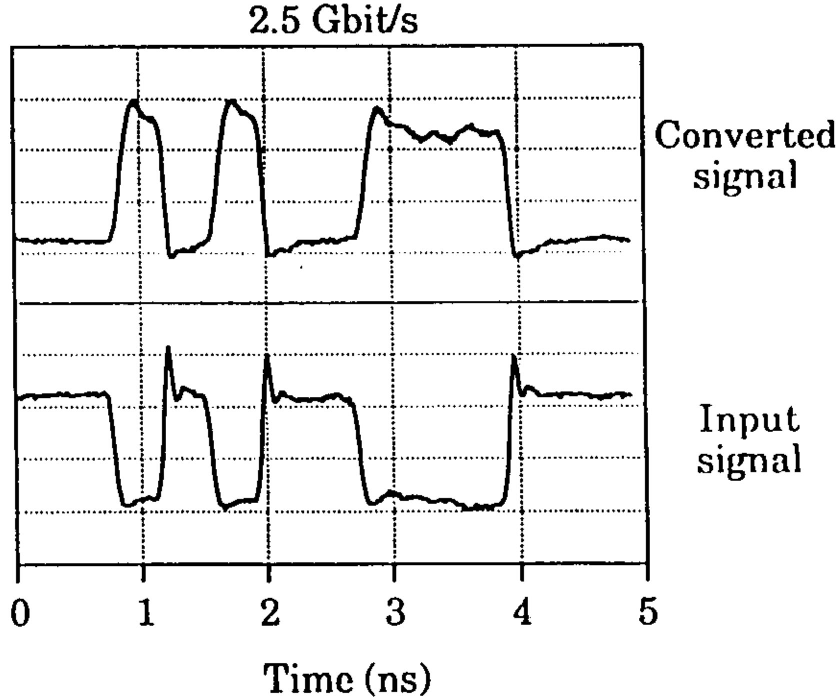

Wavelength Converter with Semiconductor Optical Amplifiers in Mach-Zehnder Configuration

Penalty Free Conversion of 2.5 Gb/s Signals from 1531 nm Input Wavelength to 1543 nm Output Wavelength

TUD

ETH Eidgenössische Technische Hochschule Zürich

Optoelectronic Switches Modulators and Semiconductor Amplifier Gates for High Speed Fiber-Transmission Systems

- ⇒ Motivation for Optical Switching in High Speed Fiber Optical Communication Networks
- ⇒ Basic Concepts of Optical Switches, Modulators and Semiconductor Optical Amplifier Gates
- ⇒ Physical Effects exploited in Waveguide Type Optical Switches, Modulators and Semiconductor Optical Amplifier Gates
- ⇒ Implementations of High Speed Optical Modulators
- ⇒ Implementations of High Speed Waveguide Type Space Switches
- ⇒ Semiconductor Optical Amplifier Gates and Wavelength Converters
- ➡ Summary and Conclusions

ETH Eidgenössische Technische Hochschule Zürich

COMPARISON OF VARIOUS ELECTRO-OPTIC SWITCHES BASED ON CHANGES OF INDEX OF REFRACTION OR OF ABSORPTION

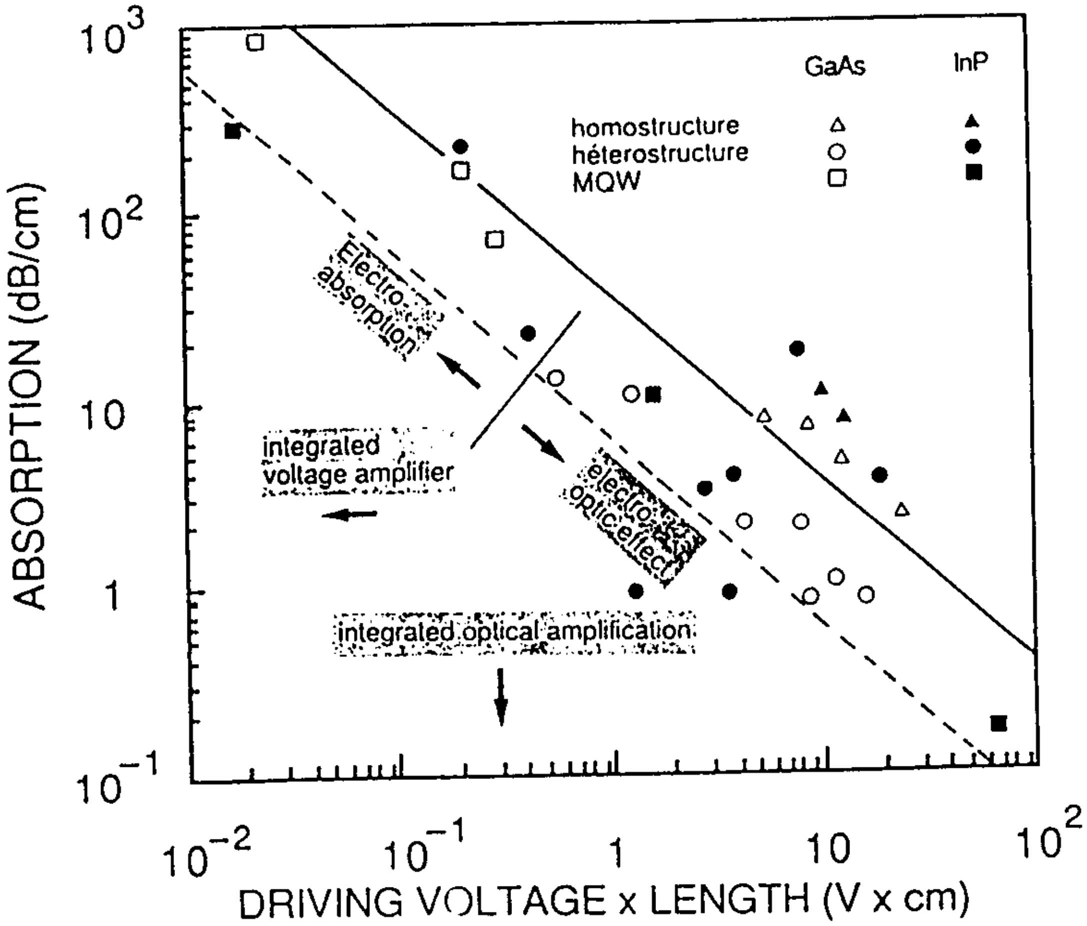

113